Physics Department annual progress report 1 January - 31 December 1989

Als-Nielsen, Jens Aage; Pedersen, J.S.; Juul Rasmussen, Jens; Lebech, Bente

Publication date:
1990

Document Version
Publisher's PDF, also known as Version of record

RISØ

Risø-R-574

Physics Department Annual Progress Report 1 January - 31 December 1989

Edited by J. Als-Nielsen, J. Skov Pedersen,
J. Juul Rasmussen and B. Lebech

Risø National Laboratory, DK-4000 Roskilde, Denmark
February 1990

ATTENTION MICROFICHE USER,

The original document from which this microfiche was made was found to contain some imperfections that reduce full comprehension or some of the text despite the good technical quality of the microfiche itself. The failures may be:

- missing or illegible pages/figures;
- wrong pagination;
- poor overall printing quality, etc...

We normally refuse to microfiche such a document and request a replacement document (or page) from the national INIS Centre concerned. However, our experience shows that many months pass before such documents are replaced. Sometimes the Centre is not able to supply a better copy or, in some cases, the pages that were supposed to be missing correspond to a wrong pagination only. We feel that it is better to proceed with distributing the microfiche made of these documents than to withhold them till the imperfections are removed. If the removals are subsequently made then replacement microfiche can be issued. In line with this approach then, our specific practice for microfiching such documents is as follows:

1. A microfiche of an imperfect document will be marked with a special symbol (black circle) on the left of the title. This symbol will appear on all masters and copies of the document (1st fiche and trailer fiches) even if the imperfection is on one fiche of the report only.

2. If the incorrectnesses are not too general the reason will be specified on a sheet such as this, in the space below.

3. The microfiche will be considered as temporary, but sold at the normal price. Replacements, if they can be issued, will be available for purchase at the regular price.

4. A new document will be requested from the supplying Centre.

5. If the Centre can supply the necessary pages/document a new master fiche will be made to permit production of any replacement microfiche that may be required.

The original document from which this microfiche has been prepared has these imperfections:

- [X] ~~missing pages/figures~~ numbered: 81, 82, 83 + 84.
- [ ] wrong pagination
- [ ] poor overall printing quality
- [ ] combinations of the above
- [ ] other

INIS Clearinghouse
I.A.E.A.
P.O. Box 100
A-1400, VIENNA
AUSTRIA

RISØ-R-574

PHYSICS DEPARTMENT ANNUAL PROGRESS REPORT

1 January - 31 December 1989

edited by J. Als-Nielsen, J. Skov Pedersen, J. Juul Rasmussen and B. Lebech

Abstract

Research in the Physics Department covers two main fields: condensed matter physics and plasma physics. The principal activities in these fields are presented in this Progress Report covering the period from 1 January to 31 December 1989.

The condensed matter physics research is predominantly experimental utilising diffraction of neutrons and x-rays. The research topics range from studies of two- and three-dimensional structures, magnetic ordering, heavy fermions, phase transitions in model systems to studies of texture and recrystallization kinetics with a more applied nature. The discovery of the high T_c superconductors in 1986 has opened an important new research area, where neutron and x-ray diffraction are used to elucidate the basic mechanism responsible for the superconductivity and in the analysis of the solid state syntheses used in producing the materials.

The plasma physics research is partly experimental and partly theoretical. The plasma physics programme is also of a wide scope ranging from fundamental studies of wave propagation, instabilities, solitons and turbulence in plasmas to refuelling a fusion reactor by deuterium-tritium pellets.

February 1990

Risø National Laboratory, DK-4000 Roskilde, Denmark

This report contains unpublished results and should not be quoted without permission from the authors.

ISBN 87-550-1618-9
ISSN 0106-2840
ISSN 0107-8348

Grafisk Service Risø, 1990

CONTENTS

1. CONDENSED MATTER PHYSICS

1.1. Introduction to the work in condensed matter physics

The condensed matters physics research is predominantly experimental utilising diffraction of neutrons and x-rays. The neutron scattering experiments are carried out at the DR3 reactor, where the Physics Department operates seven spectrometers, including a small angle neutron scattering facility. The experiments using synchrotron x-ray radiation take place at HASY-laboratory, at DESY in Hamburg, F.R.G.

Neutron and x-ray diffraction are complementary techniques. The neutron has several unique properties. It can penetrate matter; the energies of neutrons are comparable to that of typical excitations in condensed matter, and so the neutron can probe such excitations. In scattering experiments, the neutron is sensitive to the magnetic moments of atoms and to nuclear isotopes and at ultralow temperatures the neutron can even be used to determine the orientation of nuclear spins. The main advantage of x-ray diffraction in our research programme stems from the astounding x-ray intensity one can obtain from synchrotron sources. This allows an improvement of resolution in diffraction experiments by several orders of magnitude over possibilities with neutron scattering, and/or a minute volume of the diffracting sample such as a single atomic or molecular layer on a surface.

The research topics described in this report cover studies of two- and three-dimensional structures, magnetic ordering, heavy fermions, phase transitions in model systems, studies of high T_c superconductivity and studies of inorganic and biological materials by small angle scattering.

1.1.1. Nuclear magnetic phase diagramme for Cu

(A.J. Annila*, K.N. Clausen, P.-A. Lindgård, O.V. Lounasmaa*, A.S. Oja*, K. Siemensmeyer*, M. Steiner*, J.T. Tuoriniemi* (*Heisinki University of Technology, Espoo, Finland) and H. Weinfurter* (*Hahn-Meitner Institute, Berlin)

A new magnetic structure, characterized by the (0 2/3 2/3) and symmetry equivalent reflections (1 1/3 1/3), (1 −1 3 −1/3), has been observed by neutron scattering from a ^{65}Cu single crystal with the external field along the $(0\bar{1}1)$ direction.

The phase diagram has been determined from intensities of the (1 1/3 1/3) and (100) reflections measured at 17 different external magnetic fields between B = 0 and B_c = 0.25 mT. This was done by monitoring the neutron signal as a function of time while the spin system was warming up at constant field; the method is schematically illustrated in the inset of Fig. 1a.

In Fig. 1a, b and c we give three examples of warm-up curves. Neutron counts are plotted as functions of time. Temperature, which can be determined only in the paramagnetic phase ($T > T_N$ = 58 nK), is monotonically increasing with time. Figure 1a, with data

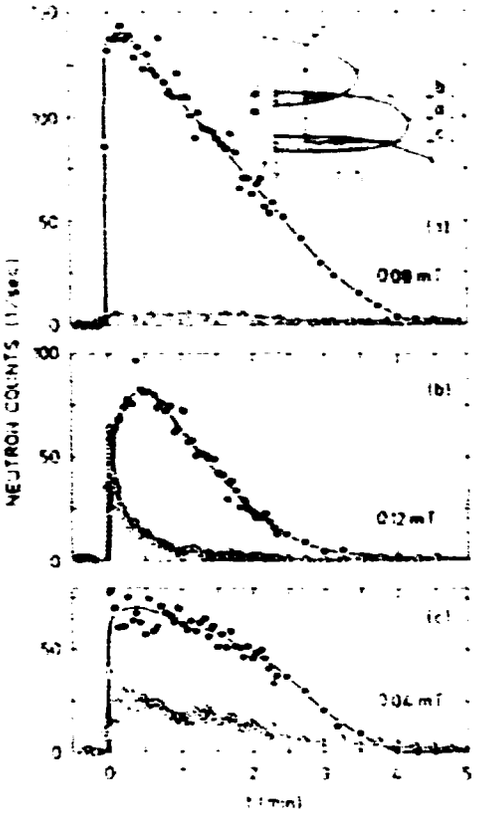

Fig. 1. (a) Time dependence of the (1 1/3 1/3) (filled symbols) and (100) (open symbols) reflection at B = 0.08 mT. A schematic phase diagram in the B-T plane is shown in the inset; the lines with arrows indicate entrance along an isentrop (S = 0.1·Rln4) into the ordered phase and subsequent measurements in a constant field; a,b,c correspond to the curves in Figs. 1a, b and c, respectively. (b) Time dependences of the (1 1/3 1/3) and (100)reflections in the vicinity of the upper phase boundary. (c) Same for the lower phase boundary.

measured at B = 0.08 mT, shows how the (1 1/3 1/3) neutron intensity

decreases due to the warm-up caused by the spin lattice relaxation process.

The data presented in Figs. 1b and 1c illustrate the kinetics of the transitions. At B = 0.12 mT, the simultaneous disappearence of the (100) signal and appearance of the (1 1/3 1/3) reflection indicate a first order phase transition. At B = 0.04 mT, the (100) neutron intensity increases during the first minute whereafter, the (1 1/3 1/3) and (100) peaks both decrease slowly during the next few minutes. This behavior could be explained by domain growth, which increases the intensity initially and tends to counteract the decrease caused by the warm-up.

The observed kinetics is a consequence of our demagnetization technique (see inset of Fig. 1a), which requires passage through the higher field phase prior to entering the lower field phase. During the passage, the upper phase is formed, and some seconds are needed for it to disappear. This time scale is very convenient for further studies of kinetic effects in the spin system.

From the neutron count versus time curves a neutron intensity contour diagram was constructed (1 1/3 1/3) reflection: full curves and (100) reflection: dotted curves); it is shown in Fig. 2. Three maxima occur: At B = 0.09 mT for the (1 1/3 1/3) reflection, and at B = 0 and B = 0.15 mT for the (100) reflection. The (1 1/3 1/3) signal is strongest when the (100) signal is weakest and vice versa, implying the presence of three distinct phases.

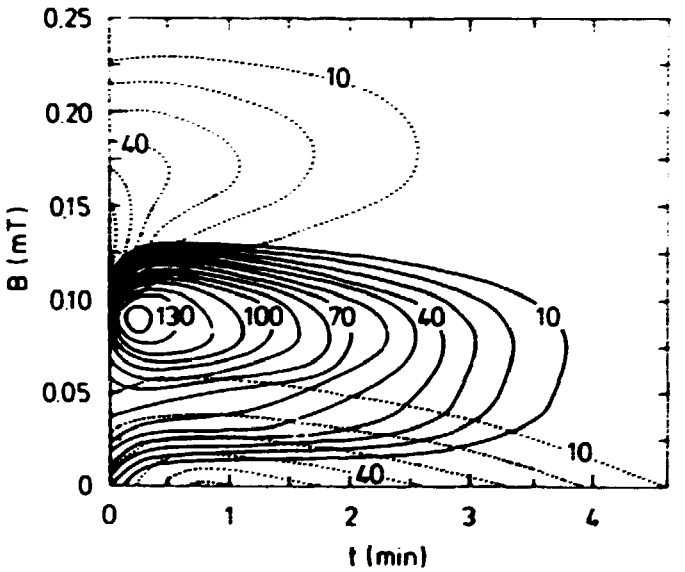

1.1.2. Theory of the magnetic ordering in a field in Cu: An ideal frustrated antiferromagnet

(P.-A. Lindgård)

The phase diagram as a function of a field of the ideal S = 3/2 f.c.c. antiferromagnet, represented by the nuclear spin system in Cu, was investigated by perturbation theory for a spin cluster. The (100) phases are stable on account of the dipole interaction and the calculated Rudermann Kittel interaction[1]. A phase with ordering vector along $\Gamma K(0\eta\eta)$ was previously predicted[2] to be penetrating along the phase separation line for two distinct (100) phases for a field along the (101) direction. A structure with an irrational η, i.e. an incommensurate structure, could not be excluded. It is found that a phase diagram with two (100) structures, separated by the indicated three sublattice, (0 2/3 2/3), structure is stabilized by quantum fluctuations (see figure). The relevant ratio of the dipolar (D) and exchange (H_c) interactions for Cu is 3D/H_c ~ 0.9. This is in agreement with recent experimental results (see 1.1.1) where three distinct phases are found, characterized by the (100) and (0 2/3 2/3) neutron reflections.

1) Lindgård, P.-A., Wang, X. and Harmon, B.N. (1986). J. Magn. Magn. Mater. 54-57, 1052.

2) Lindgård, P.-A. (1988). Phys. Rev. Lett. 61, 629.

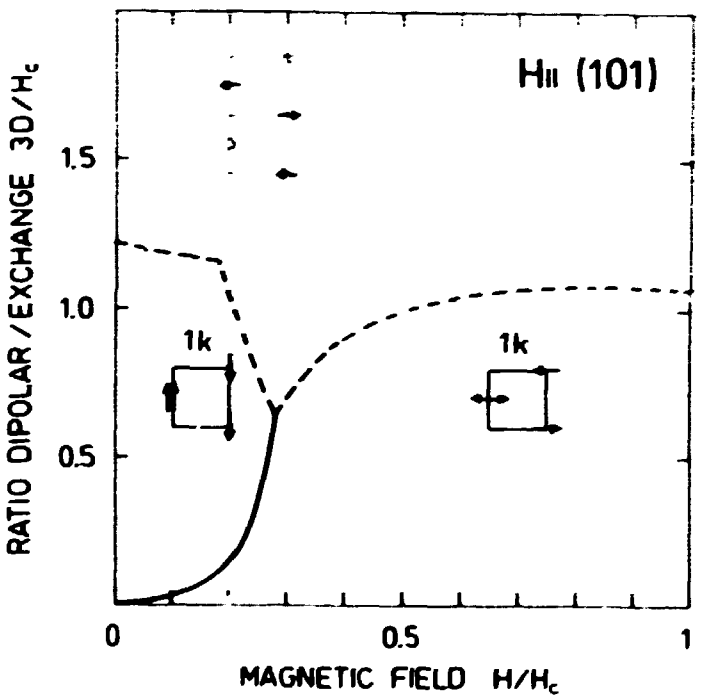

1.1.3. Structural phase diagram and equilibrium oxygen partial pressure of $YBa_2Cu_3O_{6+x}$ studied by powder neutron diffraction and gas volumetry

(N.H. Andersen, B. Lebech and H.F. Poulsen)[1]

Many structural properties related to high-T_c superconductivity in $YBa_2Cu_3O_{6+x}$ (YBCO) have been established until now. It is well-known that the CuO_2-planes in the layered structure are the basic component containing the electronic configurations that give rise to superconductivity if sufficient hole concentrations are created by the acceptor layers formed by the CuO-chains in the structure. Reduction of the oxygen concentration ($x < 1$) causes oxygen disordering in the CuO-chains, and a simultaneous decrease of the hole carrier concentration in the CuO_2-plane and the superconducting transition temperature. The main result is the existence of two levels of superconducting transition temperatures (~ 90 K and ~ 60 K) joining smoothly as x decreases. For $x = 0.4$, T_c goes to 0 K, and for $x < 0.4$ antiferromagnetic ordering of the Cu-spins develops. However, significant differences exist in the literature with respect to the details in the variation of T_c with x, probably as a result of the differences in the sample preparation causing variations in the oxygen disorder configurations. Disorder of the oxygen positions in the chain structure develops with decreasing x and/or increasing temperature leading to a structural transformation from orthorhombic to tetragonal symmetry. There are strong indications that orthorhombic symmetry is favourable for high-T_c superconductivity, but details in the correlations between defect structure and superconductivity have not been established.

We have studied the structural phase diagram and determined the equilibrium oxygen partial pressures of YBCO at more than 350 points in (x,T)-space for concentrations $0.15 < x < 0.92$ and temperatures $25^{\circ}C < T < 730^{\circ}C$ by a technique in which *in situ* gas volumetric measurements are carried out on a powder neutron diffractometer. The advantage of the method is that very accurate values of oxygen stoichiometry ($\Delta x < 0.005$) may be obtained under equilibrium conditions by use of the ideal gas law in combination with structural and iodiometric titration analyses. Hereby, simultaneous studies of structural properties and oxygen equilibrium partial pressure may be carried out.

The structural data have been used to establish the structural phase diagram with respect to the transition temperature from orthorhombic to tetragonal symmetry as function of x. Our experimental results together with predictions of theoretical model calculations (— from Ref. 3, ⊷ and from Ref. 4) are shown in the figure. Lattice constants as function of temperature and x have also been deduced. Results at room temperature are in good agreement with recently

published values[2], although orthorhombic distortions are observed only for $x > 0.28$ and not down to $x = 0.18$. Analysis of the structural data did not reveal the presence of mixed phase structures, which we have observed from alternative oxidation procedures[5], and which have been suggested theoretically[3]. Neither do we observe the superstructures which have been inferred from electron microscopy studies, probably because the defect ordering is two-dimensional, and therefore may be determined only from single crystal studies. The oxygen equilibrium partial pressures P in (x,T)-space has been used to establish the oxygen chemical potentials in the disordered chain structure. At higher temperatures log P versus x approaches a linear behaviour, whereas a more complex dependence, which to some extent correlates with the $T_c = 60$ K plateau and the disappearence of orthorhombic phase, is observed at lower temperatures. A significant result is also a strong increase in the low temperature oxygen equilibrium partial pressure as x approaches 0.92. This indicates that $x = 0.92$ corresponds to the maximal oxygen concentration which may be obtained in the material at an oxygen partial pressure of one atmosphere. Finally it should be mentioned that some measurements carried out with essentially the same starting parameters resulted in quite different values of oxygen equilibrium partial pressures and variations in the final oxygen stoichiometry. This observation support our previous suggestion of possible metastable structures in the phase diagram[5].

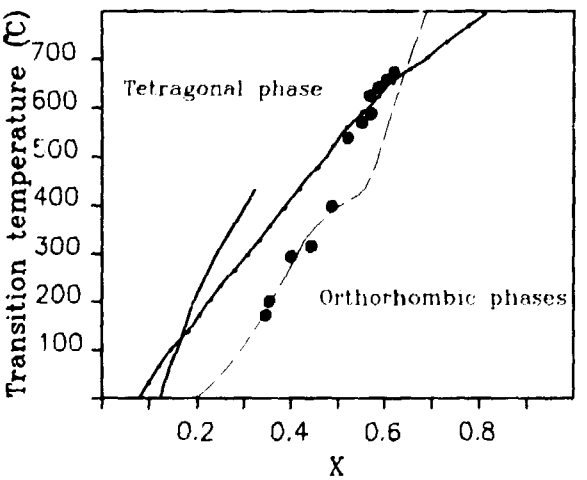

Structural phase diagram of $YBa_2Cu_3O_{6+x}$. Notice that a sample with $x = 0.28$ showed weak broadenings of the (200)-peaks, indicating weak orthorhombic distortions below 20°C. Theoretical model calculations from Ref. 3 (———) and Ref. 4 (Figs. 1 (----) and (-•-•-) are also included.

1) Larsen, J.G. and Røen, S. H. Topsøe Corporation are greatly acknowledged for supplying the sample and performing iodiometric titration analyses.

2) Nakazawa, Y. and Ishikawa, M. (1989). Physica **C158**, 381.

3) Khachaturyan, A.G. and Morris Jr., J.W. (1987). Phys. Rev. Lett. **59**, 2776.

4) Kikuchi, R. and Choi, J.-S. (1989). Physica **C160**, 347.

5) Als Nielsen, J., Andersen, N.H., Broholm, C., Clausen, K.N., Lebech, B., Nielsen, M. and Poulsen, H.F. (1989). IEEE Transactions on Magnetics **25**, No. 2, 2254.

1.1.4. Crystal structure and oxidation properties of $Nd_{1.85}Ce_{0.15}CuO_{4-y}$ studies by neutron powder diffraction and gas volumetry

(N.H. Andersen, B. Lebech, I. Mangelschots (IBM Research Laboratory, Zürich, Switzerland) and A. Wisniewski (Polish Academy of Sciences, Warszawa, Poland))

The discovery of superconductivity in $Nd_{2-x}Ce_xCuO_{4-y}$ has attracted considerable interest recently. The material is derived from the archetype high-T_c superconductor $La_{2-x}Ba_xCuO_{4-y}$ by standard substitution on the La-site. However, instead of Ba^{2+}-, Ce^{4+}-ions are introduced in the lattice resulting in an increased electron carrier density in the CuO_2-planes. Valence considerations, assuming $y > 0$, and measurements of Hall-coefficients and thermopower suggest that the system is an electron conductor, and not as the other high-T_c materials a hole conductor. Further support for this suggestion is the observation, made from a single crystal study at the IBM Research Laboratory, Zürich, that oxidation in pure oxygen for one hour destroys superconductivity. Recent neutron powder diffraction studies by Izumi et al.[1] have revealed that $Nd_{1.845}Ce_{0.155}CuO_{4-y}$ (NCCO) has essentially full occupation on the oxygen sites O(1) and O(2), whereas $La_{2-x}Ba_xCuO_{4-y}$ has essentially full occupation on sites O(1) and O(3) (see figure). In their studies of both superconducting and non-superconducting samples Izumi et al. found no significant changes in the oxygen occupations on sites O(1) and O(2), but they do not indicate whether they have tried to include the possible O(3) site in their analysis.

We have carried out a powder neutron diffraction study of superconducting NCCO with respect to occupation on site O(3) and the structural stability as a result of oxidation and reduction. In order to improve on the limited accuracy by which occupation numbers may be determined from powder data we have combined our structural measurements with gas volumetric determinations of the oxygen concentration changes in the sample. Neglecting oxygen adsorption on the grain surfaces an accuracy better than $\Delta y = 0.001$ is obtained using a sample of weight 3.09 g. The sample was prepared by standard solid state reaction methods. It was single phase and has been made superconducting ($T_c = 23$ K) by reduction at 890°C for 15 hours in a flow of nitrogen (4N5). Structural determinations were carried out on the sample as prepared (run No. 1), after oxidation in pure oxygen at 399°C for two hours (run No. 2) and at 794°C for 1.5 hours (run No. 3), and after reduction under vacuum (pressure variations between 0.1 and 0.3 torr during the experiment) at 414°C for 3.5 hours (run No. 4) and at 796°C for 3.5 hours (run No 5). All structural determinations were carried out at room temperature without moving the sample, thereby allowing for direct comparison of the diffraction patterns. Analysis of the structural data obtained from run No. 1

resulted in the structure shown in the figure with occupancies on oxygen sites: O(1) = 1.000 (fixed), O(2) = 1.00 ± 0.03, and O(3) = 0.03 ± 0.01. This gives an oxygen content corresponding to $y = -0.06 \pm 0.08$, which is very close to the critical oxygen content ($y_c = -0.075$) where transition from electron ($y > y_c$) – to hole ($y < y_c$) – conduction is expected. Within the statistical error the diffraction patterns from run No. 1-5 were identical. Also the gas volumetric measurements support that no structural changes have occurred since only minor variations in the oxygen content were observed relative to run No. 1: $\Delta y = -0.006$ after run No. 2, $\Delta y = -0.011$ after run No. 3, $\Delta y = -0.008$ after run No. 4, and $\Delta y = 0.000$ after run No. 5. Part of the sample was subsequently given the heat treatments corresponding to run No. 2-5 and their superconducting properties were studied by measurements of the Meissner effect. Only small changes in the widths of the superconducting transitions were observed. In contrast to the single crystal results we therefore conclude that NCCO is stable at least for short times up to 800°C under oxidizing as well as reducing atmospheres. The limits of stability are currently under investigation by measurements of Meissner effect. Studies of the structural and stoichiometric changes resulting in the destruction of superconductivity are planned using the same methods.

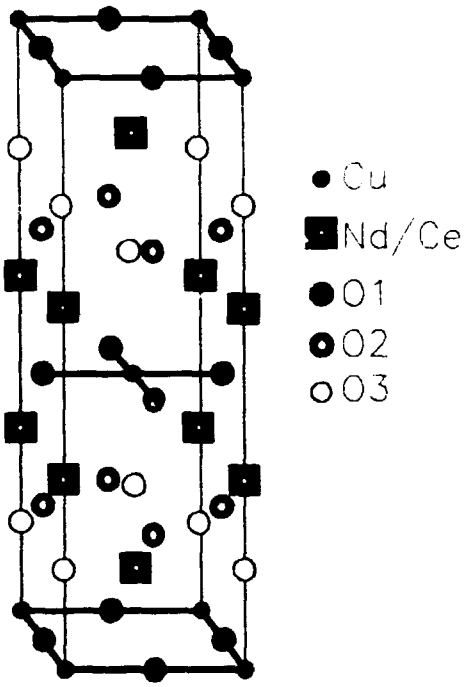

Crystal structure of $Nd_{1.85}Ce_{0.15}CuO_{4-y}$.

[1] Izumi, F., Matsui, Y., Takagi, H., Uchida, S., Tokura, Y. and Asano, H. (1989). Physica C158, 433-439.

1.1.5. Measurement of texture in high T_c thin films

(R. Kromann, J. Fossum and N. H. Andersen)

Ceramic high T_c superconductors exhibit a strong anisotropy in the critical current density J_c with the highest values for current flowing along the a-b plane. This suggests that thin films should be grown with the c-axis perpendicular to the substrate. Furthermore, since grain boundaries significantly decrease J_c it is of interest to monitor and eventually control the in-plane ordering. For this purpose we have established a facility for texture analysis of thin films using the standard Euler cradle technique. This yields a measure of the preferred crystallographic orientations in the form of a pole figure.

Measurements have been performed on two kinds of film on single crystalline MgO, one kind made by laser ablation and the other kind by high temperature recrystallization of a 10 μ thick tape casted foil. Films have been prepared by NKT Corporation and H. Topsøe Corporation. The latter has a very dull appearance both visually and in terms of the pole figure which contains many small, broad peaks. The first kind of film, on the contrary, is highly textured with only a few very strong peaks at the theoretically correct angles (see figure) for the thin film to be epitaxial, and with peak widths approaching those of the single crystal substrate. We conclude therefore that the laser ablation technique is very good for preparation of epitaxial films whereas the high temperature recrystallization technique needs further development.

In the near future we expect to include films grown on $LaGaO_3$ substrates which have lattice parameters closer to those of $YBa_2Cu_3O_7$ than has MgO. They should therefore be better suited for epitaxial growth.

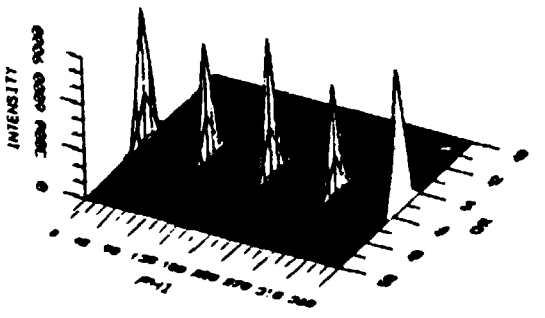

Partial pole figure for a laser ablated film based on the $YBa_2Cu_3O_7$ (103)-peak. Theoretical values: χ = 45.5°; ϕ = 0, 90, 180 and 270°.

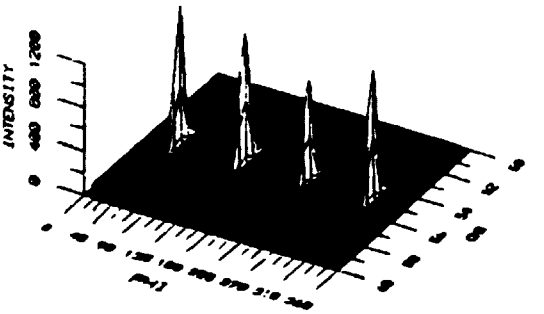

Partial pole figure for a laser ablated film based on the $YBa_2Cu_3O_7$ (113)-peak. Theoretical values: χ = 55.0°; ϕ = 45, 135, 225 and 315°.

1.1.6. A powder neutron diffraction study of Co-substituted $YBa_2(Cu_{1-x}Co_x)_3O_{9-\delta}$

(H. Fjellvåg*, R. Glenne*, P.H. Andresen*, P. Karen* (*University of Oslo, Norway) and B. Lebech)

All metallic elements in the high temperature superconducting material $YBa_2Cu_3O_{9-\delta}$ can easily be substituted by several other metallic elements. As a part of an extensive study of the correlation between slight changes in the crystal structure brought about by chemical substitution and various superconducting properties, three selected powder samples of $YBa_2(Cu_{1-x}Co_x)_3O_{9-\delta}$, x = 0.015, 0.030 and 0.250 were studied by neutron diffraction at temperatures between 10 and 300 K. The symmetry changes from orthorhombic (Pmmm) to tetragonal (P4/mmm) when the substitution level exceeds 2.5 ± 0.2 at. % at room temperature. The upper limit for solid solubility is x = 0.30. The diffraction study provides information on two major structural implications of the substitution; (i) the distribution of Co among the two different Cu-sites and (ii) the amount and distribution of oxygen atoms in the two structure modifications. The results show that Co mainly substitute at the Cu_1 site, i.e. in the (0 0 0) position. Simultaneously, the increased oxygen content is achieved by a higher degree of filling of the (0 1/2 0) and (1/2 0 0) sites. It is possible that Co thereby obtains octahedral coordination.

Powder diffraction data were also collected for Y_2BaO_4 and $Y_2Ba_3O_6$. The former has a well-known structure, and position coordinates were obtained by Rietveld refinements. For the latter, structure solution and refinement based on powder diffraction data is in progress.

1.1.7. Intermetallic magnetism in $NpCo_2$ - experiment and theory

(M. Wulff (Centre d'Etudes Nucleaires, Grenoble, France), B.Lebech, G.H. Lander+, P.J. Brown (Institute Laue-Langevin, Grenoble, France), M.S.S. Brooks+ (+Commission of European Communities Joint Research Centre, Karlsruhe, F.R.G.), O. Eriksson* and B. Johansson* (*University of Uppsala, Uppsala, Sweden))

Actinide intermetallic compounds exhibits a rich variety of magnetic properties and it has been pointed out[1] that there seems to be a critical actinide-actinide distance such that magnetic order vanishes below this distance. In a simplified picture these ideas can be understood quantitatively by noting that as the actinide atoms are brought together the overlap of the 5*f*-wavefunctions increases and this broadens the effective 5*f*-band. When the 5*f*-band width becomes sufficiently large the Stoner criterion for magnetism is no longer fulfilled and the ground state is paramagnetic.

$NpCo_2$ crystallizes in the cubic Laves phase (C-15 structure). Mössbauer spectroscopy[2] and neutron diffraction studies have shown that $NpCo_2$ orders antiferromagnetically below 15 K[3], but the nature of the magnetic structure has not yet been established. However, in the presence of a large magnetic field ($H > 2.5$ T) Aldred at al.[3] observed a metamagnetic transition in which a moment $\mu_{Np} = 0.5\ \mu_B$ is induced on the Np sites and with $\mu_{Co} < 0.15\ \mu_B$ is induced on the Co sites. Normally, in actinide intermetallics the exchange field is so great that a magnetic field applied to an antiferromagnet yields a neglible induced magnetic moment. $NpCo_2$ is exceptional in this respect. Based on our own and previous difficulties[3] in establishing the magnetic structure, the high susceptibility may possibly arise from a complex long-range antiferromagnetic structure. The Mössbauer effect is unfortunately of little use in the study of $NpCo_2$ because of the observed relaxation effects[2].

In order to study in detail the magnetic properties of $NpCo_2$ we have used a 40 mg single crystal grown by the Czochralski technique at the Institute for Transuranium Elements, Karlsruhe. The crystal was fully characterised by 4-circle neutron diffractometry at Risø, and the sample was found to be within 1% of stoichiometry.

In order to obtain the induvidual induced moments μ_{Np} and μ_{Co} and their distribution in real space, we have used the polarised neutron diffractometer D3B at the Institute Laue-Langevin, Grenoble. The instrument utilises the interference between the induced magnetic signal ($H_{appl} = 4.6$ T) and the

known nuclear structure factors to determine the induced magnetic amplitude at each Bragg reflection. By an appropriate data analysis[4], it is possible to determine the induced magnetic amplitudes on the Np and the Co sites separately. The results are shown in the figure. The open squares

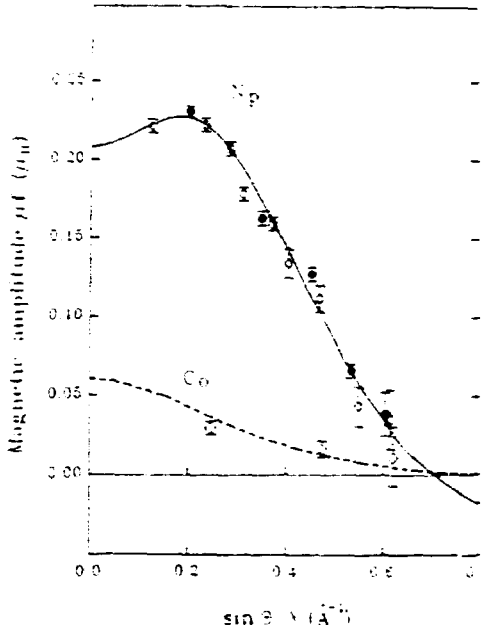

correspond to Co-only reflections, the closed circles to Np-only reflections. The open circles to mixed reflections with contributions from both sites where we have corrected for $(\mu \cdot f(\mathbf{Q}))_{Co}$ before plotting the $(\mu \cdot f(\mathbf{Q}))_{Np}$ open circles. The dashed curve is the form factor $(f(\mathbf{Q}))_{Co}$ of elemental Co normalised to $\mu_{Co} = 0.06\ \mu_B$. The solid curve is a fit to the Np form factor described the dipole approximation by

$$\mu f(Q) = \mu(\langle j_0 \rangle + C_2\langle j_2 \rangle), \qquad (1)$$

where $\mu = \mu_s + \mu_\ell$, $C_2 = \mu_\ell/\mu$ and $Q = 4\pi\frac{\sin\theta}{\lambda}$

In Eq. (1) μ_s and μ_ℓ are the spin and orbital moments, respectively, and $\langle j_l \rangle$ are Bessel transforms[5] of the single electron charge density distribution for the 5*f*-electrons. From the fit we found $\mu_{Np} = 0.21(1)\ \mu_B$, $\mu_{Co} = 0.06(1)\ \mu_B$ and $C_2 = 3.7(3)$, leading to $\mu_s = -0.6(1)\ \mu_B$ and $\mu_\ell = 0.8(1)\ \mu_B$.

In order to compare the magnetic properties obtained from the neutron scattering experiments with theory, we have calculated the spin and orbital contributions and the resulting magnetic formfactor from first principles[6]. The theoretical values were obtained from a self-consistent enegy band calculation, using the linear muffin tin orbital (LMTO) method. In addition to the socalled combined correction terms the calculation incorporated relativistic effects and allowance were made for both spin and orbital polarisation. With no input parameters we find a total Np moment of 0.87 μ_B and $C_2 = 4.1$. When comparing these results with the experimental results above, it is important to realise that the experiment was performed on an antiferromagnet, whereas the theory refers to a ferromagnet. However, the composition in terms of relative magnitude of the spin and orbital components is less sensitive to the type of magnetic order than is, for example, the total moment at each site. If we consider the experimental results of high field (8 T) magnetization data[7] which show that

the yet unsaturated moment is 0.55 μ_B, we may assume that about one third of the total moment is induced in our experiment at 4.6 T. By scaling, this corresponds to a high-field induced moment of 0.63(3) μ_B which compares reasonably well with the calculated value of 0.87 μ_B. When comparing the C_2 values, where no scaling applies (see Eq. (1)) the agreement is even better (C_{2exp} = 3.7(3) and C_{2theo} = 4.1).

1) Hill, H. in "Plutonium 1970 and other actinides", edited by W.N. Miner (AIME, New York, 1971), p. 2.
2) Gal, J., Hadari, Z., Atzmony, U., Bauminger, E.R., Nowik, I. and Ofer, S. (1973). Phys. Rev. B8, 1901.
3) Aldred, A.T., Dunlap, B.D., Lam, D.J., Lander, G.H., Mueller, M.H. and Nowik, I. (1975). Phys. Rev. B11, 530.
4) Wulff, M., Lander, G.H., Lebech B. and Delapalme, A. (1989). Phys. Rev. B39, 4719.
5) Desclaux, J.P. and Freeman, A.J. (1978). J. Magn. Magn. Mater. 8, 119.
6) Wulff, M., Eriksson, O., Johansson, B., Lebech, B., Brooks, M.S.S., Lander, G.H., Rebizant, J., Spirlet J.C. and Brown, P.J. Experiment and theory of actinide intermetallic magnetism: A test case of $NpCo_2$, accepted for publication in Europhysics Letters.
7) Sanchez, J. P., private communication.

1.1.8. Giant magnetic anisotropy in US

(G.H. Lander*, M.S.S. Brooks* (*Commission of European Communities Joint Research Centre, Karlsruhe, F.R.G.), B. Lebech, P.J. Brown (Institute Laue-Langevin, Grenoble, France) and O. Vogt (Laboratorium für Festkörperphysik ETH, Zürich, Switzerland))

One of the key parameters of device applications in permanent magnets is the anisotropy constant which may be characterised as an effective K_1. The values of K_1 for transition metals are always low ($< 10^6$ ergs/cm^3) and this is one of the reasons that permanent magnets are now usually composed of a transition metal (3*d*) in conjunction with a rare earth metal (4*f*). The 3*d*-element increases the Curie temperature, whereas the 4*f*-element can be considered as increasing K_1. It is well known that compounds containing 5*f*-actinide elements exhibit even more anisotropic behaviour than the analogous 4*f*-compound, but the size of the anisotropy has never been measured.

We have now measured the magnetic anisotropy in a simple cubic (NaCl structure) ferromagnet US. The measurements were done at D3B at the Institute Laue-Langevin using polarised neutron diffractometry. A magnetic field of 4.6 T was applied along a direction approximately 26° from the easy [111]

axis. From the polarised diffraction data the precise direction of the magnetic moment and its magnitude were determined as a function of temperature. The U-moment at 0 K was found to be 1.70 μ_B/f.u. in agreement with earlier work[1]. From 5 to 140 K the moment is locked along the easy [111] axis, but then it starts to rotate. Because of the high applied field we observe appreciable magnetic moment at T_c (178 K) and the moment finally turns parallel to the magnetic field at 195 K, at which temperature the reduced moment is 0.23. Using standard formulae[1] to relate the nisotropy to the magnetic energy we determined an effective K_1 in US as a function of reduced moment. This is plotted in the figure (open circles), where temperature is an implicit parameter.

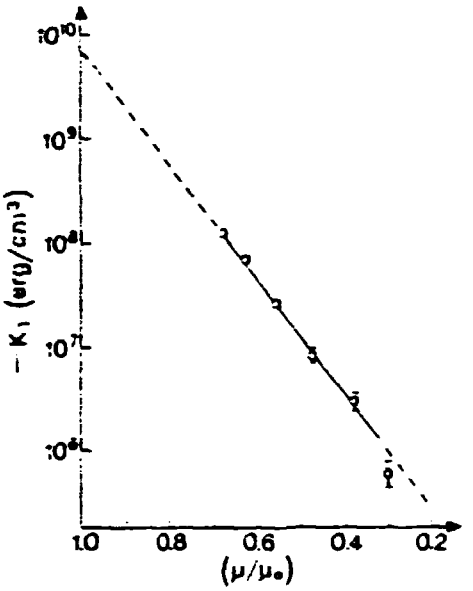

It should be noted that the effective K_1 in cubic US is ~20 times greater than that found in the cubic Laves phase $TbFe_2$ (~5.2 10^8 erg/cm^3), and this make 5*f*-compounds promising as possible candidates for permanent magnet devices. Theoretical studies suggest that the strong hybridisation of the 5*f*-electrons with the conduction electrons (and with *d*-electrons in the case of compounds containing transition metals) is the primary cause of this giant anisotropy in actinide compounds.

1) A. Clark in "Ferromagnetic materials", edited by E.P. Wohlfart, North-Holland, Amsterdam, 1980, p. 540.

1.1.9. Magnetic properties of $MgCu_2O_3$

(Th. Zeiske*, H.A. Graf*, H. Dachs* (*Hahn-Meitner-Institute, Berlin) and K.N. Clausen)

The chemical structure of $MgCu_2O_3$ was determined by Drenkhahn and Müller-Buschbaum[1]. It is orthorhombic, space group Pmmn, and can be described as a derivative of the NaCl structure. The lattice parameters are a = 3.99 Å, b = 9.34 Å and c = 3.19 Å.

The static magnetic susceptibility χ of polycrystalline $MgCu_2O_3$ was measured with a Faraday balance. Figure (a) shows the reciprocal specific susceptibility $1/\chi$ in SI units as a function of temperature in the range $12 < T < 292$ K. In order to correct for small ferromagnetic impurities, each measurement was made at five different magnetic fields and the data points plotted represent values extrapolated to high field, i.e. $1/B \rightarrow 0$, as shown in the inset for one particular temperature. The diamagnetic contributions have been calculated and subtracted.

$1/\chi$ decreases continuously with decreasing temperature and only a slight discontinuity is noticeable at the magnetic ordering temperature around 95 K. The magnetic structure of $MgCu_2O_3$ was determined by neutron diffraction from powder samples.

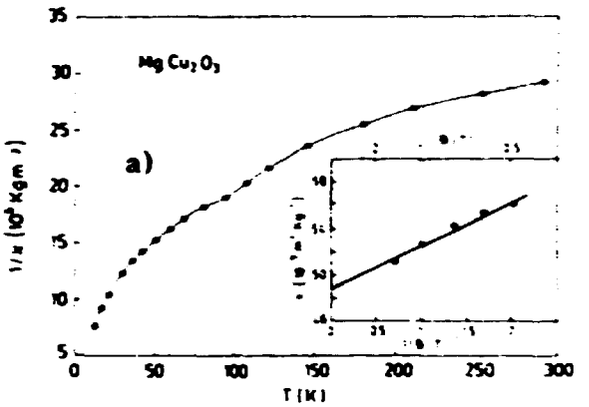

Below 94.5(5) K, peaks of magnetic origin appear in addition to the nuclear reflections. The magnetic peaks are commensurate and can be indexed as $([2n+1]/2\ [2m+1]/2\ \ell)$ on the basis of the chemical cell, with n, m and ℓ integers. The a and b axes of the magnetic unit cell are thus doubled, as compared with the chemical cell, while the c-axis remains unaltered. The intensity of the strongest magnetic peak, (1/2 1/2 0) as a function of T can be fitted with the expression $I(T) = I_0[(T_c-T)/T_c]^{\beta}$ with $\beta = 1/2$. This curve demonstrates, that $MgCu_2O_3$ undergoes a second order antiferromagnetic phase transition with a Néel temperature $T_N = 94.5(5)$ K.

Only a few magnetic peaks, could be observed in the present measurements. From these reflections a model of the magnetic structure was derived, which is shown in (b): The Cu^{2+} ions are arranged in slightly corrugated layers, which are parallel to the (220) lattice planes of the magnetic unit cell. Within one layer all

copper ions have parallel spin, which is opposite to the spin of the copper ions in the neighbouring layers. To a first approximation, the spin is parallel to [010]. By scaling the magnetic scattering to the nuclear scattering, a magnetic moment of 0.33 μ_B per Cu^{2+} ion was deduced.

[1] Drenkhahn, H. and Muller-Buschbaum, H. (1975). Z. anorg. allg. Chem. 418, 116.

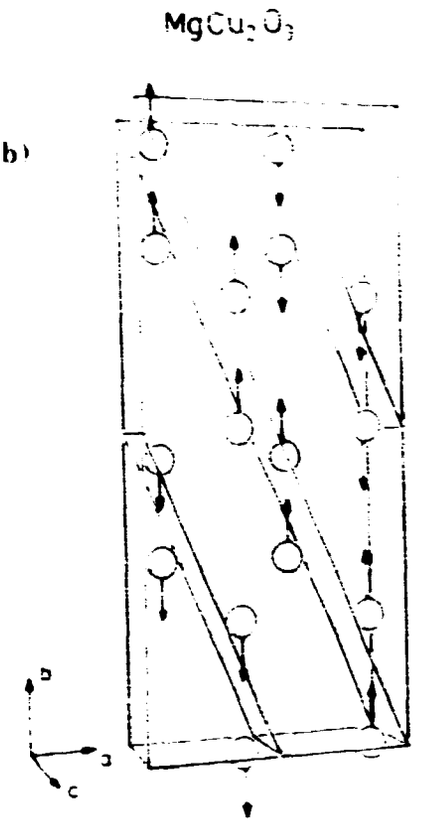

1.1.10. The magnetic structure of RbMnSb, CsMnAs and CsMnSb

(R. Müller*, H.-U. Schuster* (*Institut für Anorg. Chemie der Universität Köln, F.R.G.), P. Müller+, W. Bronger+ (+Institut für Anorg. Chemie der RWTH Aachen, F.R.G.) and K. N. Clausen)

The series of compounds AMnX with A = Li, Na, K, Rb, Cs and X = P, As, Sb, Bi crystallizes in a structure type shown in Fig. 1 (Space Group P4/nmm). The structure is characterized by edge sharing tetrahedra of X-atoms, centered by manganese. These layers are separated by the alkali atoms. Susceptibility measurements showed antiferromagnetism for all of these compounds with Néel temperatures above room temperature for most of them. Earlier investigations on the light alkali metal compounds revealed their magnetic structures and the correlation of magnetic moments with crystal field parameters[1]. In order to determine the spin structures of RbMnSb, CsMnAs and CsMnSb neutron diffraction experiments were carried out on TAS 1 at room temperature and at 11 K. The low temperature powder pattern could be indexed by doubling the c-axis. The spins are directed parallel to the c-axis and are coupled antiferromagnetically in the a-b-plane. The magnetic Space Group is found to be P4'/n'cc'. Table 1.1.10. (next page) shows the results of the Rietveld refinements. The magnetic structure is shown in figure 2.

1) Bronger, W., Müller, P., Höppner, R. and Schuster, H.-U. (1986). Z. allg. anorg. Chem. **539**, 175.

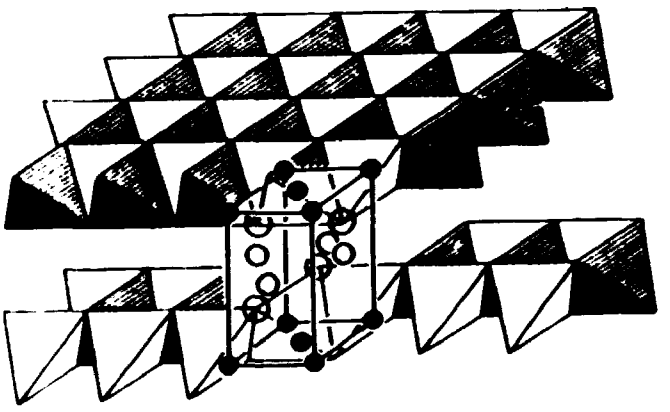

Fig. 1: Structure of AMnX

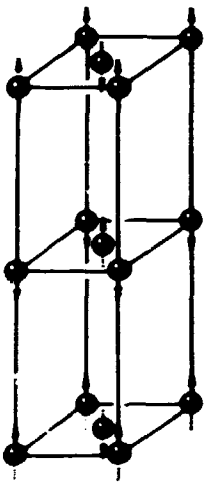

Fig. 2: Magnetic Structure of AMnX

Table 1.1.10. Results of Rietveld refinements on AMnX compounds. A and X are in 2c positions 0 1/2 z_A ; 1/2 0 $-z_X$ and Mn in 2a positions 0 0 0 and 1/2 1/2

Compound		RbMnSb		CsMnAs		CsMnSb	
T	[K]	9.9	295	10	295	10	295
a	[Å]	4.7172(2)	4.7329(1)	4.4171(1)	4.4632(3)	4.7618(2)	4.7763(4)
c	[Å]	8.4499(4)	8.4644(4)	8.6850(5)	8.6941(4)	8.8909(4)	8.8974(4)
z_A		0.646(2)	0.646(3)	0.650(2)	0.648(2)	0.650(2)	0.646(4)
z_X		0.184(1)	0.178(4)	0.170(1)	0.176(4)	0.176(3)	0.182(3)
$B_{overall}$	[Å^2]	0.2(1)	0.3(2)	1.5(2)	1.0(1)	0.1(3)	0.5(2)
μ_{Mn}	[μ_B]	4.22(3)		4.07(2)	2.19(1)	4.31(3)	
$R_{nuclear}$		0.054	0.036	0.058	0.033	0.048	0.032
$R_{magnetic}$		0.041		0.035	0.057	0.056	

1.1.11. $CaPdH_2$, a new perovskite-type hydride

(W. Bronger*, K. Jansen*, P. Muller* (*Institut fur Anorg. Chemie, Aachen, F.R.G.) and K. N. Clausen)

$CaPdH_2$ has been synthesized by the reaction of calciumhydride with palladium in a hydrogen atmosphere at 850°C. X-ray investigations on powdered samples reveaied a primitive cubic cell with a lattice constant a = 3.690(1) Å. Ca and Pd was assumed to order in the CsCl type structure. The results of least squares calculations are shown in Table 1.1.11. (next page).

In order to determine the hydrogen positions elastic neutron diffraction experiments on TAS I were carried out on a deuterated sample in an Al-container of 8 mm diameter and 30 mm length. The structure refinement with the integrated intensities led to an atomic arrangement which is related to a perovskite-type structure with a 2/3 occupation of the anion position. Thus palladium is found to be in the oxidation state 0 with a d^{10}-configuration, which favours a linear coordination of the ligands. The 2/3 occupation of the anion positions in a perovskite structure might result in a superstructure, caused by ordering of the PdH_2 dumb-bells.

Since we could not find any reflections caused by a superstructure we assumed either a statistical arrangement of the PdH_2 dumb-bells or dynamical disorder. A dynamical behavior should cause a transition to an ordered phase at low

temperature as it is found in other hydrides[2]. However, the neutron diffraction experiments at 10 K showed an identical diffraction pattern to that found at room temperature. Therefore, a statistical distribution of the hydrogen atoms on the anion positions in the perovskite-type structure is assumed.

1) Bronger, W., Jansen, K. and Müller, P. (1990). Journal Less Comm. Met., in press.

2) Bronger, W., Auffermann, G. and Müller, P. (1988). Journal Less Comm. Met. 142, 243.

Table 1.1.11. Parameters for $CaPdH_2$ and $CaPdD_2$ (space group P m 3 m) (n = number of reflections; PPD = occupation parameter for D)

		X-ray $CaPdH_2$	Neutron diffraction $CaPdD_2$	
T	[K]	295	295	10
λ	[Å]	1.54051	2.014	2.014
n		10	6	6
a	[Å]	3.690(1)	3.687(2)	3.683(1)
Pd in		(0 0 0)	(0 0 0)	(0 0 0)
B_{Pd}	[Å^2]	0.7(5)		
Ca in		(1/2 1/2 1/2)	(1/2 1/2 1/2)	(1/2 1/2 1/2)
B_{ca}	[Å^2]	0.8(6)		
D in			(0 0 1/2)	(0 0 1/2)
$B_{overall}$	[Å^2]		4.4(1.6)	7.3(2.1)
PPD			0.667	0.667
R-value		0.066	0.052	0.066

1.1.12. Structural investigations of lithiated chromium oxides and of perovskite-type oxides

(P. Norby (University of Odense, Denmark), A. Nørlund Christensen (University of Aarhus, Denmark) and B. Lebech)

Chromium oxides with composition MCr_3O_8, (M = Li, Na, K) are of interest as potential cathode materials in lithium batteries[1]. KCr_3O_8 and $NaCr_3O_8$ are isostructural having a layer-like structure. The structure consists of octahedrally coordinated Cr(III) linked together by single chromate groups (Cr(VI)) to form sheets. The layers are held together by the Na- and K-ions. Lithium insertion and de-insertion are to a certain extent possible both chemically and electrochemically[1] without notable structural changes. Thus the insertion reaction is suggested to involve reduction of Cr(VI) to lower oxidation states (V and IV), while retaining the tetrahedral oxygen coordination.

Neutron powder diffraction of the starting material ($NaCr_3O_8$ and KCr_3O_8) and of chemically lithiated compounds ($Li_1NaCr_3O_8$ and $Li_1KCr_3O_8$) were performed in order to:

1) Refine the structure of $NaCr_3O_8$.
2) Determine the position of the inserted lithium ions and determine its oxygen coordination.
3) Investigate the Cr-O distances in the CrO_4-tetrahedra, which are reflecting the oxidation state of the chromium atom.

The refinement of the crystal structure of $NaCr_3O_8$ confirmed that the material is isostructural with KCr_3O_8, but the oxygen coordination around sodium is octahedral instead of the ten-fold coordination around the bigger potassium cation. The Cr-O bond distances in the CrO_4-tetrahedra show variations which indicate a change in oxidation state of the chromium atoms.

Refinement of the structures of a number of oxides with perovskite and related structure types were performed in order to investigate the influence of chemical composition on the structure and the superconducting properties. The oxides synthesized and investigated thus covered a broad range in chemical composition: $La_{1.8}Ba_{0.2}CuO_4$, $La_{1.9}Ca_{0.1}CuO_4$, $La_2Ni_{0.5}Cu_{0.5}O_4$, $La_2Zn_{0.2}Cu_{0.8}O_4$, $HoSrBaCu_3O_7$, $NdSrBaCu_3O_7$, $LaSrBaCu_3O_7$, $NdCaBaCu_3O_7$, $LaCaBaCu_3O_7$.

1) Koksbang, R., Fauteux, D., Norby, P. and Nielsen, K.A. (1989). J. Electrochem. Soc. **136**, 598.

1.1.13. Investigation of compounds with very short hydrogen bonds

(N. Kalsbeek*, S. Larsen*, B. Lebech, K. Schaumburg* (*University of Copenhagen, Denmark) and M. H. Nielsen (University of Aarhus, Denmark)

A study of compounds containing very short O-H-O hydrogen bonds has been initiated. The study combines diffraction techniques (x-rays and neutrons) with solid state NMR experiments in order to determine the proton positions.

Very short hydrogen bonds are characterised by O-O distances of 2.4-2.6 Å and anomalously broad O-H stretching bands below 1600 cm^{-1} in the infrared spectrum. These bonds may either be symmetric, with the proton situated between the two oxygen atoms, or asymmetric, with the proton associated specifically with one of the oxygen atoms. Generally, the symmetric coordination is the most probable for short O-O distances. The symmetric hydrogen bond may either be truly symmetric, i.e. the hydrogen atom may be placed exactly between the oxygen atoms, or there may be statistical or dynamical disorder of the proton position, i.e. the proton oscillates around the centre position between the oxygen atoms of the O-H-O bond. In the former case the potential energy has a single minimum, in the latter case the potential energy has a double minimum.

The selected compounds are acid salts of malonic acid and succinic acid. Crystal growth of a number of salts containing alkali metals and aliphatic amines as cations has been attempted using H_2O and D_2O. So far seven salts have been crystallized in a size adequate for diffraction studies. Studies of these crystals have shown that six compounds ($KDC_3H_2O_4$, $NaDC_4H_4O_4$, $KHC_4H_4O_4$, $CH_3NH_3HC_4H_4O_4$, $((CH_3)_2NH_2HC_4H_4O_4$ and $(C_2H_5)_2NH_2HC_4H_4O_4$) contain very short symmetric hydrogen bonds (2.4295-2.4612 Å) binding the anions in long chains. The hydrogen bond in the seventh compound ($NaHC_3H_2O_4$) is longer (2.5547 Å) and asymmetric.

For the non-deuterated compounds with symmetric bonds the x-ray diffraction results indicate that the O-H-O bonds are not truly symmetric, but rather disordered around the centre position (statistically or dynamically). Crystals of the deuterated salts are used for the neutron diffraction studies which give more precise information about the proton position. So far a set of room temperature neutron diffraction 4-circle data has been collected for one deuterated crystal ($NaDC_4H_4O_4$) and the data analysis is in progress. Data collection on a second crystal ($NaDC_3H_2O_4$) is initiated.

1.1.14. Reverse Monte Carlo analysis of powder neutron diffraction data: Structural disorder in AgBr

(D.A. Keen*, R.L. McGreevy*, W. Hayes* (*Clarendon Laboratory, Oxford OX1 3PU, U.K.) and K.N. Clausen)

AgBr is a fast ion conductor at elevated temperatures. The ionic conductivity increases anomalously as the melting temperature is approached (T_m = 701 K). Just below T_m the Ag^+ ion conductivity reaches approximately 1 $(\Omega cm)^{-1}$, and the lattice is highly disordered. A neutron powder pattern from such a system exhibits both Bragg peaks and strong diffuse scattering. In a conventional analysis these two contributions are analysed separately. The new Reverse Monte Carlo (RMC) technique models the complete structure factor, i.e. Bragg and diffuse scattering simultaneously.

The RMC method uses a configuration cell with N atoms in a box with sides L and periodic boundary conditions. The atoms are moved randomly one at a time. After each attempted move the radial distribution function $G_c(r)$ is calculated and compared to the experimentally observed $G_e(r)$. A move is accepted/rejected using a test based on the assumption that the difference between the calculated and experimental G(r) at each r follows a normal probability function.

The powder spectrum from AgBr at 669 K has been measured on the D20 diffractometer at the ILL Grenoble, using an incident wavelength of 0.92 Å. The pattern has been analysed by RMC using a configuration cell of 16^3 unit cells (L = 16a, i.e. 32768 atoms). With this size of cell comparison between observed and calculated G(r) could be taken out to R = 8a ≈ 40 Å. As initial configuration the f.c.c. lattice was used.

The converged configuration cell is an instantaneous three dimensional representation of the ion positions, i.e. site occupancy factors and mean square displacements (m.s.d.) of atoms from the regular sites can be calculated without any assumptions for the distribution of m.s.d. The resulting m.s.d.'s along the high symmetry directions are shown in the following table:

Direction	Ag^+ (Å^2)	Br^- (Å^2)
<100>	0.15	0.13
<110>	0.19	0.14
<111>	0.32	0.14

The Br^- distribution is isotropic, but the Ag^+ distribution is enhanced along the <111> direction with some density in the (1/4 1/4 1/4) interstitial site.

The confidence in the RMC analysis can be substantiated by comparing the diffuse scattering calculated from the

configuration (left hand figure) with the diffuse scattering measured on a single crystal at 669 K (right hand figure). The diffuse (1 −1 0) contour diagram was measured at TAS 6, using an incident wavelength of 2.02 Å.

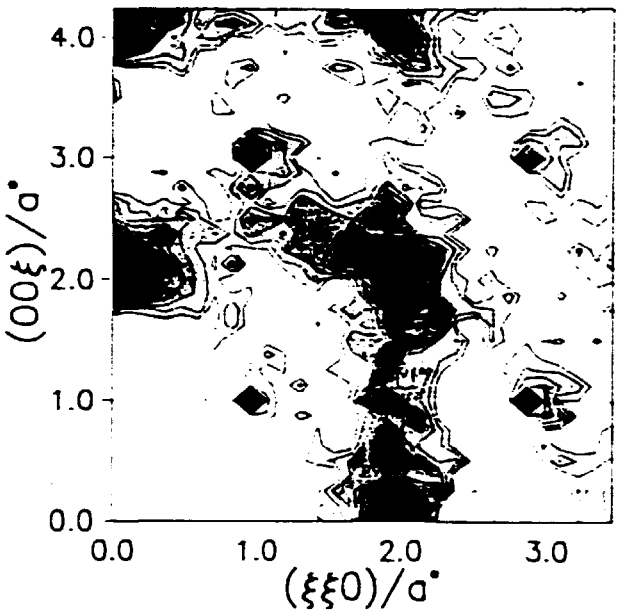

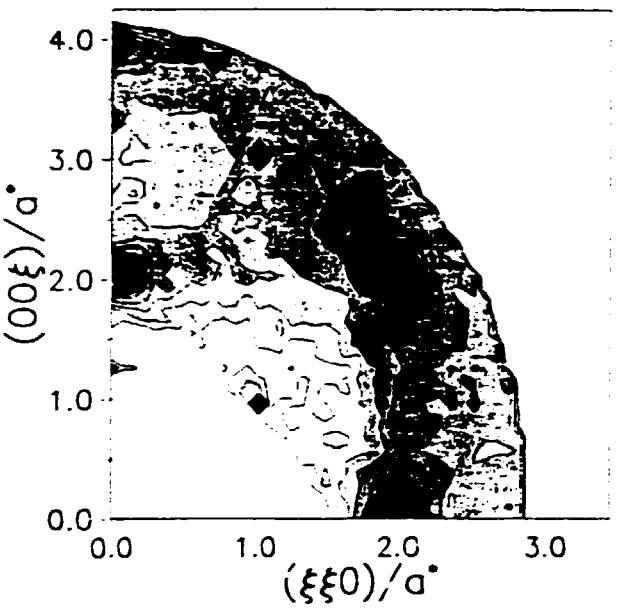

1.1.15. Kinetics of domain growth for model system for Martensitic transformation

(P.-A. Lindgård and T. Castán (University of Barcelona, Spain))

The domain growth after a quench to very low, finite temperatures T has been analysed by scaling theory and Monte Carlo simulation. The growth exponent for the excess energy $\Delta E(t) \sim t^{-n}$ was found to be $n \sim 1/4$. However, for quenches to higher temperatures a clear cross-over to $n = 1/2$ is found (see figure). The scaling theory for low T gives exactly $n = 1/4$ for cases of hierarchical movement of domain walls. This explains the existence of a slow growth universality class. It is shown to be a singular Allen-Cahn class, to which belongs systems with domain walls of both exactly zero and finite curvature. The model studied has continous variables, non-conserved order parameter and two kinds of domain walls: sharp, straight stacking faults and broad, curved soliton-like walls. The cross-over to the Allan-Cahn exponent $n = 1/2$ at higher temperatures is in agreement with similar studies by Mouritsen and Præstgård[1].

1) Mouritsen, O.G. and Præstgård, E. (1988). Phys. Rev. B38, 2703.

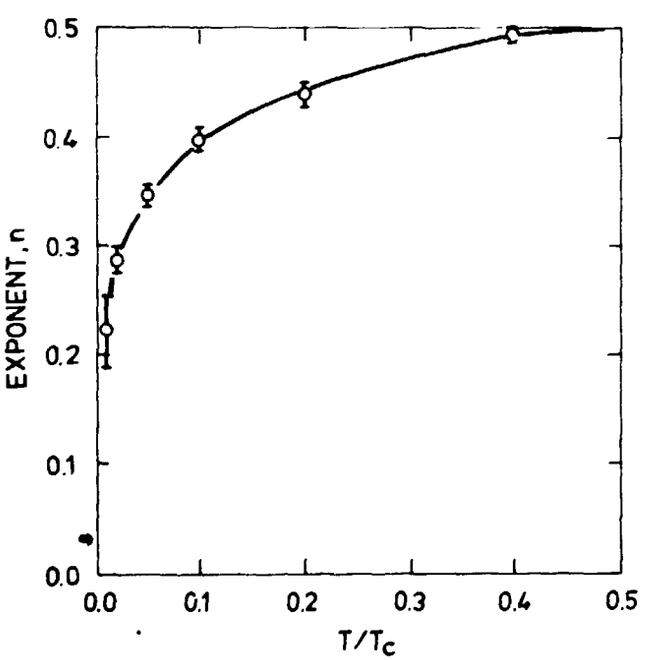

1.1.16. Homogeneous nucleated annihilation of the 2q-phase in $Cu_{.78}Pd_{.22}$

(J. Bohr, D. Broddin* and A. Loiseau*
(*University of Antwerp, Belgium))

The kinetics of the phase transition in $Cu_{.78}Pd_{.22}$ from the two-dimensional long period structure to the one dimensional (2q to 1q) has been investigated by time-resolved x-ray scattering. Over two-and-a-half decades an exponential decay law is accurately obeyed. Model considerations of bulk and interfacial annihilation at the 1q-2q interface shows that the annihilation is a bulk proces and not driven by the 1q-2q interface. Because of the finite difference in the free energy of the 1q and 2q phases, mean field theory predicts that the annihilation shall be exponential. However, due to the anti-phase nature of domain walls, the annihilation of the 2q phase cannot be homogeneous on an atomic scale but must require the simultaneous dissociation of two domain walls. To understand the time behavior, it is therefore necessary to take into account the topology of the structure. A topological defect is needed in the mesh of domain walls if the annihilation takes place by local rearrangements of atoms. The data can be explained by a two stage model involving nucleation of topological defects and the subsequent motion of these.

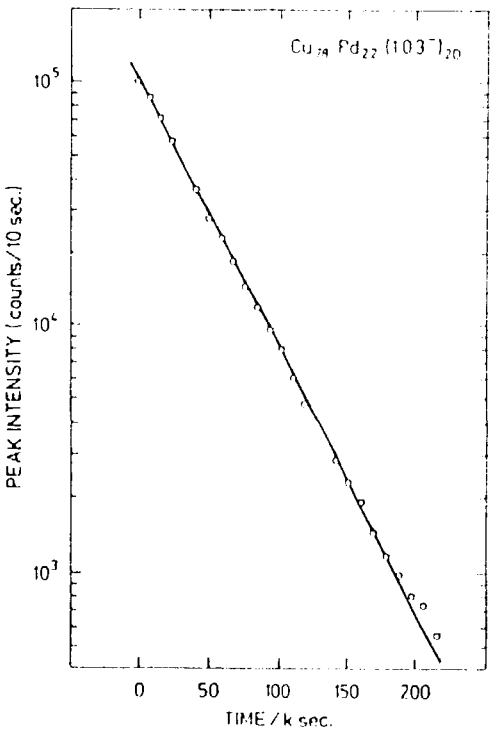

A single logarithmic plot of the background subtracted peak intensity versus time. The straight line is the best fit to the data by an exponential decay law.

1.1.17. X-ray diffraction studies of the magnetic state of thulium

(J. Bohr, D. Gibbs* and K. Huang*
(*Brookhaven National Laboratory, Upton, U.S.A.))

X-ray diffraction has been applied to investigate the magnetic structure of thulium. In addition to magnetic scattering at q, charge scattering is observed at 2q and 4q. A high-resolution study of the temperature dependence of the wavelength of the 2q modulation showed two regimes: one incommensurate and the other commensurate. An analysis of the charge scattering at 2q shows that the ordering transition is continuous. The magnetic states of thulium were also probed by a resonance study of the magnetic scattering at the fundamental wave vector. Near the L_{III} absorption edge, an enhancement of the magnetic scattering of approximately 50 was observed. The results of polarization analysis of the magnetic scattering shows that it is entirely rotated. This agrees with simple one-electron multipole scattering.

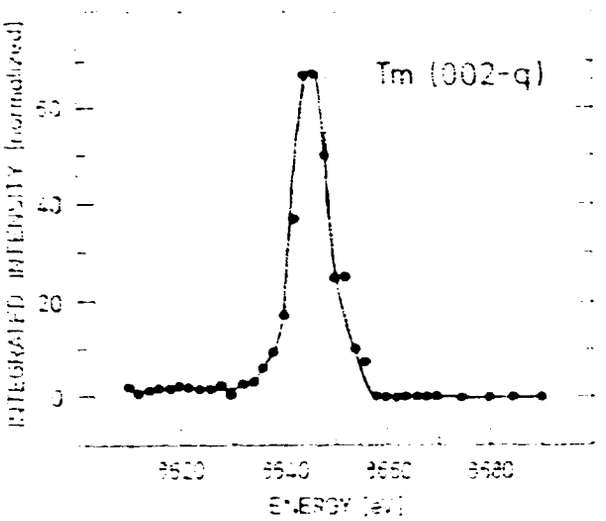

The resonance enhancement of the integrated intensity at the (0 0 2-q) magnetic satellite as a function of energy. A subsequent polarization analysis showed that the signal is rotated, i.e. with π polarization. No scattering with the σ polarization was observed at q.

1.1.18. Superheating and supercooling of lead precipitates in aluminum

(L. Gråbæk, J. Bohr, E. Johnson, H.H. Andersen*, A. Johansen* and L.M. Sarholt-Kristensen* (*University of Copenhagen, Denmark))*

Small precipitates of lead formed in an aluminum single crystal after ion implantation have been studied by x-ray diffraction at the rotating anode in the Physics Department at Risø. These insoluble precipitates offer a unique model system in which the melting transformation can be studied reversibly, or non-destructively. The formed precipitates grow during annealing from a mean size of 140 Å to a mean size of 270 Å. This is determined from the decrease of the width of the (111) reflection originating from the precipitates. In our study we have observed super-heating and super-cooling of the lead precipitates (see the figure). The narrowing of the hysteresis loop between the melting and solidification transition, observed from the first to the third temperature cycle, is closely connected with the growth of the precipitates during the annealing in the previous temperature cycles.

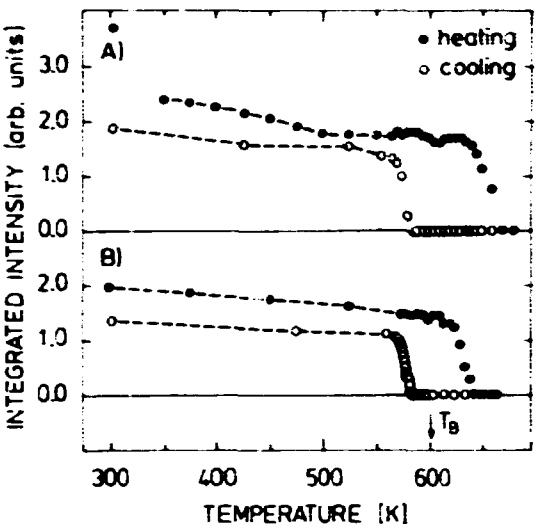

The figure shows the integrated intensity as a function of temperature for the first A) and third B) temperature sequences. Filled and open circles represent data obtained during heating and cooling, respectively. The arrow T_B marks the bulk melting point of lead (601 K). In the first heating sequence, superheating prevails to 67 K above T_B and solidification begins 21 K below T_B. In the third heating sequence, superheating prevails to 44 K above T_B and solidification begins 18 K below the bulk melting point.

1.1.19. Structure of Pb/Si(1 1 1)7×7

(F. Grey, R. Feidenhans'l, M. Nielsen and R.L. Johnson (University of Hamburg, F.R.G.))

The clean Si(1 1 1) surface is known to have a 7×7 reconstruction involving a stacking-faulted bilayer of Si atoms[1]. Upon deposition of Pb at room temperature, the diffraction pattern, as observed with low-energy electron diffraction, changes: strong reflections appear just outside the main hexagonal Si (1 0)-type reflections, and have been attributed to an incommensurate Pb layer which has its main axes aligned parallel with those of the Si substrate[2].

We have studied Pb/Si(111) by surface x-ray diffraction at the Wiggler beamline W1 at HASYLAB in Hamburg. We find that the strong reflection is in fact at the commensurate position (8/7 0), and all other observed reflections can be indexed in terms of a 7×7 unit cell. In other words, the size of the surface unit cell is preserved on Pb deposition, but the intensities of the reflections change greatly, reflecting a change of structure within the unit cell.

We have measured 97 symmetry inequivalent structure factor intensities. A Fourier transform of the data gives directly the electron density autocorrelation function, which is shown in the figure for a 7×7 unit cell. The figure

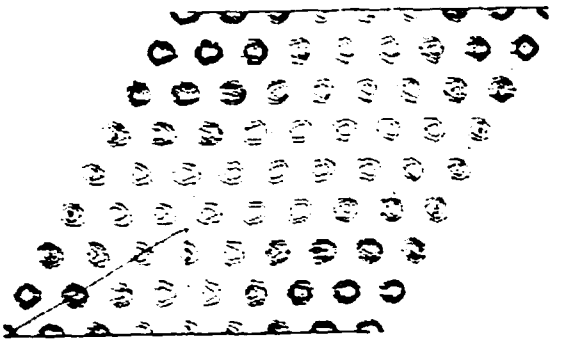

Contour plot of electron density autocorrelation function for Pb/Si(1 1 1)7×7. The dashed lines show underlying 1×1 unit cells. The 8×8 mesh of atoms is apparent.

suggests an 8×8 mesh of Pb atoms within the 7×7 unit cell. Such a simple dense-packed Pb structure is compressed 5% relative to bulk Pb.

Least-squares refinement of this model leads to in-plane relaxations of the Pb atoms, with those near the centre of the unit cell moving apart, adopting interatomic separations closer to that in bulk Pb. Allowing the occupation of the atoms to vary, we find that the Pb atom at the corner is absent, and its nearest neighbours have partial occupation (50%) indicating disorder in the structure.

1) I. K.Robinson, W. K.Waskiewicz, P.H. Fuoss, and L.J. Norton, Phys. Rev. B37, 4325(1988)
2) P. J. Estrup and J. Morrison, Surf. Sci. 2, 465 (1964).

1.1.20. Structure and melting of the incommensurate phase of Pb/Si(111)

(F. Grey, R. Feidenhans'l, M. Nielsen and R.L. Johnson (University of Hamburg, F.R.G.))

Upon adsorption of Pb on Si(1 1 1) and annealing at 120°C or higher, Pb forms a close-packed phase with the principal axes of the Pb layer rotated 30° relative to those of the Si substrate. This epitaxy is similar to that of the $\sqrt{3}\times\sqrt{3}$R30° phase of Pb/Ge(1 1 1), except that on Si(1 1 1), the Pb structure is incommensurate, because of the larger lattice mismatch (5% on Si versus 1% on Ge).

We have studied the incommensurate structure as a function of temperature. Results of radial scans of the $(1\ 0)_i$ reflection are summarized in the figures.

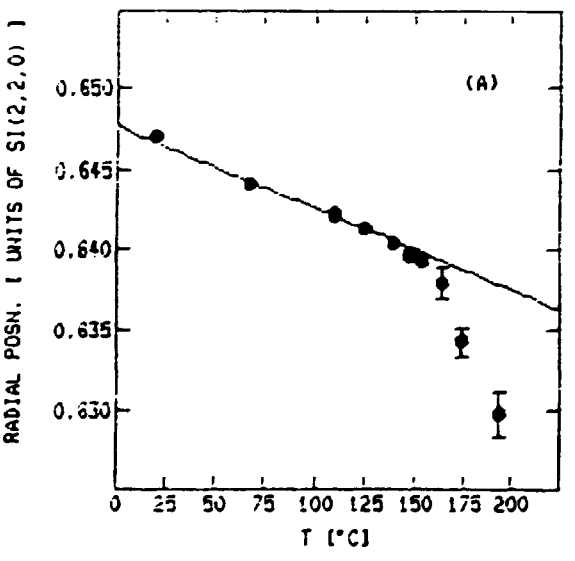

Fig. A. Position of $(1\ 0)_i$ reflection in units of Si(2,2,0) = 3.27 Å^{-1}.

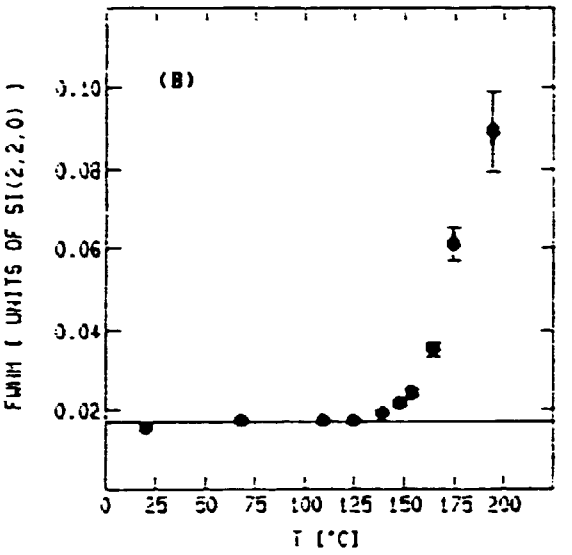

Fig. B. FWHM of the $(1\ 0)_i$ reflection.

Below about 150°C the layer expands linearly with T, the commensurate position being 0.667 in Fig. a. The full width at half maximum (FWHM) is roughly constant in this range (Fig. b). The expansion coefficient deduced from the measurements below 150°C is $1.0\pm 0.1\times 10^{-4}$, compared with the linear thermal expansion coefficient of bulk Pb, 0.3×10^{-4}. Above 150°C, the layer expands more rapidly and the FWHM diverges. We interpret this to be a melting transition. The reflection diverges also in the azimuthal direction. At 195°C we observe modulated ring-like scattering, similar to that seen for Pb/Ge(1 1 1) at high temperatures, which is characterisitic of a 2D liquid on a periodic substrate.

1.1.21. The structure of Au monolayers on the Si(111) surface

(R. Feidenhans'l, F. Grey, M. Nielsen, R.L. Johnson (University of Hamburg, F.R.G.) and D. Degenhardt (HASYLAB, Hamburg, F.R.G.)

We have pursued our studies of the atomic structures of monolayers of Au on the Si(111) surface. After deposition of 0.4 monolayer (ML) of Au the surface shows a 5×1 LEED pattern; at 1 ML of Au the structure has changed into $\sqrt{3}\times\sqrt{3}R30°$ and finally at 1.5 ML the structure is 6×6. At intermediate coverages, the LEED pattern shows mixed phases and/or disorder. Our task is to determine the atomic geometry of each of the three structures and to explain the origin of the disorder at intermediate coverages. For each structure we collect integrated intensities for in-plane reflections. Data for the 5×1 and the $\sqrt{3}$ structure were collected in 1988, in 1989 we have made a more precise data set of the $\sqrt{3}$ structure and also measured a set for the 6×6 structure.

The 5×1 structure is quite complex. A contour plot of the Patterson function is shown in figure 1a. Because Au is a stronger scatterer for x-rays than Si, the strong peaks in the plot must correspond to Au-Au interatomic vectors. One conclusion can immediately be made because no Au-Au vector corresponds to

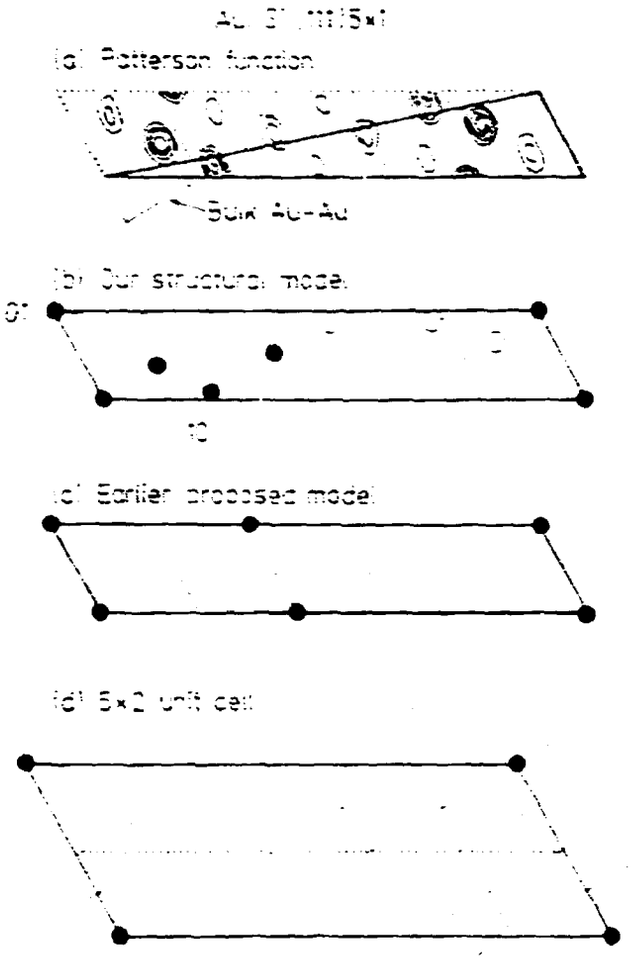

Fig. 1. Au Si(111)5×1:
(a) A contour map of the Patterson function. The origin rises 10 contour levels. The triangle is the irreducible unit.
(b) Our model for the Au-structure in the projected 5×1 unit cell. The atoms indicated with full circles have full occupancy, the atoms with open circles have partial occupancy.
(c) The model for the Au-atoms as proposed by Huang and Williams.
(d) A 5×2 unit cell. Note the 5×2 unit cell breaks the mirror line (dashed) from the Si bulk, whereas the 5×1 unit cell does not.

the bulk Si interatomic vector: the Au atoms are not residing on high-symmetry sites on the surface. A structural model describing the data reasonably well is shown in figure 1b. The sharp reflections belonging to the 5×1 structure are accompanied by streaks of intensity running thr ugh the half-order positions. They were first observed by LEED, the explanation for them being that the structure is not 5×1 but a random mixture of rows of 5×2 and c(10×2) unit cells. A 5×2 (or a c(10×2)) unit cell, however, is forced to break the mirror symmetry of the underlying bulk (see figure 1). This explains the anomalously large Debye-Waller factors necessary to get a good fit of the model in figure 1b. The structure shown is a projection of the two 5×1 sub-units of the 5×2 cell into one 5×1 cell. The real atomic structure must then be obtained by transforming the atoms in figure 1b back into a 5×2 cell. On basis of the present d· · set we are not able to do this.

The √3 structure is much simpler. It consists basically of a trimer of Au-atoms with a Au-Au interatomic distance close to that of bulk Au and a relaxed Si layer. In order to obtain a satisfactory fit to the data, it is necessary to partly occupy the positions inside the trimer. It is unlikely that Si-atoms occupy all these sites since the resulting interatomic distances would be very short. It might be that the partly occupied positions are precursors of the 6×6 structure.

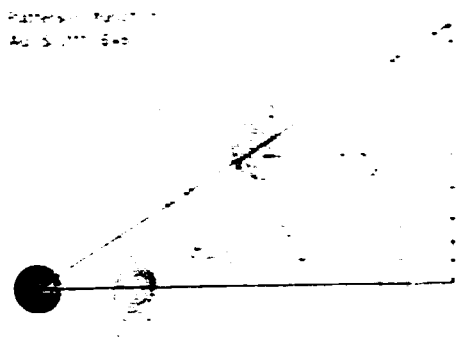

Fig. 2. Patterson map for Au/Si(111)6×6. The origin rises 10 contour levels.

The Patterson plot for the 6×6 structure is shown in figure 2. The two main peaks are similar to those in the √3 structure. Peak 1 is the same as the interatomic vector in the trimer, whereas peak 2 is the vector connecting one √3 cell to the next, but slightly longer. The 6×6 structure might therefore be a super-structure of the √3 structure, however, we have not been able to pinpoint in detail the atomic positions of the Au atoms.

1.1.22. Investigation of the Ag/Ge(111) surface

(R. Feidenhans'l, F. Grey, R.L. Johnson (University of Hamburg, F.R.G.), G. LeLay (University of Marseilles, France), I. Robinson (AT&T Bell Laboratories, Murray Hill, New Jersey, U.S.A.) and M. Nielsen)

Depositing one monolayer of Ag on the Ge(111) surfaces makes a $\sqrt{3}\times\sqrt{3}$ R30° structure, as for Au/Si(111) (see 1.1.21). The difference in scattering amplitude between Au and Si makes it difficult to determine the positions of the Si atoms in the $\sqrt{3}$ structure. If the Ag/Ge(111)-$\sqrt{3}$ were isomorphic to Au/Si(111)-$\sqrt{3}$, this difficulty could be overcome. We therefore made a crystallographic investigation of the Ag/Ge(111)$\sqrt{3}$ structure. We collected in-plane integrated intensities for 13 inequivalent reflections. One feature of the data set was immediately striking. The intensity of the (4/3 1/3) reflection was about 50 times stronger than any other reflection we measured. This means that the structure is considerably different from Au/Si(111), and has essentially only one Fourier component.

We have not been able to find a simple two-dimensional model that can account for the Ag/Ge(111)$\sqrt{3}$ data: the trimer model of Au/Si(111) fails. The structure may involve more than one layer of Ag, since Ag grows on Ge(111) in a layer by layer mode (Frank-van-der-Merwe growth), unlike Au and most other metals which grow by a layer plus island mode (Stranski-Krastanov growth).

We have also studied thicker films of Ag/Ge(111). For ten monolayers deposition we observe Ag growing in parallel epitaxy with the Ge substrate. Somewhat damped multilayer oscillations are observed, indicating a rather uniform film thickness over areas of about 1 mm^2 (the illuminated area of the surface). We have also studied the irreversible coagulation of the film into islands on heating to ~ 120°C.

1.23. The $\sqrt{2}\times\sqrt{2}R45^\circ$ and $c(5\sqrt{2}\times\sqrt{2})R45^\circ$ structures of Pb/Cu(100)

(F. Grey, R. Feidenhans'l, M. Nielsen, R.L. Johnson (University of Hamburg, F.R.G.) and C. Ocal (Autonomous University of Madrid, Spain))

The interatomic distance of bulk Pb, 3.5 Å, is close to the lattice constant of Cu, 3.6 Å. Thus a (100) layer of Pb, rotated 45°, makes good epitaxy with Cu(100).

We have made surface x-ray diffraction measurements of Pb/Cu(100) at the wiggler line W1 at HASYLAB in Hamburg. For the $\sqrt{2}\times\sqrt{2}R45^\circ$ phase, we have measured 14 inequivalent reflections, and find that, indeed, a simple square lattice of Pb atoms, rotated 45° relative to the Cu(100) substrate, fits the data well, with the only adjustable parameter being the Debye-Waller factor.

At higher coverages, Pb forms a $c(5\sqrt{2}\times\sqrt{2})$ structure. Two models have been proposed for this structure, which seem at first to be very different. The first model requires that the simple square mesh of atoms of the $\sqrt{2}\times\sqrt{2}R45^\circ$ phase form a regular array of dense domain walls every third unit cell, in order to accomodate the extra Pb[1]. This model is shown in the figure, with the Pb atoms at the domain walls relaxed from the high-symmetry

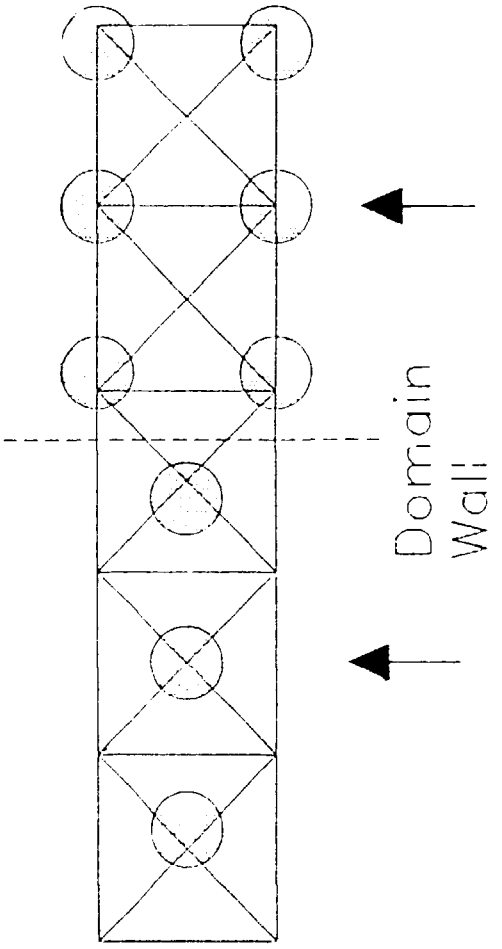

Domain-wall model of Pb/Cu(100) $c(5\sqrt{2}\times\sqrt{2})R45^\circ$. The domain wall is shown (dashed line). The atom rows which must be shifted (0 1/2 1/2) along the arrow direction to obtain the hexagonal model are arrowed.

positions to preserve more equal Pb-Pb distances throughout the unit cell. The second model is a "hexagonal" structure, which is in fact a distorted triangular array of Pb atoms[2].

We have measured 26 inequivalent reflections for the c(5√2×√2) structure. The domain wall model explains qualitatively the main features of the diffraction pattern, provided the atoms at the domain walls are relaxed 0.35 Å away from the walls. However, to obtain good quantitative agreement, it is necessary to assume that about 40% of the surface has the hexagonal structure.

The coexistence of the two structures has a possibly simple explanantion. The hexagonal structure can be formed from the domain-wall structure by simply shifting the two rows marked by arrows in the figure by (0 1/2 1/2) along the arrow direction. This allows the Pb atoms to adopt a close-packed structure (presumably energetically favourable), but places some Pb atoms between Cu(100) adsorption sites (presumably unfavourable). We note that the shift of (0 1/2 1/2) can be described as two cancelling domain walls, and so our results suggest that there are regions on the surface of higher domain-wall density than given by the simple domain-wall model.

1) J. Henrion and G.E. Rhead, Surf. Sci. **29**, 20 (1972).

2) W. Höesler and W. Moritz, Surf. Sci. **175**, 63 (1986).

1.1.24. Oxygen chemisorption on Cu(110)

(R. Feidenhans'l, F. Grey, R.L. Johnson (University of Hamburg, F.R.G.), S.G.J. Mochrie (Massachusetts Institute of Technology, Cambridge, U.S.A.), J. Bohr and M. Nielsen)

The atomic structure of oxygen chemisorbed on the Cu(110) surface has long been a matter of debate. The surface forms a 2×1 reconstruction after exposure to 10 Langmuir (1 Langmuir = 10^{-6} torr sec). This corresponds to a coverage of 0.5 monolayer of atomic oxygen on the surface. It remains controversial whether the copper atoms in the first layer reconstruct into a missing-row structure with every second (001) row missing, and what exactly is the location of the oxygen in the unit cell. We have performed a structural study by x-ray diffraction. To resolve these issues, we have obtained in-plane integrated intensities for fifteen fractional-order and seven integer-order inequivalent reflections. All in-plane, integer-order reflections (non bulk Bragg points) are weak. This is a strong signature of a missing row structure, because the scattering from the crystal truncation rod exactly cancels the scattering from a half-filled copper layer. The scattering observed at the integer-order positions is therefore originating from the oxygen only.

Due to the simplicity of the structure, all in-plane fractional-order structure factors are real and positive. This allows us directly to plot the electron density as shown in the figure. The oxygen atom is positioned in the long-bridge position. Furthermore, as determined from a least-square analysis the second copper layer is slightly relaxed laterally by 0.031 ± 0.005 Å. An analysis of the out-of-plane crystal truncation rods at (h k) = (1 0) and (1 1) shows that the remaining copper atoms in the first layer are displaced outwards by 0.37 ± 0.05 Å relative to the ideally terminated surface and that the oxygen atom is sitting 0.34 ± 17 Å below the first copper layer.

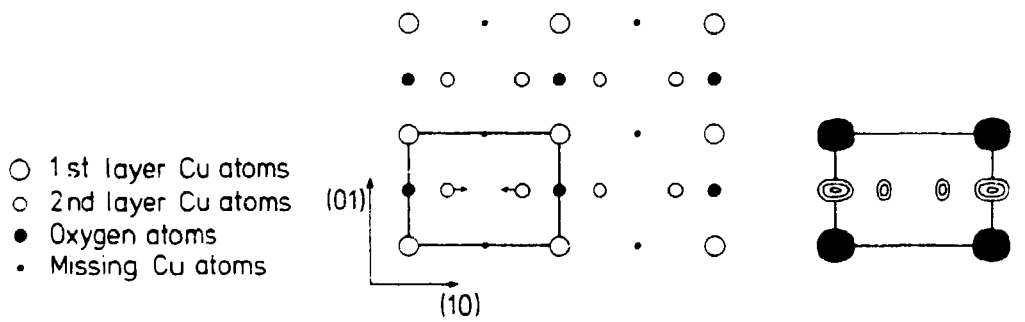

The left side shows a model of the missing row reconstruction. The right side is a contour plot of the electron density

1.1.25. Pressure-, pH- and time-dependence of two-dimensional self-aggregation

(D. Jacquemain*, S. Grayer Wolf*, F. Leveiller*, M. Lahav*, L. Leiserowitz* (*Weizmann Institute, Israel), M. Deutsch (Bar-Ilan University, Israel), K. Kjær and J. Als-Nielsen)

2D-"crystalline" monolayer domains of PFA, CF_3-$(CF_2)_9$-$(CH_2)_2$-OCO-CH_2-$CH(NH_3^+)CO_2^-$ at the air-water interface (with coherence lengths exceeding 1500 Å) were detected for low lateral densities and zero lateral pressure by grazing incidence synchrotron x-ray diffraction (GID) at HASYLAB, DESY, Hamburg.

2D-"crystallinity" was detected for three different regimes: (i) at high pH (pH ≥ 11.2) over aqueous KOH solutions; (ii) over pure water; and (iii) over a subphase containing HCl at pH = 1.5.

(i) At pH ≥ 11.2, the diffraction data are consistent with vertically aligned molecules arranged in a hexagonal net[1]. This molecular arrangement is preserved at all surface pressures upon compression and decompression. The diffracted intensity, as a function of pressure, strongly suggests that all the

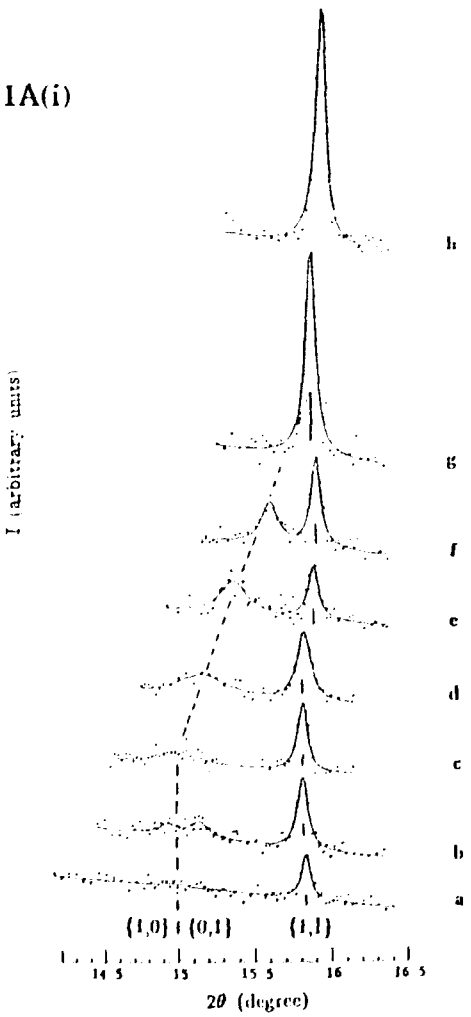

Fig. 1Ai. GID data for PFA on H_2O versus pressure (cf. Fig. 1C). Integrated over $0 \leq Q_z \leq 0.3$ Å^{-1}.

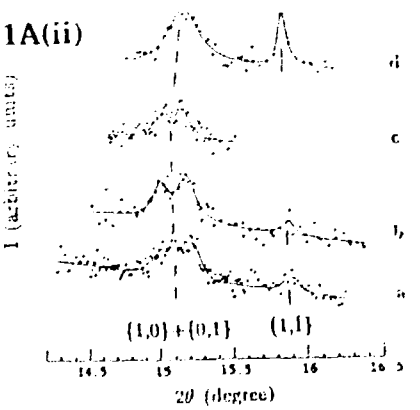

Fig. 1Aii. GID data for PFA on H_2O versus pressure. Integrated over $0.2 \leq Qz \leq 0.5$ Å^{-1}.

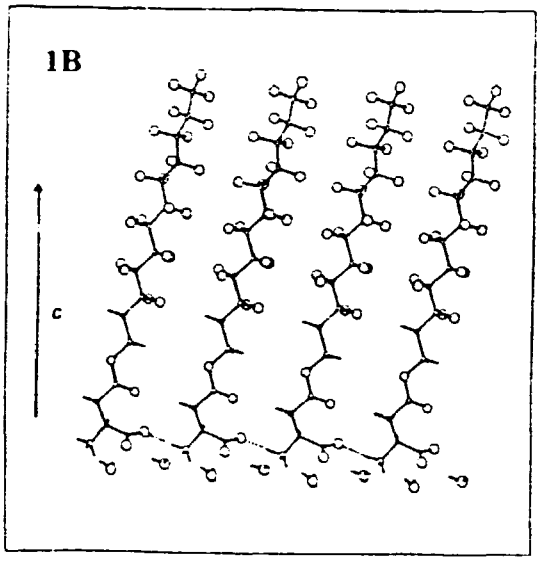

Fig. 1B. Model arrangement of PFA molecules in self-aggregated crystallites over pure water.

molecules in the uncompressed state are in the crystalline phase.

(ii) Over pure water, in the uncompressed state, three GID peaks were observed (Fig. 1A, a-b) indicating an oblique cell. The Bragg rods (not shown) are consistent with tilted molecules[1], cf. Fig. 1B. Upon compression the three peaks coalesce (Fig. 1A); the resulting cell is hexagonal with the molecules standing upright[2]. Upon complete decompression, the diffraction peaks disappear[2], indicating hysteresis.

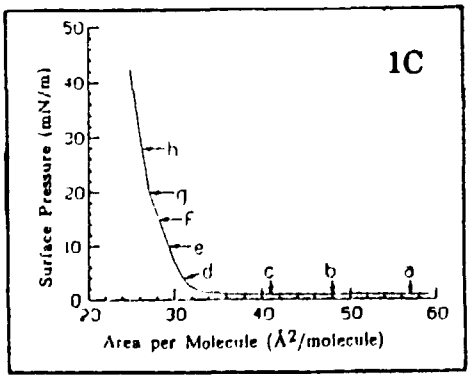

(iii) Over acidic subphases (pH = 1.5), in the uncompressed state, the diffraction data were interpreted in terms of a centered rectangular cell with the PFA molecules tilted from the vertical[1].

The growth of the two-dimensional crystallites of PFA was monitored as a function of time (Fig. 2). Glycine in the water subphase impeded the growth of the crystallites; over pure water the growth was too fast to be observed.

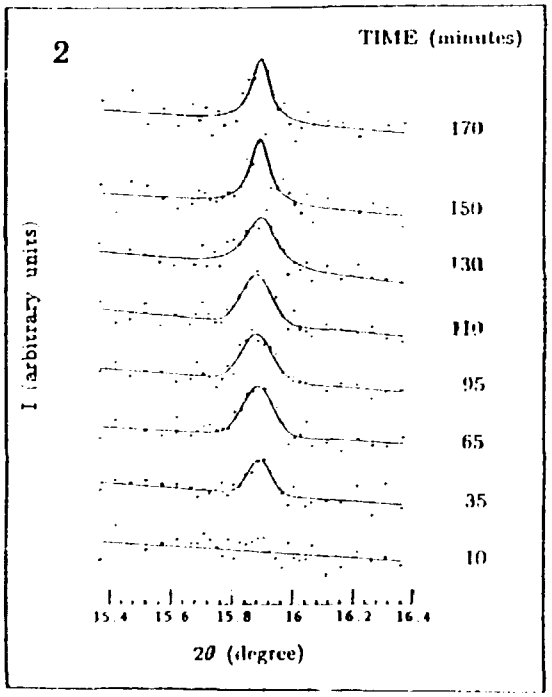

Fig. 2. PFA over glycine subphases (0.015 M) at 45 Å² per molecule, 0 mN/m. GID data ((1 -1) reflection) versus time after spreading.

1) Jacquemain, D., Grayer Wolf, S., Leveiller, F., Lahav, M., Leiserowitz, L., Deutsch, M., Kjaer, K. and Als-Nielsen, J., subm. J. Am. Chem. Soc.

2) Grayer Wolf, S., Deutsch, M., Landau, E.M., Lahav, M., Leiserowitz, L., Kjaer, K. and Als-Nielsen, J. (1988), Science 242, 1286.

1.1.26. Bragg rod scattering from phospho-lipid monolayers

(R. Kenn*, H. Möhwald* (*University of Mainz, F.R.G.), D. Degenhardt (DESY, Hamburg, F.R.G.), J. Als-Nielsen and K. Kjær)

At the air-water interface, monolayers of the phospho-lipid Di-Myristoyl-Phosphatidic-Ethanolamine (DMPE) at 20°C exhibit the pressure versus area isotherm shown in Fig. 1d. Between 75 and ~ 40 Å²/molecule, a fluid and a condensed phase coexist. On approaching 40 Å²/molecule, the lateral pressure π rises steeply, and the positional correlation length of the condensed phase increases, as shown by x-ray grazing incidence diffraction. By resolving the intensity variation *along* the Bragg rods of scattering (perpendicular to the monolayer), the conformation of the diffracting moities can be studied in more detail. At lower pressures (1c and 1b), the intensity peaks at non-zero vertical scattering vector Q_z, indicating uniformly tilted molecules. At high pressure (Fig. 1a), the intensity peaks at $Q_z = 0$, indicating vertical molecules.

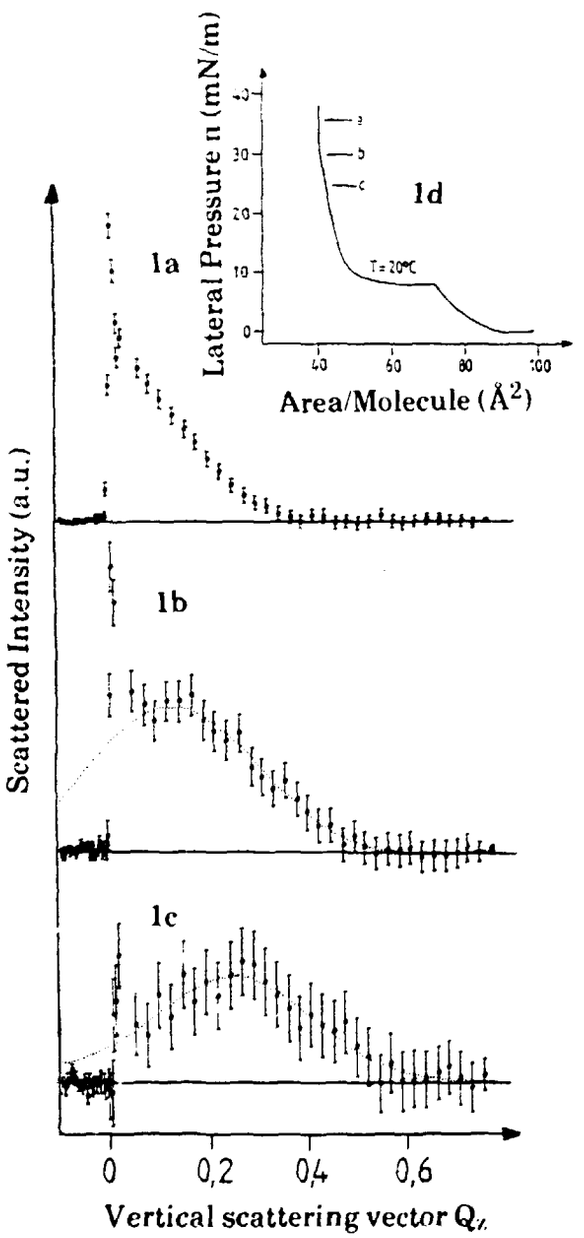

The rod-like character of the scattering is illustrated by the intensity landscape in Fig. 2. The intensity versus Q_{hor} peaks sharply, but it extends in Q_z.

At 6°C, the fluid phase is suppressed, but qualitatively similar results were obtained for the condensed phase.

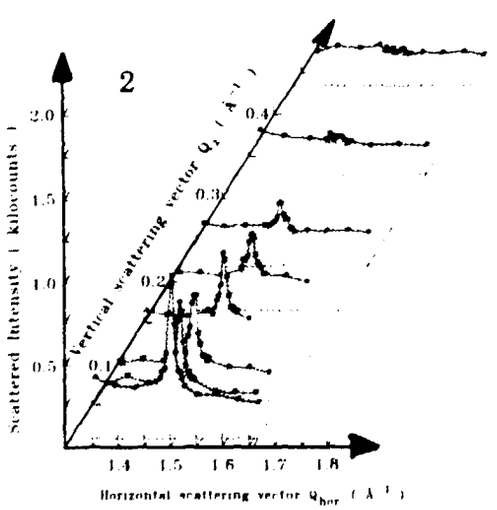

1.1.27. X-ray diffraction studies of behenic acid monolayers on water

(R. Kenn*, C. Böhm*, H. Möhwald* (*University of Mainz), J. Als-Nielsen and K. Kjær)

Behenic acid ($CH_3(CH_2)_{19}COOH$) is a useful model system for surfactant layers on water, since it displays a richness of two-dimensional phases in an easily accessible temperature range. These phases were studied by x-ray diffraction (and reflection) with scattering vector parallel (and perpendicular) to the surface. At all investigated temperatures and pressures the lateral structure was found to be centered rectangular. The data indicate that the molecules assume a uniform orientation with a low kink density. At low lateral pressures they are tilted towards a nearest neighbour molecule, and on compression the tilt angle is continuously reduced. On compression at temperatures > 12°C the pressure/area isotherm (Fig. 1) changes slope at a distinct pressure. This corresponds to a transition from a tilted to an untilted state (Fig. 2a). In both phases the area per molecule is large enough that, presumably, the tails can rotate about their axes and thus be considered as cylinders. At temperatures < 10°C compression of the tilted state leads to zero tilt (Fig. 2b). In this case a first order phase transition occurs with a change in two-dimensional density of order 5%. The resulting phase is distinguished by narrower diffraction peaks indicating a larger positional coherence length. This is assumed to correspond to a crystalline packing of the *methylene groups* as also observed in crystals of alcanes at low temperatures, where the projected molecular area per chain is 18.5±0.1 Å^2. Bragg rod data (not shown) reveals a zero tilt angle for this phase.

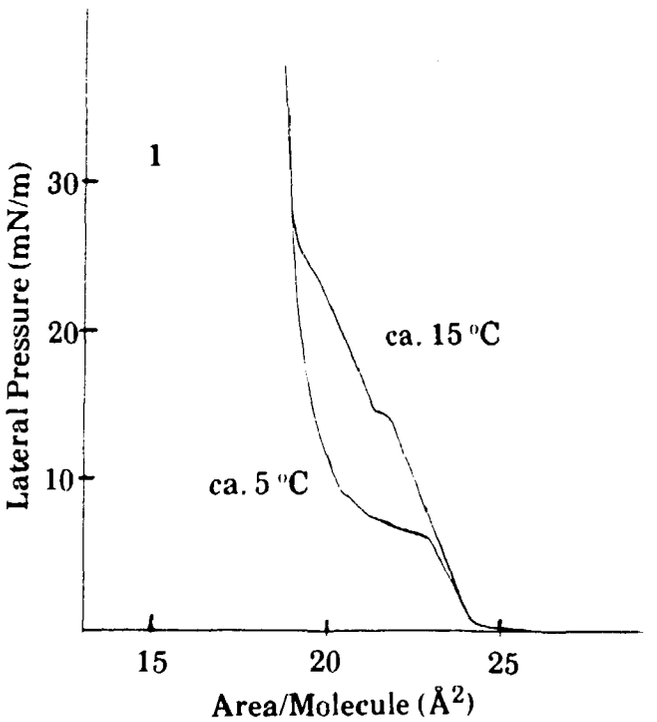

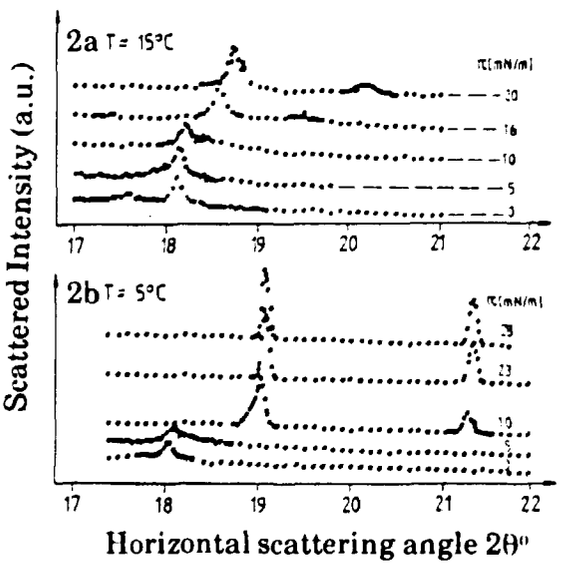

1.1.28. Three-dimensional x-ray diffraction from a quasi-two-dimensional mono-molecular film of a fatty acid

(K. Kjær, J. Als-Nielsen, P. Tippmann-Krayer* and H. Möhwald* (*University of Mainz, F.R.G.))

The structure of Langmuir films (i.e., monolayers at the air-water interface) of Arachidic acid, $CH_3(CH_2)_{18}COOH$, was earlier investigated by means of X-ray Reflection (XR) from the interface (vertical scattering vector **Q**) and Grazing Incidence Diffraction (GID: almost horizontal **Q**).

For a two-dimensional (quasi-)periodic structure, the scattering is concentrated in Bragg Rods instead of spots.The intensity profile along the rod (non-zero horizontal *and* vertical **Q** components) reveals the molecular structure factor. As explained in Fig. 1 the rod profile is quite sensitive to the orientation of these linear molecules.

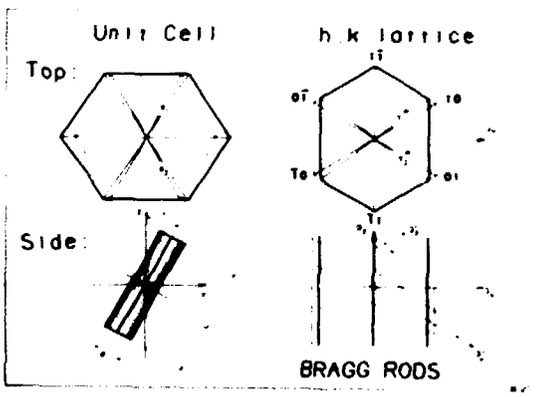

Fig. 1. The molecule is represented by a cylinder. At high surface pressures a hexagonal lattice is formed (broken lines). At lower pressures the molecules tilt and the unit cell is distorted (full lines). Lower right: Bragg Rods and form factor of a tilted molecule (ellipse).

The results (Fig. 2) confirm in more detail a model already proposed on the basis of XR and GID data: At high surface pressure, the molecules are upright and form a hexagonal lattice. Upon relaxation of pressure, the molecules tilt towards nearest neighbours while remaining in clo- -ntact (Model 1 in Fig. 2).

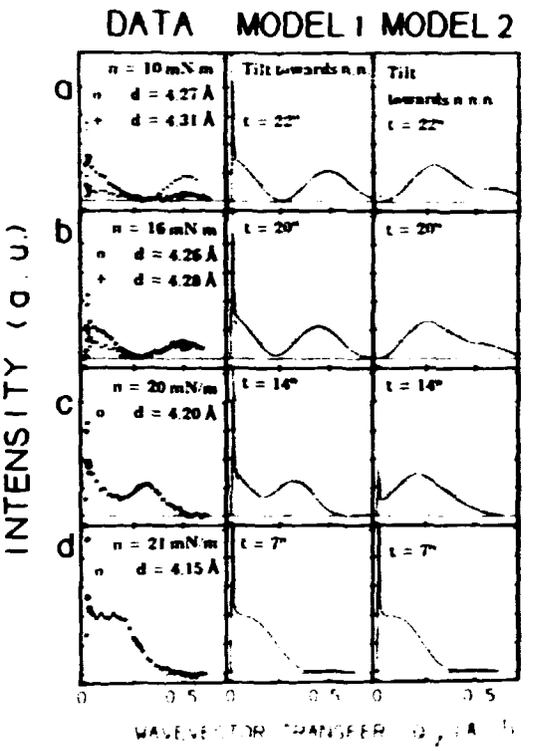

Fig. 2. DATA: Bragg rods for surface pressures of 10, 16, 20, 21 mN/m (a to d). In case c and d the <1 0> and <1 -1> peaks coincide, but in case a and b they split as indicated by open circles and crosses. Model 1: The molecules tilt towards nearest neighbours. Model 2: Tilt towards next nearest neighbours.

1.1.29. Specific heat and thermal conductivity of silica aerogel at low temperatures

(D. Posselt, A. Bernasconi*, T. Sleator*, H.R. Ott* and E. Felder* (*ETH-Hönggerberg, Zürich, Switzerland))

Silica aerogels have thermal properties which are clearly distinct from glasses. First of all the thermal conductivity λ is very low; in the range from 100 mK to 10 K the value is 1-2 orders of magnitude smaller than for amorphous silica, while the specific heat C_p in contrast is ~ 2 orders of magnitude larger. The temperature dependence of the low temperature properties also establish aerogels in a class of their own.

Measurement of the low temperature properties of aerogels is very difficult due to the low thermal conductivity and the low density of the samples (density down to ~ 1/25 of the value for amorphous silica). A dynamic technique based on a generalisation of a thermal relaxation method has been developed especially for aerogel measurements at the Labor für Festkörperphysik, ETH, Zürich. The technique allows the determination of both thermal conductivity and specific heat in a single measurement. The temperature region from 100 mK to 1.5 K is covered using a $^3He/^4He$ dilution cryostat, whereas data in the interval from 1.5-30 K is obtained in a conventional ^4He cryostat. Cooling down in the dilution refrigerator is done without use of exchange gas to avoid contributions to the specific heat from gas adsorbed onto the huge surface of the aerogel.

We have investigated a series of base catalyzed aerogels with densities in the range from 0.10-0.30 g/cm^3. From small angle neutron scattering data we know that the structure of the investigated aerogels can be described in terms of a mass-fractal model within a length scale of 10-100 Å. The dynamical behaviour in the fractal range is described by theory using a 'fracton' concept implying localized vibrational states; i.e. fractons are vibrational modes which are not expected to contribute to the thermal conductivity. The sound velocity in aerogels is very low (~ 10^2 m/s) and correspondingly the relevant temperature range for observation of the fracton regime is expected to be in the range of 100 mK to 1 K given the above length scales.

In accordance with the structural model we do observe three different regimes in the specific heat: At high temperatures the specific heat is approaching that of glass, i.e. the modes excited are particle modes in the amorphous silica units building up the fractal network. Between 0.15 K and 2 K, C_p varies approximately linearly in temperature while at very low temperatures our data indicates the onset of a Debye regime corresponding to travelling phonons in a homogeneous solid. The thermal

conductivity follows a power law, $\lambda \sim T^{\alpha}$, where $\alpha \sim 1.6$, from 3-30 K. At lower temperatures there is a slight upturn in the value of λ, but further evaluation of the data is necessary before we can state the existence of a plateau due to modes which cannot transport heat.

1.1.30. Neutron Brillouin scattering from silica aerogels

(D. Posselt, J. Skov Pedersen, K. Mortensen, J.K. Kjems, H. Mutka* and G. Kearley* (*Institute Laue-Langevin, Grenoble, France))

The vibrations of solids with a fractal mass distribution can be described in terms of fracton theory. So far many experimental techniques have been applied to confirm the application of the fracton concept and most of these experiments have been carried out on fractal silica systems (Cab-O-Sil, aerogel).

Brillouin scattering gives the possibility of direct investigation of the fracton excitations. While Brillouin light scattering covers only a small range in q,ω (see figure), neutrons are ideal for the interesting q,ω range. With a new setup at the instrument IN5, Institute Laue-Langevin, Grenoble, Brillouin neutron scattering has recently become accessible. We have performed experiments on two aerogel samples with different densities, i.e. with highest possible variation of sound velocity within the experimental accessible limits. We measured at two different wavelengths: 10 Å with an energy resolution of 13 μeV and 3 Å with 500 μeV energy resolution. In order to check the temperature dependence of the scattering assigned to inelastic processes we performed the measurements at 300 K and 90 K. The 3 Å measurement was done in order to investigate the inelastic scattering from particle modes in the amorphous silica spheres building up the fractal network.

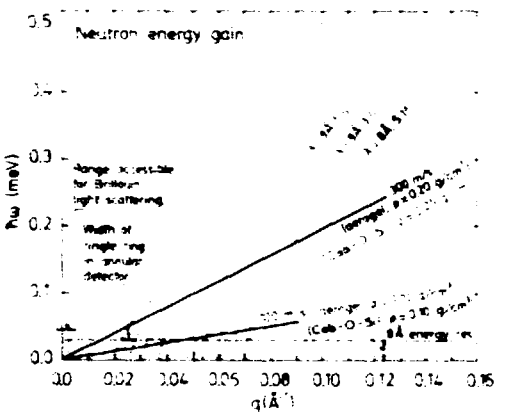

The figure shows extrapolations of the dispersion curves for samples with different densities. The extrapolation is based on values of the sound velocity measured both directly and obtained from Brillouin light scattering. Also shown are the tracks in q, ω space along which time-of-flight data from a single ring on the area sensitive detector are collected.

A huge small angle scattering peak from the aerogel samples together with contributions to the background originating from scattering in the argon filled flight tank made the experiment very difficult. Beforehand we calculated the ratio between the elastic and inelastic count rate to be of the order 10^3 integrated over the whole area sensitive detector; a number which from our data seems to be realistic.

Data processing are in advance and we can so far conclude that if present the inelastic events in both the fracton and particle regime are very broad in energy as well as in scattering vector.

1.1.31. A SAXS study of freeze dried silica gels

(D. Posselt, J. Skov Pedersen, K. Mortensen and E. Degn Egeberg (The Technical University of Denmark, Lyngby. Denmark))

The detailed structure of a silica network made by removing the solvent in the pores of a SiO_2 gel is very sensitive towards parameters characterizing the gel formation, i.e. pH, temperature and aging time, where 'aging' refers to the relaxation of a gel before drying.

We have characterized dried silica gels made by acid catalyzed hydrolysis of $Si(OCH_2CH_3)_4$ diluted by tertiary butanol. The experimental technique used is small angle x-ray scattering (SAXS) performed at the JUSIFA spectrometer, DESY, Hasylab, Hamburg. The investigated gels were aged from 96-864 hours before drying using a freeze drying technique. A typical example of radial averaged data is shown in the figure in a log-log plot of intensity (I) versus q, where q is the scattering vector.

We analyzed the data by fitting to a modified expression for scattering from a fractal mass distribution[1]. A fit to the data is shown in the figure. The modification consists basically in excluding contributions from the basic structural units. If such basic building blocks were present their size would give the lower cut off length for fractal

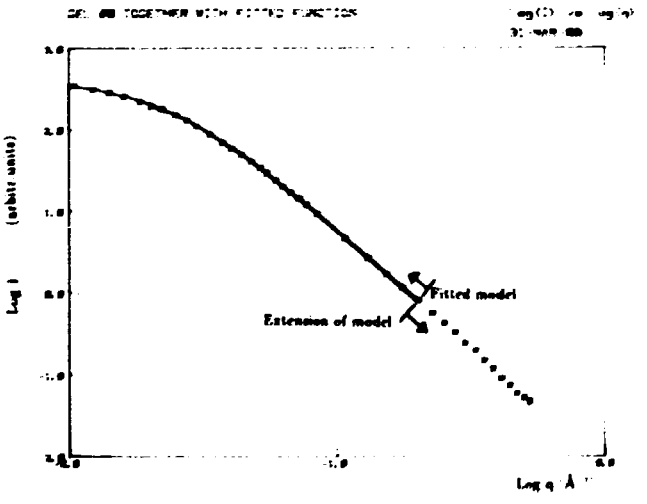

behaviour. We conclude that the network is of a polymeric type rather than

being built from aggregation of basic structural units in consistence with the fact that we do not observe a crossover to a Porod regime ($I \sim q^{-4}$) or surface fractal behaviour ($I \sim q^{-6+D}$, $2 < D < 3$). Our data extends down to a length scale of the order of 5 Å which are to be compared with typical Si-O bond distances of 1.5 Å. That basic particles do not exist in the gel network can be understood from the pH dependence of the reaction rates of the gel forming processes.

On a microscopic level the structure of our freeze dried gels is similar to silica aerogels, which are produced by hyper-critical drying of the wet gel. The fractal dimension d_f is increasing with aging and stabilizes at a value of 2.6 after aging longer than 200 hours. The value of the upper cut off for fractal behaviour is of order 50 Å and decreases as function of aging time. Again a qualitative understanding can be achieved in terms of reaction chemistry.

1) Freltoft, T., Kjems, J.K. and Sinha, S.K. (1986). Phys. Rev. B33, 269.

1.1.32. A SANS study study of solutions of Cab-O-Sil in pentadecane under shear flow

(P. Lindner (Institute Laue-Langevin, Grenoble, France), J. Skov Pedersen and K. Mortensen)

Cab-O-Sil is a commercially available low-density powder of silica aggregates produced by flame hydrolysis of silicon tetrachlorine vapor in a gas of hydrogen and oxygen. A previous small angle scattering study[1] has shown that the structure of the aggregates is a branched network made up of small primary particles having a radius of about 20 Å. In the range from 20 Å to the upper cut-off length scale of 500-1000 Å the structure is a fractal with a dimension of 2.4-2.6.

Cab-O-Sil is used as a thickening agent in many commercially available products like food, paints and other chemical products. When dispersed in a non-hydrogen bonding liquid the Cab-O-Sil gives a viscosity that depends on the shear and stearing history of the sample. The present work concerns the structure of Cab-O-Sil as a thickener in a well-characterized oil, pentadecane. The hydrogen bonds between the hydroxyl groups on the surface of the aggregates are expected to play an important role in processes giving rise to the modification of the viscosity of the solvent. Therefore physisorbed water was removed from the

Cab-O-Sil by annealing the samples at 120°C for 2-3 days before dispersing it in the pentadecane. The samples used in the small angle scattering study contained 5 grams of Cab-O-Sil per 100 ml pentadecane. The samples were allowed to rest for more than one week at room temperature before the scattering experiment.

The new small angle scattering facility at Risø was not fully optimized when the experiment was carried out and therefore the quality of the experimental data do not allow a detailed quantitative analysis. Scattering experiments were performed under laminar flow conditions and at rest using the ILL Couette type shear apparatus[2]. For shear rates of 0, 10 and 100 s^{-1} the scattering curves are identical. At small scattering vectors (0.003-0.016 $Å^{-1}$) the scattering follows a power law with the exponent $D = -1.1 \pm 0.1$. At a shear rate of 1000 s^{-1} the power reduces to $D = -0.86 \pm 0.06$. In the range 0.016-0.053 $Å^{-1}$ the exponent is -2.25 ± 0.05 at all four shear rates. We did not check whether the sample returned to the original scattering curve when having rested after being exposed to the shear rate of 1000 s^{-1}. The samples described above consisted of two phases: a thick one and a more fluid one. We took this as an indication of the Cab-O-Sil being poorly dispersed. Therefore we put the sample in an ultrasonic bath for 12 hours at 80°C. This gave a more gel-like sample. The small angle scattering curves of this sample gave a lower power for small scattering vectors: -1.30 ± 0.05 in the range 0.003-0.016 $Å^{-1}$ for the shear rates 0 and 100 s^{-1}. In the range 0.016-0.053 $Å^{-1}$ the power law was unchanged. After having sheared the sample we observed a tendency for the sample to separate into a thick and a thinner phase similar to the samples that have not been ultra-sonicly treated. However, the power of the scattering curve had the value of -1.30 which is significantly higher than for the non-treated samples. We were not able to detect any anisotropy in the scattering pattern for any of the samples.

1) Freltoft, T., Kjems, J.K. and Sinha, S.K. (1986). Phys. Rev. B33, 269.

2) Lindner, P. and Oberthür, R.C. (1984). Rev. Phys. Appl. 19, 759.

1.1.33. A SANS study of copper containing a high concentration of krypton

(J. Skov Pedersen and M. Eldrup (Metallurgy Department, Risø))

Recent years have shown an increased interest in the properties of rare gas precipitates ("bubbles") in metals. Often such bubbles are produced in a thin layer by ion implantation. The sample used for the present study is remarkable in the sense that it contains 3-4% Kr throughout the bulk of a Cu matrix. The sample was obtained from Harwell, U.K., where it had been produced by a combined implantation and sputtering process developed there[1]. (The original aim was to develop a safe and efficient way to store radio active Kr-85 resulting from nuclear fuel reprocessing). Previous transmission electron microscopy and electron diffraction studies[1,2] have revealed that the krypton forms microscopic bubbles of about 15-20 Å diameter in which the Kr pressure of several GPa is high enough for Kr to be solid even at room temperature. The aim of the present study was to characterize the bubble structure by SANS.

The small angle scattering spectrum has been measured in the range from 0.002 $Å^{-1}$ to 0.5 $Å^{-1}$. For scattering vectors q smaller than 0.050 $Å^{-1}$ the curve follows a power law with the power close to −3.0. At about 0.1 $Å^{-1}$ the curve levels off and for scattering vectors larger than 0.2 $Å^{-1}$ the intensity falls off again. We interpret the scattering for q smaller than 0.05 $Å^{-1}$ to be caused by inhomogenities at the grain boundaries. Similar scattering is observed for a pure polycrystalline annealed Cu sample. The scattering for q larger than 0.1 $Å^{-1}$ is interpreted as arising from the krypton bubbles. An indirect Fourier transformation of this part of the scattering curve using Glatter's method[3] (see 1.1.41) gives a distance distribution function with two significant features: A bubble self-correlation peak with a maximum at 10 Å and a negative correlation extending up to about 50 Å. This shows that the average bubble radius is close to 10 Å and that the bubbles have a separation of the order of 50 Å. If one assumes a close-packed lattice of bubbles with a bubble separation of 50 Å a bubble radius of 10 Å gives a krypton concentration of 4.5 vol.%. Using the lattice constant of 5.2 Å for Kr in the f.c.c. structure determined by electron diffraction[2] and a lattice constant of 3.6 Å for Cu this gives an atomic concentration of 1.7 at.%. This is somewhat low compared to the estimated value of 3-4 at.%. Probably the remaining Kr is contained in small gas-vacancy complexes.

1) Evans, J.H., Williamson, R. and Whitmell, D.S. (1985). In: "Effects of Radiation on Materials: 12th Int. Symp." (STP 870) (edited by F.A. Garner and J.S. Perrin (Philadelphia: American Society for Testing and Materials)), 1225.

2) Evans, J.H. and Mazey, D.J. (1985). J. Phys. F: Met. Phys. 15, p. L1.

3) Glatter, O. (1977). J. Appl. Cryst. 10, 415.

1.1.34. SANS of microstructure in microphase-separated poly-siloxane-imide) segmented copolymers

(R.J. Spontak*, J. Samseth* (*Institute for Energy Technology, Kjeller, Norway) and K. Mortensen)

Poly(siloxane-imide) (PSI) segmented, or multiblock, copolymers constitute a relatively new class of organosiloxane materials which possess desirable properties of each parent homopolymer: Mechanical and chemical stability from the imide component and flexibility and physiological inertness from the siloxane segments. Microphase separation may occur in these materials resulting in the formation of microstructures typically of the same order as the r.m.s. end-to-end distance ($<r^2_D>^{1/2}$) of the domain-forming segment. In traditional diblock and triblock copolymers the microstructural characteristic dimension are controlled by the chain length. In the multiblock PSI copolymers, it has been possible to alter the molecular architecture so that $<r^2_D>^{1/2}$ is varied while both the molecular weight (M_n) and molecular weight distribution (MWD) of the copolymer molecules remain unchanged.

Three PSI copolymers derived from polyetherimide and polydimethyl-siloxane, have been provided by the General Electric Co. Each copolymer is composed of 40 wt.% siloxane and possesses an M_n and a polydispersity index of about 25,000 g/mol and 4, respectively. In the first copolymer (PS11), the degree of polymerization (DP) of the soft and hard segments is approximately 5, while in PS12 the DP is about 3. In PS13 the DP of each segment is statistical, varying along the copolymer backbone. Specimens investigated at Risø National Laboratory were either slow-cooled from the melt state or quenched to below ambient temperature so as to determine the effect of cooling on resultant microstructure.

SANS spectra and integrated intensities clearly revealed interesting features of each copolymer. Scattering patterns from all three prepared according to the slow-cooling and quenching methods, exhibited an isotropic scattering peak. The intensity of this peak did not differ appreciably between slow-cooling and quenching for PS11 and PS12, indicating that the microstructure formed at 230°C was thermodynamically stable. This was not the case with PS13, whose peak upon slow-cooling was sharper than that corresponding to the quick quench. Thus, it was inferred that significant microstructural evolution does occur in this copolymer upon cooling. The peak positions of PS11 and PS13 were nearly equal, suggesting similar size characteristics of the dispersed microphase. The position of the peak in PS12, on the other hand, was observed to occur at a smaller scattering vector, implying a larger dispersed structure.

Funding for this project was provided by the NTNF and the NAVF.

1.1.35. SANS studies of concentrated phases in the AOT-decane-water system

(J. Samseth*, E. Skjetne* (*Institute for Energy Technology, Kjeller, Norway), S.-H. Chen (Massachusetts Institute of Technology, Cambridge, U.S.A.), R. Strey (Max-Planck Institut für Biophysikalische Chemie, Göttingen, F.R.G.) and K. Mortensen)

Three component systems of water, oil and surfactant molecules have for a long time been investigated with small angle neutron scattering. These systems form different phases depending on parameters such as composition, temperature, pressure and salinity. The structure of the simplest systems are simple microemulsion droplets in a matrix of oil (or water). The droplet itself has a water core (or oil core) coated with a monolayer of surfactant molecules. These are referred to as water-in-oil (oil-in-water) micro-emulsions. A surfactant molecule has two distinctive parts, a hydrophilic head group and a hydrophobic tail. This tail is very often a hydrocarbon chain. The investigation of these three component systems have until recently been limited to dilute and dense regions of the phase diagram where the above simple microemulsion picture can be applied.

The purpose of this study is to elucidate the structure in the *ordered* phases in these three component systems. These ordered phases can both be lamellae or liquid crystals. If the SANS spectra show asymmetric scattering patterns, this is evidence for ordering in the sample.

In our experiments we have used AOT as the surfactant and decane as the oil. At temperatures of about 50°C asymmetric scattering patterns were found as shown in the figure below. Further analysis of the data will elucidate more about the actual shape and size of the micelles in the liquid crystals or the lamellae.

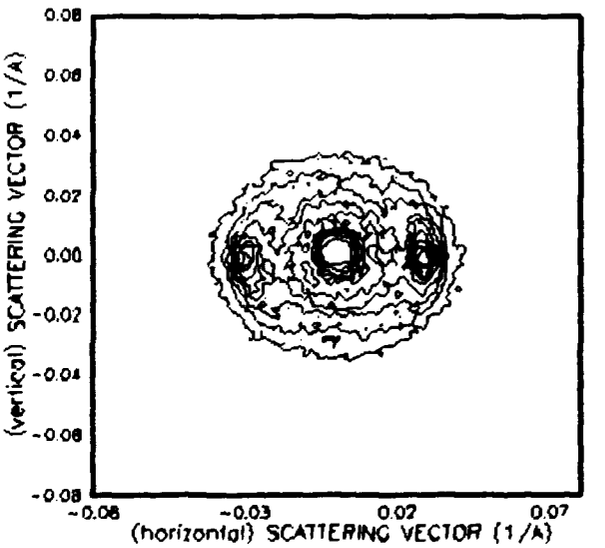

1.1.36. Structure of the membrane protein, clathrin

(S.L. Hansen*, R. Bauer* (*The Royal Veterinary and Agricultural University, Copenhagen, Denmark), T. Særmark (Protein Laboratory, Copenhagen University, Denmark), G. Jones**, M. Beran** (**Daresbury Laboratory, U.K.) and K. Mortensen)

The protein clathrin can by polymerisation form a polygonic structure enwrapping a small bilayer membrane of an approximate radius of 20 nm. These coated micro-vesicles serve the function of transporting specific hormones in and out of a living cell.

We are in the middle of a process of characterising these coated micro-vesicles by small angle x-ray, neutron and static and dynamic light scattering. X-ray scattering performed at the Daresbury Synchrotron Facility on coated micro-vesicles has shown that the structure of the coating protein clathrin is in the form of a polygonic structure (the bump in the figure is related to the polygonic structure of the clathrin polymer). Performing small angle scattering with neutrons has further shown that even the most careful preparation of these coated microvesicles contains higher aggregates and is therefore not monodisperse. This results

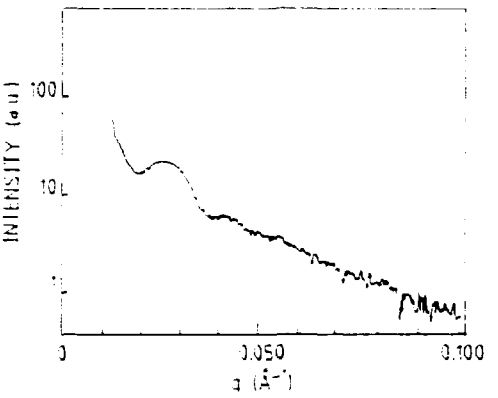

Small angle x-ray scattering results in a semilogarithmic plot of intensity versus scattering vector.

have only been possible because of the improvement in the low q-range accessible at the Risø SANS. However, the sizes of these aggregates have been shown by static light scattering to be so large that it should be possible to extract information at high q-values for the coated micro-vesicles. Extending these measurements in the near future to dynamic light scattering should give valuable information about polydispersity of the coated micro-vesicles.

In the beginning of 1990 it is also planned to do experiments which by contrast variation can determine the general protein-membrane interaction. The joint determination of small angle scattering by light, x-ray and neutrons together with electron micrographic pictures of coated micro-vesicles should make the obtained conclusions more generally applicable.

1.1.37. Anisotropic SANS of RecA-DNA complexes in flow-oriented solution

(B. Nordén*, T. Eriksson*, M. Kubista* (*Chalmers University of Technology, Gothenburg, Sweden), K. Mortensen, B. Sjöberg (University of Gothenburg, Sweden) and M. Takahashi (CNRS, Strasbourg, France))

RecA is a key protein in the general genetic recombination process and its complexes with single-stranded (ss) and double-stranded (ds) DNA's are of fundamental importance to study from both structural and thermodynamical angles. The group at Chalmers were first to stoichiometrically and structurally characterize a number of such complexes using linear dichroism (LD) spectroscopy on solutions subjected to shear in a Couette flow device, made of silica cylinders transparent to ultraviolet light.

Corresponding experiments with SANS at Risø, using a Couette cell constructed of neutron transparent niobium, have confirmed that measurable alignment of RecA-dsDNA is achieved already at small shear gradient values (less than 30 s^{-1}) with a saturation obtained at about 200 s^{-1}. A similar saturation observed by LD-spectroscopy had earlier been taken as evidence for an efficient shear orientation. Quite surprisingly, the degree of orientation as concluded from SANS is rather modest, an observation that implies, by inference from LD-spectroscopy runs made under identical conditions, that the optical chromophores in the complex are locally very well organized. More specifically, the DNA bases appear to be pointing preferentially perpendicular to the fiber axis.

Although the experiments at Risø have so far only been rather preliminary with the main purpose of assessing the potential of the method applied to partially aligned molecules in flowing aqueous solution, the measurements have been quite successful and have provided valuable information complementing the geometric information from the flow LD-spectroscopy technique.

1.1.38. Quaternary structure of α_2-macroglobulin from human blood plasma

(B. Sjöberg*, S. Pap* (*University of Göteborg, Sweden) and K. Mortensen)

Human plasma α_2-macroglobulin (α_2M) is a glycoprotein of molecular weight about 720.000 and with an approximative concentration of 2 mg/cm^3 plasma. It is generally assumed that the most important physiological role of α_2M is to protect living materia from proteolytic degradation. The molecule is a tetramer composed of identical subunits linked in pairs by disulfide bonds; two disulfide bonded pairs associate non-covalently to form the native tetramer.

Our strategy in the investigation of α_2M is to dissociate the molecule by specific reagents, followed by characterisation of the products by the SANS-technique. As a result of these investigations we obtain information about the organisation of the total α_2M-molecule, as well as about the contact areas between the subunits. The SANS-technique is ideally suited for the investigation of dissociation equilibria since, besides structural information, it also offers a rapid and non-destructive determination of the average molecular weight directly in solution.

In a first investigation of the nature of the non-covalent interaction we used dodecylsulfate as dissociating agent[1]. The non-covalent interaction can, however, also be broken by lowering the pH to below 4.5. By monitoring the relative molecular weight, as a function of pH, it was found[2] that the dissociation at low pH is driven by the uptake of protons on altogether four acid-base (most probable carboxylate) groups, one per monomeric subunit of α_2M.

The effect of urea upon α_2M has been very much debated in the literature, but the prevailing opinion is that α_2M dissociates very rapidly (within 30 minutes) in urea solutions of relatively low concentration (about 2.5 M). Our SANS-investigations, however, clearly shows that the dissociation of α_2M in urea is a very slow process requiring high concentrations of urea. For instance, in 4 M urea at room temperature, 24 hours are needed for complete dissociation of α_2M into half molecules. These findings might explain why some authors have reported that α_2M is active even after dissociation in urea.

Also regarding the products obtained after reducing the inter-subunit S-S bonds of α_2M there are contradictory results, in the literature. Some authors claim that a quarter molecular frag-

ment, consisting of just one subunit, is obtained, while other claim that a half molecular fragment, consisting of two subunits, is obtained. We have used both dithithreitol (0.5-100 mM), and the NADPH-thioredoxin-thioredoxin reductase enzyme system, as reducing agents. The SANS measurements clearly shows that the same type of half-molecular fragment is obtained in all these studies; a result which is independent of the concentration and type of reducing system used. By considering the shape and dimensions, measured for the half-molecular fragment[3], it can be easily identified within the three-dimensional model for the total α_2M-molecule[4]. From the time dependence of the reaction, after adding reductant, we can also conclude that the dissociation is a well defined process, which follows simple kinetic laws.

1) Sjöberg, B., Pap, S. and Kjems, J.K. (1987). Eur. J. Biochem. **162**, 259.

2) Sjöberg, B., Pap, S. and Mortensen, K. (1989). Submitted.

3) Sjöberg, B., Pap, S. and Kjems, J.K. (1985). Eur. Biophys. J. **13**, 25.

4) Sjöberg, B. and Pap, S. (1989). J. Biol. Chem. **264**, 14686.

1.1.39. Studies of complement proteins and their interactions

(R. Österberg*, B. Malmensten* (*University of Agricultural Sciences, Uppsala, Sweden) and K. Mortensen)

Complement proteins are part of the immunological system and it consists of about twenty proteins. This system is involved in a series of defence mechanisms. One such mechanism is the formation of the membrane attack complex (MAC) which by tube formation through the cell membrane destroys foreign cells and bacteria. The proteins C3, C4 and C5 are initially involved in the formation of MAC. Their split products activates the inflammation response of the body and thereby keep the infection localized. The C3 and C4 proteins are the key components of the complement system and they are activated via cleavage of a labile thiolester bond. It is therefore not surprising that genetic anomalies of C3 and C4 lead to serious diseases. For instance, rare haplotypes of the C4 gene have been found among humans suffering from auto-immune diseases, such as SLE, diabetes, rheumatoid arthritis and glomerulonephritis.

One of our main aims is to study the mechanism of activation of C3 and C4 and the extension of this reaction, via complex formation with the other components, into the MAC-complex. Using methylamine we simulate the activation reaction and, in a contrast variation study using SANS, we have observed that new surfaces are revealed to the solvent when C3 and C4 are activated[1]. In other studies of the same reactions and by using monoclonal antibodies as markers we observe, as a result of the activation, a dramatic conformational change; the result from these SANS and SAXS studies could be explained by a rotation of a large globular body within the molecules most probably about a single bond, a so-called domain rotation. After activation of C3 or C4, the C3 and C5 convertases are formed and we observe in a study of this step, via the SAXS technique, that C3 and C4 dimerize[2]. The initial formation of the MAC-polymer is being studied using the C3 and C5 convertases occurring naturally in cobra venom; so far, the cobra venom analogue, CVF, has been studied in relation to both factor B and its split product, Bb[3].

1) Österberg, R., Malmensten, B., Nilsson, U., Eggertsen, G. and Kjems, J.K. (1988). Int. J. Biol. Macromol. 10, 15-20.

2) Österberg, R., Nilsson, U. and Eggertsen, G. (1985). J. Biol. Chem. 260, 12970-12973.

3) Österberg, R., Malmensten, B., Nilsson, U., Eggertsen, G. and Kjems, J.K. (1986). Proceedings 17th FEBS Meeting, Berlin.

1.1.40. Analytical treatment of the resolution function for small angle scattering

(J. Skov Pedersen, D. Posselt and K. Mortensen)

Analytical expressions for the resolution function for small angle scattering in pin-hole geometry have been derived. The contributions to the resolution function due to wavelength spread, finite collimation and detector resolution have been determined separately using Gaussian functions to approximate the contributions. A general resolution function has been derived which is the result of the combined effect of the three contributions. The width of the resolution function along the nominal scattering vector for the contributions from collimation effects and detector resolution is nearly independent of the scattering vector, whereas the width of the contribution due to wavelength spread increases with increasing scattering vector. The width in the direction perpendicular to the nominal scattering vector is due to the collimation effects and detector resolution and is nearly independent of the scattering vector.

An azimuthal-integrated resolution function, which can be applied to scattering from materials with a circular symmetric scattering cross-section has been calculated. This resolution function contains a contribution from the radial-averaging procedure itself. An example is shown in figure a). The shape of the function deviates somewhat from that of a Gaussian at small scattering vectors but becomes nearly Gaussian for large scattering vectors.

The analytical results have been compared to the results of computer simulations. The comparison shows that the Gaussian function gives a good description of the resolution function and that the widths agree with those calculated by the analytical expressions.

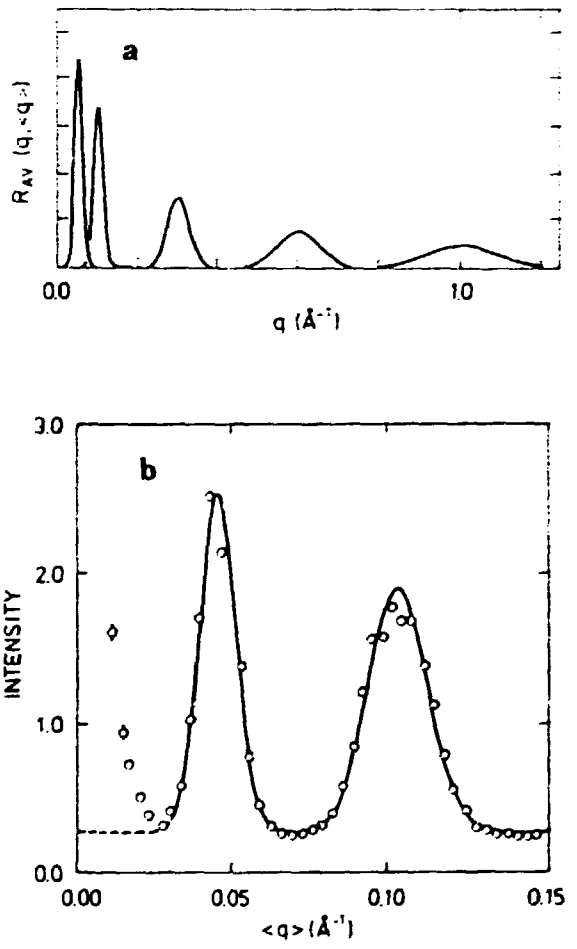

The resolution function has been applied in the analysis of experimental examples. Figure b) shows the radial-averaged scattering pattern of lamellar structures of bilayer lipid membranes (K. Mortensen, W. Pfeiffer, E. Sackmann and W. Knoll, 1988, unpublished). The curve in the figure is a least-squares fit of a cross-section consisting of two delta-functions and a flat background, convoluted with the resolution function. The width of the two peaks are determined by the instrumental resolution and using the derived analytical expressions for the resolution function, the least-squares analysis can easily be performed.

1.1.41. Analysis of small angle scattering data: Indirect Fourier transformation and deconvolution of instrumental resolution effects

(S.L. Hansen (The Royal Veterinary and Agricultural University, Copenhagen, Denmark) and J. Skov Pedersen)

The interpretation of the full range of the scattering curve in small angle scattering involves the determination of the distance distribution function. This function is equivalent to the correlation function multiplied by the distance squared. The distance distribution function is the Fourier transform of the scattering curve, but a direct Fourier transformation is impossible due to the finite range of scattering vectors for which the intensity is known and more important due to the statistical noise in the measured intensity. Therefore an indirect method has to be employed. The distance distribution function is determined by fitting its Fourier transform to the measured scattering curve. However, in general this gives an underdetermined set of equations and procedures to limit the number of free parameters has to be invented. In the indirect fitting procedure it is straight forward to include the effects of instrumental resolution as a convolution of the calculated scattering cross-section and the resolution function. In addition to the distance distribution function the fitting procedure also gives the scattering curve deconvoluted for resolution effects.

The purpose of the present work is to compare two methods for limiting the number of free parameters and to investigate the applicability of the recently derived expressions for the resolution function for deconvolution (1.1.40). The two methods that have been used are the classical method of Glatter[1] and the maximum entropy method. In Glatter's method the distance distribution function is described as a linear combination of smooth functions (cubic B-splines) having a restricted extension in real space. A measure of the smoothness of the distance distribution function in terms of the coefficients in the linear combination is added to the usual chi-

squared and the sum of these two are minimized by least-squares methods. In the maximum entropy method a measure of the multiplicity of a solution for the distance distribution function is introduced and it is optimized subject to the constraint that chi-squared of the Fourier transform is unity.

The two methods have been applied on simulated as well as real experimental scattering curves. For simulated results for fibrinogen and model proteins[2] the two methods give very similar results which are in good agreement with the original distance distribution functions. For the experimental example of scattering from a solution of polymer latex spheres[3] the two methods give similar results and they are both able to give the deconvoluted scattering curve. However, for the experimental example of scattering from lamellar structures of bilayer lipid membranes[4] the maximum entropy method used for direct deconvolution gives significantly better results.

1) Glatter, O. (1977). J. Appl. Cryst. 10, 415.
2) May, R.P. and Nowotny, V. (1989). J. Appl. Cryst. 22, 231.
3) Wignall, G.D., Christen, D.K. and Ramakrishnan, V. (1988). J. Appl. Cryst. 21, 438.
4) Mortensen, K., Pfeiffer, W., Sackmann, E. and Knoll, W. (1988). Unpublished.

1.1.42. Resolution function for small angle x-ray scattering calculated using Gaussian approximations in position-angle-wavelength space

J. Skov Pedersen and C. Riekel (European Synchrotron Radiation Facility, Grenoble, France))

The general description of synchrotron x-ray beam-lines in the position-angle-wavelength space[1] has been developed as a simple graphical method for matching the optical elements to the properties of the x-ray beam. We have made a mathematical formulation of the methods in terms of Gaussian function. The source, the transmission function for the slits, and the acceptance windows of the monochromator crystals are approximated by Gaussian functions. These approximations are far from perfect particularly for the slits and for perfect, crystal monochromators. However, they allow all of the algebra in connection with combining the different contributions to be done analytically.

The various components of the beam-line, like flight paths, monochromators and mirrors, results in coordinate transformations in the parameter space. By inserting these transformations in the expressions for the source, the transmission functions of the slits and the acceptance windows of the monochromator crystals, one can calculate the distribution of the intensity in the

position-angle-wavelength space at any position along the beam-line. It should be noted that the wavelength only correlates with the position and angle in the direction in the scattering plane of the monochromator crystals. There is no mixing between the position-angle in the vertical and in the horizontal plane. Therefore the transformations can be described by 3×3 matrices for the position-angle-wavelength in the direction of the monochromator crystals and by 2×2 matrices for the position-angle in the other direction.

The source, the transmission functions of the slits and the acceptance windows of the monochromators are transformed to the position of the sample and multiplied. This give the intensity distribution at this position and from this distribution the resolution function in reciprocal space is calculated. The resolution of the detector is easily included by a convolution. The transmissions of the slits and the acceptance windows of the monochromator crystals have been normalized to give the same integrated transmissions and reflectivities as the functions they approximate. Therefore the flux at the sample position can be calculated by multiplication of the brilliance of the source and the result obtained from an integration of the distribution over the two position parameters, the two angle parameters and the wavelength.

1) Matsushita, T. and Kaminaga, U. (1980). J. Appl. Cryst. 10, 465 and 472.

1.1.43. A controlled atmosphere x-ray *in situ* experiment for simulation of an industrial catalytic reactor

(B. Fabius*, B.S. Clausen*, G. Steffensen*, J. Villadsen* (*Haldor Topsøe Research Laboratories, Lyngby, Denmark) and R. Feidenhans'l)

A new experimental set-up designed for real time *in situ* measurements of the reaction dynamics taking place under high gas pressure and at elevated temperature has been tested at the D4 beam line at HASYLAB. A gas flow system controls a continuous gas flow through the powder sample and the exit gas is analyzed by a gas chromatograph. The *in situ* cell has been designed for simultaneous investigation of changes in the solid state of catalytic materials, but the set-up is equally suitable for studies of phase transitions and other aspects of materials science.

The set-up was used to elucidate the reduction of a $CuO/ZnO/Al_2O_3$ methanol synthesis catalyst. The catalyst, which is composed of small crystallites giving rise to rather broad diffraction peaks, is not a strong scatterer, but by using a position sensitive detector, it is possible to make time resolved studies at a time scale less than two minutes and with counting statistics sufficiently good for profile analysis.

The integrated intensity of CuO(111) and Cu(111) as a function of reduction temperature is shown in the figure.

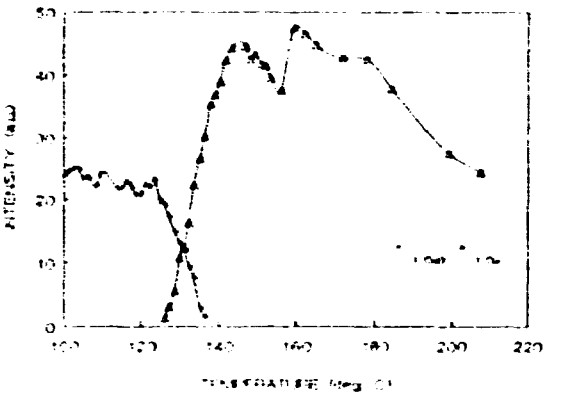

The integrated intensity of the (111) peak of Cu (Δ) and CuO (+), respectively as a function of temperature of a Cu ZnO Al_2O_3 catalyst in a reduction gas. At T ~ 130°C the CuO phase transforms to metalic copper.

It is the intention to use the experimental set-up to study the effect of sintering on the catalytic activity together with lattice strains that might occur in the catalyst while working.

1.1.44. The metal-MBE machine

(R. Feidenhans'l and T. Kjær)

The assembling of the metal MBE machine started early 1989 when the vacuum vessel was delivered from the Risø workshop. The assembling has been problem-free and no leaks were found in the vessel. The system is now under vacuum and has a base pressure of 4×10^{-11} torr after 24 hours bake out at 200°C. Most of the components are tested. The ion-sputter guns and the gas inlet system are still to be installed and the heat shield for the electron beam evaporators has been redesigned.

We aim to start metal film preparations by studying Pb layers on Si(111) and Ge(111) surfaces. This is a relatively easy system to handle experimentally and is a continuation of a project we have started in our measuring program in HASYLAB. The first results are expected in early 1990.

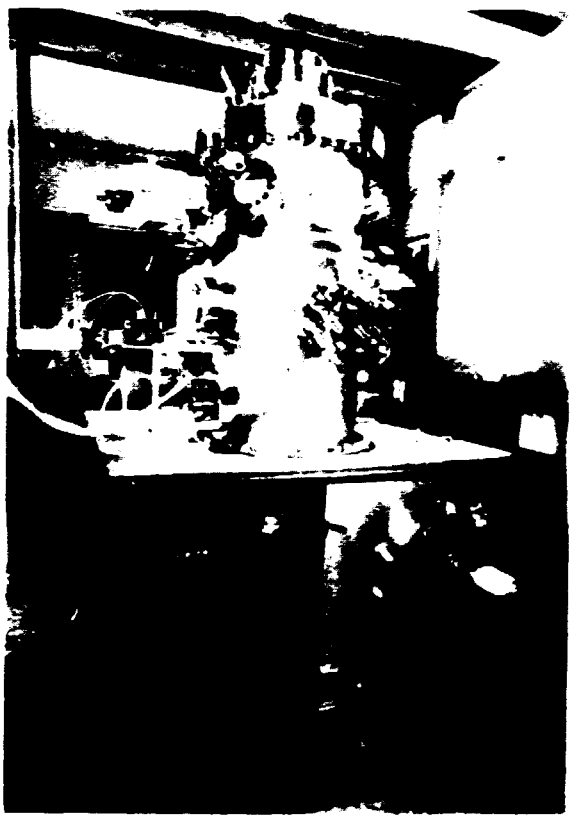

The MBE-vacuum chamber

1.1.45. The liquid He plant

(K. Christensen and M. Nielsen)

For the year 1989 the following quantities of liquid He were delivered: 56.800 liter. Of this 45.200 liter He are used outside Risø.

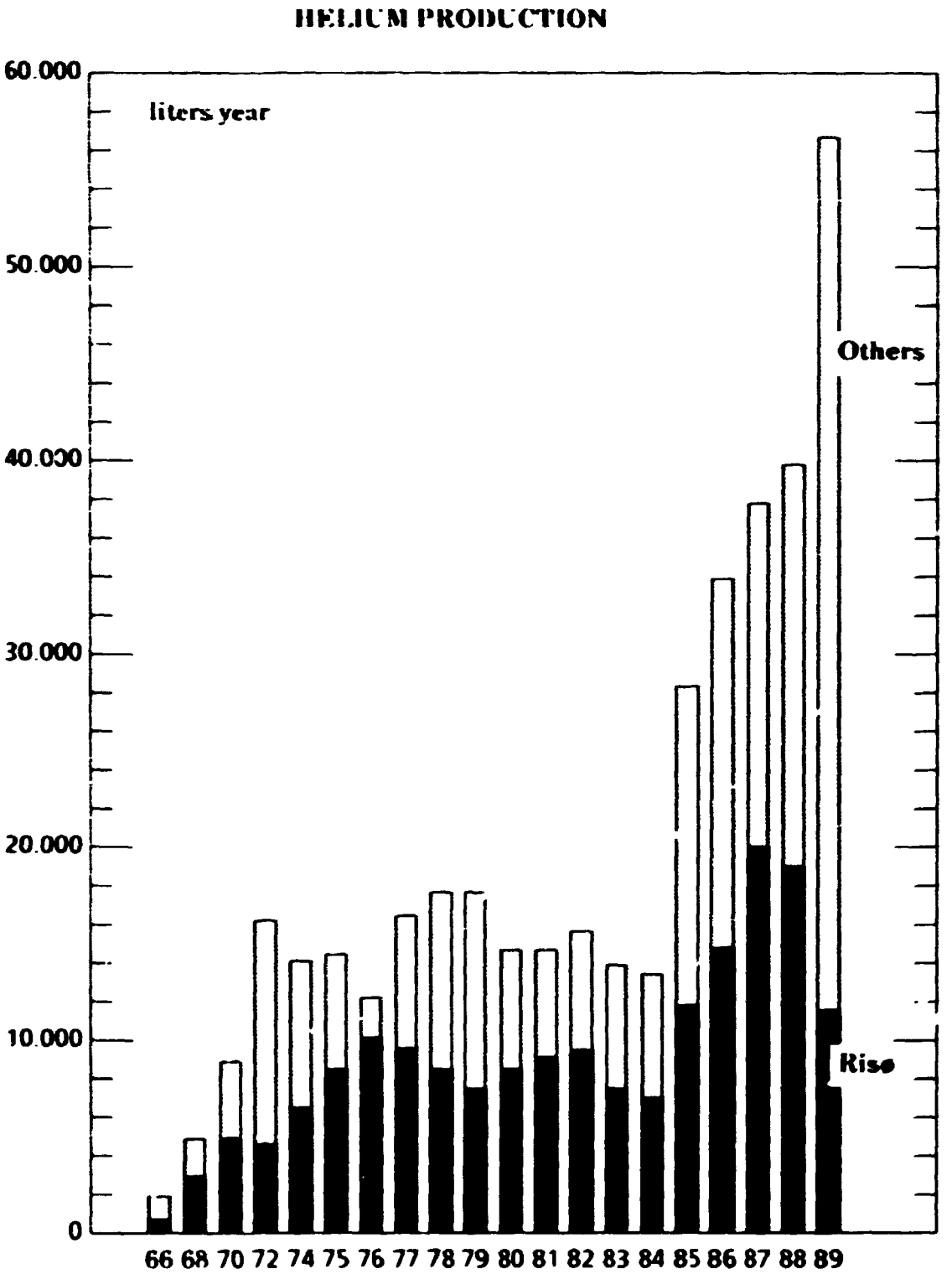

1.2. PARTICIPANTS IN THE WORK ON CONDENSED MATTER

Scientific Staff

Als-Nielsen, Jens
Andersen, Niels Hessel
Bohr, Jakob
Buras, Bronislaw*
Clausen, Kurt Nørgård
Feidenhans'l, Robert
Grey, François
Kjær, Kristian
Lebech, Bente
Lindgård, Per-Anker
Mortensen, Kell
Nielsen, Mourits
Skov Pedersen, Jan
Wulff, Michael

Ph.D. Students

Kromann, Rasmus (from February 1)
Gråbæk, Lars
Kalsbeek, Nicoline§
Posselt, Dorthe
Poulsen, Henning Friis (from February 1)

Technical Staff

Bang, Sten
Breiting, Bjarne
Christensen, Kaj
Dietrich, Caspar** (from July 17 - August 31)
Ejbye, Jan (from August 1)
Hansen, Claus (from February 1-28)
Jeppesen, Einer Bernhard (from July 3)
Jensen, Louis Gordon
Jensen, Tina*** (from September 1)
Kjær, Torben
Kofoed, Werner
Larsen, Preben
Bang Larsen, Arild (from November 2)
Linderholm, Jens
Lund, Morits
Ottosen, Helle*** (from June 16 - September 30)
Nielsen, Sten
Theodor, Kjeld
Thuesen, Allan

---

* Part time consultant
** Temporary assistant
*** Laboratory apprentice
§ From the University of Copenhagen

Secretaries

Astradsson, Lone
Frederiksen, Lajla
Kjøller, Kæth
Kloster, Margit (from February 1)

Guest Scientists

Annila, A.	University of Helsinki, Finland
Bojsøe-Jørgensen, P.	Ferroperm, Copenhagen, Denmark
Bruce, H.	Cavendish Laboratory, Cambridge, U.K.
Fossum, J.	Norwegian Natural Science Foundation, Norway
Jyrkkiö, T.	Helsinki University of Technology, Finland
Oja, A.	Helsinki University of Technology, Finland
Siemensmeyer, K.	Hahn-Meitner-Institute, Berlin
Tuoriniemi, J.	Helsinki University of Technology, Finland
Vaknin, David	University of Pennsylvania, U.S.A.
Weinfurter, H.	Hahn-Meitner-Institute, Berlin

Short time visitors (more than one week)

Alliborn, J.	Institute Laue-Langevin, Grenoble, France
Aeppli, G.	AT&T Bell Laboratories, Murray Hill, New Jersey, U.S.A.
Broddin, D.	University of Antwerp, Belgium
Caciuffo, R.	University of Ancona, Italy
Christensen, A. Nørlund	University of Århus, Århus, Denmark
Broholm, C.	AT&T Bell Laboratories, Murray Hill, New Jersey, U.S.A.
Falcao, A.	LNETI, Sacavem, Portugal
Fjellvåg, H.	University of Oslo, Blindern, Norway
Glenne, R.	University of Oslo, Blindern, Norway
Habekost, S.	University of Århus, Århus, Denmark
Hayden, S.	Institute Laue-Langevin, Grenoble, France
Hutchings, M.	AERE Harwell, Oxfordshire, England
Keen, D.	Clarendon Laboratory, Oxford, U.K.
Klauda, M.	Hahn-Meitner Institute, Berlin
Loiseau, A.	ONERA, Chapilon, France
Luke, G.	University of Colombia, U.S.A.
Lounasmaa, O.*	University of Helsinki, Finland
Malmensteen, B.	University of Uppsala, Sweden
Mayer, H.M.	Hahn-Meitner Institute, Berlin
McGreevy	Clarendon Laboratory, Oxford, U.K.
McMorrow, D.	University of Edinburg, Scotland
Mochrie, S.	Massachusetts Institute of Technology, U.S.A
Müller, P.	Technische Hochschule, Aachen, F.R.G.
Norby, P.	University of Odense, Odense, Denmark
Patterson, C.	University of Edinburg, Scotland
Robinson, I.	AT&T Bell Laboratories, Murray Hill, New Jersey, U.S.A.
Rothard, H.	University of Johan Wolfgang, Frankfurt am Main, F.R.G.

---

* Supported by the Danish Research Academy

Sinha, S.K.	Brookhaven National Laboratory, U.S.A.
Samseth, J.	IFF Kjeller, Norway
Shirane, G.	Brookhaven National Laboratory, U.S.A.
Sjöberg, B.	University of Göteborg, Sweden
Skjetne, E.	IFF Kjeller, Norway
Smetana, Z.	Charles University, Prague, Czechoslovakia
Spontak, R.	IFF Kjeller, Norway
Stassis, C.	Brookhaven National Laboratory, U.S.A.
Ströbel, J.	Hahn-Meitner Institute, Berlin
Viertiö, H.	University of Helsinki, Finland
Wisniewski, A.	Polish Academy of Sciences, Warsaw, Poland
Wolf, S.G.	Weizmann Institute, Israel
Österberg, R.	University of Uppsala, Sweden

Awards and degrees

Jens Als-Nielsen has been appointed a member of the Accelerator- og Synchrotron Committee for a period of January 1 1990 till January 1 1993.

Students working for their Master's Thesis

Poulsen, Henning Friis	From the Technical University of Denmark, Lyngby

IAESTE-STUDENT

Grigorie, M.	Switzerland
Knappe, J. B.	Gemini House, Hemel Hempstead, U.K.

1.3. PUBLICATIONS AND EDUCATIONAL ACTIVITIES IN CONDENSED MATTER PHYSICS

1.3.1. Publications

ALS-NIELSEN, J. (1989). Lipid and simple liquid surfaces. Colloq. Phys. **50**, No. C7, 21-22.

ALS-NIELSEN, J. and KJÆR, K. (1989). X-ray reflectivity and diffraction studies of liquid surfaces and surfactant monolayers. In: Proceedings of the NATO Advanced Study Institute, Phase Transitions in Soft Condensed Matter, Geilo, Norway, 4-14 April (editors T. Riste and D. Sherrington), Plenum Press, pp. 113-138.

ALS-NIELSEN, J., ANDERSEN, N.H., BROHOLM, C., CLAUSEN, K.N., LEBECH, B., NIELSEN, M. and POULSEN, H.F. (1989). Oxidation kinetics in oxygen deficient $YBa_2Cu_3O_{7-x}$ studied by neutron powder diffraction. IEEE Transactions on Magnetics, **25**, No. 2, 2254-2261.

ALS-NIELSEN, J., ANDERSEN, N.H., CLAUSEN, K.N., MICHELSEN, P. and POULSEN, F.W. (1989). Experiments on palladium- and titanium-deuterium systems with reference to studies on cold fusion. Risø-M-2806, 12 p.

BOHR, J., GIBBS, D., AXE, J.D., MONCTON, D.E., D'AMICO, K.L., MAJKRZAK, C.F., KWO, J., HONG, M., CHIEN, C.L., and JENSEN, J. (1989). Diffraction studies of rare earth metals and superlattices. Physica **B159**, 93-105.

BOGÉ, M., BONNESSEAU, D., BURLET, P., FOURNIER, J.M., PLESKA, E., QUEZEL, S., REBIZANT, J., ROSSAT-MIGNOT, J., SPURLET, J.C. and WULFF, M. (1989). Magnetic and electrical properties of $NpRu_2Si_2$. Journ. Nucl. Mat. **166**, 77-82.

BROHOLM, C.L. (1989). Magnetic fluctuations in heavy fermion systems. A neutron scattering study of UPt_3, U_2Zn_{17} and URu_2Si_2. Risø-M-2731, 79 p.

BURAS, B. and GERWARD, L. (1989). Applications of x-ray energy dispersive diffraction for characterization of materials under high pressure. Prog. Crystal Growth and Charact. vol. **18**, pp. 93-138.

BURAS, B. and THOMPSON, D.J. (1989). The European Synchrotron Radiation Facility. In: "Synchrotron Radiation Sources and Applications" (edited by G.N. Greaves and I.H. Munro), Scottish Universities' Summer Schools in Physics, 72-81.

BURAS, B. and GERWARD, L. (1989). Energy dispersive devices. In: "International Tables of Crystallography (edited by A.J. Wilson, vol. **C**).

CASTÁN, T. and LINDGÅRD, P.-A. (1989). Kinetics of domain growth, theory, and Monte Carlo simulations: A two-dimensional martensitic phase transition model system. Phys. Rev. **B40**, 5069-5083.

CLAUSEN, K.N., HACKETT, M.A., HAYES, W., HULL, S., HUTCHINGS, M.T. MacDONALD, J.E., McEWEN, K.A., OSBORN, R. and STEIGENBERGER, U. (1989). Coherent diffuse neutron scattering from UO_2 and ThO_2 at temperatures above 2000 K. Physica **B156 & 157**, 103-106.

CLAUSEN, K.N., HAYES, W., KEEN, D.A., KUSTERS, R.M., McGREEVY, R.L. and SINGLETON, J. (1989). Neutron scattering and electrical transport in $Nd_{0.5}Pb_{0.5}MnO_3$. J. Phys.: Condens. Matter **1**, 2721-2726.

ELSENHANS, O., FISCHER, P., FURRER, A., CLAUSEN, K.N., PURWINS, H.-G. and HULLIGER, F. (1988). Magnetic neutron scattering investigations of $TbPd_3$ and of $DyPd_3$. J. de Physique **C8**, 425-426.

FEIDENHANS'L, R. (1989). Surface structure determination by x-ray diffraction. Surface Science Reports **10**, 105.

FEIDENHANS'L, R., GREY, F., BOHR, J., NIELSEN, M. and JOHNSON, R.L. (1989). Investigation of the Au/Si(111) surface structures by x-ray diffraction. Colloq. Phys. **50**, No. C7, 175-179.

GAY, J.M., PLUIS, B., FRENKEN, J.W.M., GIERLOTKA, S., VEEN, J.F. VAN DER, MACDONALD, J.E., WILLIAMS, A.A., PIGGINS, N., ALS-NIELSEN, J. (1989). X-ray reflectivity study of surface melting on Pb(110). Colloq. Phys. **50**, No. C7, 289-293.

GIEBULTOWICZ, T.M., RHYNE, J.J., CHING, W.Y., HUBER, D.L., FURDYNA, J.K., LEBECH, B. and GALAZKA, R.R. (1989). Harmonic magnons in $Cd_{1-x}Mn_xTe$ and $Zn_{1-x}Mn_xTe$. Phys. Rev. **B39**, 6857-6870.

GREY, F., FEIDENHANS'L, R., NIELSEN, M. and JOHNSON, R.L. (1989). The relationship between the metastable and stable phases of Pb/Si(111). Colloq. Phys. **50**, No. C7, 181-187.

GREY, F. and KJEMS, J.K. (1989). Aggregates, broccoli & cauliflower. Physica **D38**, 154-159.

GRÅBÆK, L., BOHR, J., JOHNSON, E., ANDERSEN, H.H., JOHANSEN, A. and SARHOLT-KRISTENSEN, L. (1989). X-ray studies of krypton, xenon and lead inclusions in aluminum single crystals. Mater. Sci. Eng. **A115**, 97-101.

GRÅBÆK, L., JOHNSON, E. and WOOD, J.V. (1988). Phase distributions in rapidly solidified stainless steels. Met. Trans. A **20**, 2259-2265.

JACQUEMAIN, D., GRAYER WOLF, S., LEVEILLER, F., LAHAV, M., LEISEROWITZ, L., DEUTSCH, M., KJÆR, K., ALS-NIELSEN, J. (1989). Crystalline self-aggregation and a pressure driven solid-solid phase transition in a fluorinated Langmuir monolayer. Colloq. Phys. **50**, No. C7, 29-37.

JYRKKIÖ, T.A., HUIKU, M.T., SIEMENSMEYER, K. and CLAUSEN, K.N. (1989). Neutron diffraction studies of nuclear magnetic ordering in copper. J. of Low Temp. Phys. **74**, Nos. 5/6, 435-473.

KJÆR, K., ALS-NIELSEN, J., HELM, C.A., TIPPMANN-KRAYER, P. and MÖHWALD, H. (1989). Synchrotron x-ray diffraction and reflection studies of arachidic acid monolayers at the air-water interface. J. Phys. Chem. **93**, 3200-3206.

KJÆR, K., ALS-NIELSEN, J., LAURSEN, I. and KREBS LARSEN, F. (1989). A neutron scattering study of the dilute dipolar-coupled ferromagnets $LiTb_{0.3}Y_{0.7}F_4$ and $LiHo_{0.3}Y_{0.7}F_4$. Structure, magnetisation and critical scattering. J. Phys. Condens. Matter **1**, 5743-5757.

KNAK JENSEN, S.J. and KJÆR, K. (1989). Dipolar spin systems: models for $LiHoF_4$ and $LiHo_{0.3}Y_{0.7}F_4$. J. Phys. Condens. Matter **1**, 2361-2368.

KRUMMACHER, S., SEN, N., GUDAT, W., JOHNSON, R., GREY, F. and GHIJSEN, J. (1989). Comparative study of the electronic structure of the ordered and disordered $Cu_3Au(100)$ and $Cu_3Au(110)$ surfaces. Z. Phys. B **75**, 235-43.

LANDAU, E.M., GRAYER WOLF, S., SAGIV, J., DEUTSCH, M., KJÆR, K., ALS-NIELSEN, J., LEISEROWITZ, L. and LAHAV, M. (1989). Design and surface synchrotron x-ray structure analysis of Langmuir films for crystal nucleation. Pure and Appl. Chem. **61**, 673-684.

LEBECH, B., BERNHARD, J. and FRELTOFT, T. (1989). Magnetic structures of cubic FeGe studied by small angle neutron scattering, J. Phys: Condens. Matter 1, 6105-6122.

LEBECH, B. and SØNDERBERG PETERSEN, L. (1989). Neutron scattering facilities at the research reactor DR3. ISBN 87-550-1560-3 (20 pp).

LEBECH, B., WULFF, M., LANDER, G.H., REBIZANT, J., SPIRLET, J.C. and DELAPALME, A. (1989). Neutron diffraction studies of the crystalline and magnetic properties of UFe_2. J. Phys.: Condens. Matter 1, 10229-10248.

LINDGÅRD, P.-A., VIERTIÖ, H.E. and MOURITSEN, O.G. (1988). Monte Carlo simulation of adiabatic cooling and nuclear magnetism. Phys. Rev. **B38**, 6798-6806.

LINDGÅRD, P.-A. (1988). Theory of the nuclear magnetic ordering in Cu in a field. J. Phys. Colloq. **49**, No.C8, 2051-2052.

MORTENSEN, K. (1989). New facility for neutron scattering at Risø. Rådslaget, No. 2, 1-2.

NILSSON, L., ANDERSEN, N.H. and LUNDÉN, A. (1989). The structure of the solid electrolyte $LiAgSO_4$ at 803 K and of $LiNaSO_4$ at 848 K. Solid State Ionics **34**, 111-119.

NØRLUND CHRISTENSEN, A. and LEBECH, B. (1989). Preparation of superconducting $Tl_2Ba_2CaCu_2O_{8+y}$ by a fast solid-state reaction at 955°C. Acta Chem. Scand. **43**, 908-910.

PEDERSEN, J. SKOV, FEIDENHANS'L, R., NIELSEN, M., GREY, F. and JOHNSON, R.L. (1988). X-ray diffraction study of the Ge(111)5×5-Sn and Ge(111)7×7-Sn surfaces. Phys. Rev. **B38**, 13210-13221.

PEDERSEN, J. SKOV. (1989). Surface relaxations by the Keating model: A comparison with ab-initio calculations and x-ray diffraction experiments. Surface Science **210**, 238-250.

PLUIS, B., GAY, J.M., FRENKEN, J.W.M., GIERLOTKA, S., VAN DER VEEN, J.F., MACDONALD, J.E., WILLIAMS, A.A., PIGGINS, N. and ALS-NIELSEN, J. (1989). X-ray reflectivity study of surface-initiated melting: density profile at the Pb(110) surface. Surface Science **222**, L845-L852.

ROBINSON, I.K., BOHR, J., FEIDENHANS'L, R., NIELSEN, M., GREY, F. and JOHNSON, R.L. (1989). Reexamination of the InSb(111) and GaSb(111) structures: Comment on "disorder in the reconstructed (111)2×2 surfaces of InSb and GaSb" (by A. Belzner, E. Ritter and H. Schulz). Surf. Sci. **217**, L435-440.

SCHOUTEN, M., DORREPAAL, J., STASSEN, W.J.M., VLAK, W.A.H.M. and MORTENSEN, K. (1989). Thermal stability of polystyrene-b-poly(ethylene/propylene) diblock copolymer micelles in paraffinic solvents. Polymer **30**, 2038.

ŠIMA, V., SMETANA, Z., DIVIŠ, M., SVOBODA, P., ZAJAC, Š., BISCHOF, J., LEBECH, B. and KAYZEL, F. (1988). Magnetism and crystal field in $TmCu_2$. J. Phys. Paris **49**, C8, 415-416.

VIERTIÖ, H.E., MOURITSEN, O.G. and LINDGÅRD, P.-A. (1988). Computer simulation and mean field calculation of phase diagram and adiabatic demagnetization paths for an antiferromagnet. J. Phys. Colloq. **49**, 2053-2054.

WALISZEWSKI, J., ANDERSEN, N.H., DOBRZYNSKI, L., IHRINGER, J., LEBECH, B., PRANDL, W. and WISNIEWSKI, A. (1989). X-ray, neutron and magnetization studies of $YBa_2Cu_3O_{7-x}$ irradiated by fast neutrons. Physica **C160**, 189-196.

WOLNY, J. FRELTOFT, T. and LEBECH, B. (1989). SANS experiments on amorphous Fe-Ni and Co-Ni based materials. Acta Physica Polonica **A76**, 127-131.

WULFF, M., LANDER, G.H., LEBECH, B. and DELAPALME, A. (1989). Cancellation of orbital and spin magnetism in UFe_2. Phys. Rev. **B39**, 4719-4721.

WULFF, M., LEBECH, B., DELAPALME, A., LANDER, G.H., REBIZANT, J. and SPIRLET, J.C. (1989). U form factor and 3d-5f hybridization in UFe_2. Physica **B156/157**, 836-838.

ZEISKE, TH., GRAF, H.A., DACHS, H. and CLAUSEN, K.N. (1989). Electrical conductivity and magnetic properties of $MgCu_2O_3$. Sol. State Comm. **71**, 501-504.

1.3.2. Conferences

ANDERSEN, N.H., LEBECH, B., NIELSEN, M. and POULSEN, H.F., Oxygen equilibrium and structural phase properties of $YBa_2Cu_3O_{6+x}$. Danish Physical Society, Spring Meeting, Nyborg, Denmark (May).

ANDERSEN, N.H., DOBRZYNSKI, L., IHRINGER, J., LEBECH, B., PRANDL, W., WALISZEWSKI, J. and WISNIEWSKI, A., On the impact of fast neutrons on $YBa_2Cu_3O_{1-x}$ properties. Twelfth European Crystallographic Meeting ECM-12, Moscow, U.S.S.R. (August).

ANDERSEN, N.H., LEBECH, B. and POULSEN, H.F., Structural phase properties of ceramic $YBa_2Cu_3O_{7-x}$. European Conference on High-T_c Thin Films & Single Crystals (HTC USTRON 89), Ustron, Poland (30 September - 4 October).

BEGUM, R.J., LEBECH, B. and RAINFORD, B.D., X-ray and neutron diffraction studies of some pseudo two-dimensional magnetic systems. Third Asia-Pacific Conference, Hong Kong (June).

BERNASCONI, A., SLEATOR, T., OTT, H.R. and POSSELT, D., Low temperature properties of silica aerogels. Swiss-Italian Physical Society Meeting, Como, Italy (May).

BOHR, J., Magnetic x-ray scattering: A new tool for magnetic structure investigations. EMMA 89, Rimini, Italy (September).

CLAUSEN, K.N., KEEN, D.A., McGREEVY, R.L. and HUTCHINGS, M.T., Determination of defect correlations in crystalline materials from diffuse scattering using a Monte-Carlo method. Danish Physical Society, Spring Meeting, Nyborg, Denmark (May).

FEIDENHANS'L, R., GREY, F., BOHR, J., NIELSEN, M. and JOHNSON, R.L., Investigation of the Au/Si(111) surface structures by x-ray diffraction. International Conference on Surface and Thin Film Studies Using Glancing-Incidence X-Ray and Neutron Scattering, Marseilles, France (31 May - 1-2 June).

FEIDENHANS'L, R., GREY, F., NIELSEN, M. and JOHNSON, R.L., Structure and ordering of metal overlayers on Si(111) and Ge(111) surfaces. Nato Advanced Research Workshop entitled "Kinetics of Ordering and Growth at Surfaces", Acquafredda, Italy (September).

GREY, F., What is a two-dimensional liquid? Danish Physical Society, Spring Meeting, Nyborg, Denmark (May).

GRÅBÆK, L., BOHR, J., JOHNSON, E., ANDERSEN, H.H., JOHANSEN, A. and SARHOLT-KRISTENSEN, L., Superheating and supercooling of lead inclusions in aluminum. Danish Physical Society, Spring Meeting, Nyborg, Denmark (May).

JØRGENSEN, J.E. and ANDERSEN, N.H., Preparation and characterization of $Pb_2Sr_2YCu_3O_8$ and $Pb_2Sr_2HoCu_3O_8$. Twelfth European Crystallographic Meeting ECM-12, Moscow, U.S.S.R. (August).

LINDGÅRD, P.-A. and CASTÁN, T., Monte Carlo simulation of a model for the Martensitic transformation, domain growth kinetics. March Meeting of the Americal Physical Society, St. Louis, U.S.A. (March).

LINDGÅRD, P.-A. and CASTÁN, T., Kinetics of slow domain growth: The $\Delta E(t) \sim t^{-1/4}$ universality class. Danish Physical Society, Spring Meeting, Nyborg, Denmark (May).

LINDGÅRD, P.-A., Kinetics of slow domain growth in complex systems. Interdisciplinary Workshop on Complexity and Chaos, Risø, Denmark (June).

LINDGÅRD, P.-A. and CASTÁN, T., The $t^{-1/4}$ universality class: theory and simulation of slow domain growth after quenches to low and finite temperatures. The "R.J. Elliott Symposium", Oxford, U.K. (July).

LINDGÅRD, P.-A. and CASTÁN, T., Kinetics of slow domain growth: The $\Delta E(t) \sim t^{-1/4}$ universality class. 17th International Conference on Thermodynamics and Statistical Physics, Rio de Janeiro, Brazil (July-August).

NIELSEN, M., Magnetic excitations in high T_c superconductors. Interdisciplinary Workshop on Complexity and Chaos, Risø, Denmark (June).

MORTENSEN, K., PFEIFFER, W., SACHMANN, E. and KNOLL, W., Structural properties of a lecithin-cholesterol system. NATO ASI on Phase Transitions in Soft Condensed Matter, Geilo, Norway (April).

POSSELT, D., SKOV PEDERSEN, J., MORTENSEN, K. and EGEBERG, E.D., SAXS studies of freeze dried silica gels. NATO ASI on Phase Transitions in Soft Condensed Matter, Geilo, Norway (April).

POSSELT, D., SKOV PEDERSEN, J., MORTENSEN, K. and EGEBERG, E.D., SAXS studies of freeze dried silica gels. Danish Physical Society, Spring Meeting, Nyborg, Denmark (May).

WULFF, M., LANDER, G.H., REBIZANT, SPIRLET, J.C., LEBECH, B., DELAPALME, A. and GUILLOT, A. The cancellation of orbital and spin magnetism in UFe_2. Journee des Actinides, Madonna de Campeglio, Italy (April).

1.3.3. Lectures

ALS-NIELSEN, J., Reflectivity and diffraction studies of the structure of liquid surfaces. VI European Liquid Crystal Conference, Schladming, Austria (March).

ALS-NIELSEN, J. and KJÆR, K. (1989). X-ray reflectivity and diffraction studies of liquid surfaces and surfactant monolayers. Phase Transitions in Soft Condensed Matter, Geilo, Norway (April).

ALS-NIELSEN, J., Lipid and simple liquid surfaces. International Conference on Surface and Thin Film Studies, Marseilles, France (31 May - 4 June).

ANDERSEN, N.H., Højtemperatur superledere: Egenskaber og anvendelser (High-T_c Superconductors: Properties and applications).
1) Danish Engineering Society, Ålborg, Denmark (March).
2) University Extension, Roskilde, Denmark (March and October).
3) Experimenting Danish Radio-Amateurs, Roskilde, Denmark (March).
4) High-School Summer Course on Physics, Herlufsholm, Denmark (June).
5) Teachers Refresher Course on Physics, Randers, Denmark (September).
6) Danish Engineering Society, Odense, Denmark (October).

BURAS, B., X-ray energy dispersive diffraction and its applications. Second Topsøe Summer School, Aarhus, Denmark (August).

CLAUSEN, K.N., Materialefysik på Risø (Solid State Physics at Risø). Danish Magnetic Society, Risø, Denmark (May).

FEIDENHANS'L, R., X-ray scattering from solid surfaces, Modena, Italy (December).

FEIDENHANS'L, R., X-ray scattering from solid surfaces, HASYLAB, Hamburg, F.R.G. (December).

GREY, F., What is a two-dimensional liquid?, Kernforschungsanlage Jülich, F.R.G. (January).

GREY, F., What is a two-dimensional liquid?, Danish Physical Society, Spring Meeting, Nyborg, Denmark (May).

GREY, F., Pb/Ge(111): phases and phase transitions.
1) Brookhaven National Laboratory, N.Y., U.S.A. (August).
2) Stanford Synchrotron Laboratory, California, U.S.A. (August).
3) IBM Almaden Research Center, California, U.S.A. (August).

GREY, F., Pb/Si(111): phases and phase transitions.
1) FOM Institute, Amsterdam, The Netherlands (November).
2) Groningen University, The Netherlands (November).

KJÆR, K., Theory of x-ray reflection and diffraction from monolayers at the air-water interface and on solid supports. NATO Adv. Study Inst. on Phase Transitions in Soft Condensed Matter, Geilo, Norway (April).

LEBECH, B., Magnetic structures (3 lectures). University of Bialystok, Summer School on Magnetism, Bialowieza, Poland (June).

LEBECH, B., Magnetic ordering in iron monogermanides. Institute of Physics, Polish Academi Nant, Warszawa, Poland (June).

LEBECH, B., Powder neutron diffraction at Risø National Laboratory. Institute Laue-Langevin, Grenoble, France (February).

LINDGÅRD, P.-A., Theory and computer simulations of domain growth. Ames Laboratorium, Iowa, U.S.A. (March).

WULFF, M., Spin and orbital magnetism in the actinides. The European Synchrotron Radiation Facility, Grenoble, France (May).

1.3.4. Conferences and schools

SURFACE MELTING SYMPOSIUM

24-25 August 1989

Since the discovery of surface melting on the Pb(110) surface, the phenomena has been investigated intensively, both theoretically and experimentally. The symposium brought together some of the most active researchers in the field. The symposium extended over two days and inc ed 10 oral contributions, each of 45 min.

Organising committee:

François Grey, Risø National Laboratory, Denmark
Robert Feidenhans'l, Risø National Laboratory, Denmark

The symposium contained the following lectures:

J. Frenken, FOM Amsterdam	Experimental investigations of surface melting
H. Löwen, Univ. München	Crystallinity in quasi-liquid films
B. Pluis, FOM Amsterdam	Role of short and long-range interactions in the melting of a metallic surface
U. Breuer, KFA Jülich	XPD and LEED investigation of surface melting on Pb(110)
J. Bohr, Risø	Crystalline inclusions: a model system for studies of melting and roughening transitions of microcrystals

P. Stoltze, DTH, Copenhagen	The onset of disorder in Al(111) surfaces below the melting point
S. Mochrie, MIT Cambridge	Surface disordering of Au(100) and Au(111)
P. von Blanckenhagen, KFZ, Karlsruhe	Indications for surface premelting at krypton and aluminum surfaces
H. Dosch, Univ. München	Surface 'melting' of superlattices
F. Grey, Risø	Two dimensional quasi-liquids

SCHOOL ON SCATTERING METHODS IN POLYMER RESEARCH

30-31 May 1989

In connection with the opening of the new Small Angle Neutron Scattering facility at the DR3 reactor at Risø, a school on scattering methods was arranged in May 1989. The school was supported by the Danish Research Academy and Risø National Laboratory. 40 persons participated in the school, 20 Danish, 10 from other Nordic countries and 10 from the rest of Europe. Approximately half of the participants were Ph.D. students.

The school treated various scattering methods used in polymer research, including static and dynamic light scattering and small angle X-ray and neutron scattering. The school was dominated by the four invited lecturers, but included also a few contributed papers. Dr. Higgins discussed details on the theory of small angle scattering, and emphasized the use of this technique in relation to studies of polymer blends. Dr. Boue discussed small angle scattering used for studies of dynamical aspects of polymer and gel systems. Dr. Roots described aspects of dynamic laser light scattering, and Dr. Burchard discussed the use of light scattering for investigating the architecture of macromolecules in solution.

Organizing Committee of the School on scattering methods in polymer research:

Kell Mortensen, Physics Department, Risø National Laboratory
Jan Skov Pedersen, Physics Department, Risø National Laboratory
Søren Hvilsted, Chemical Department, Risø National Laboratory
Walter Batsberg, Chemical Department, Risø National Laboratory

The school comprised the following lectures:

Julia Higgins, Imperial College, London, U.K.	Neutron scattering from polymer blends
François Boue, Lab. Leon Brillouin, CEN Saclay, France	Some of the possibilities of small angle neutron scattering as applied to the study of polymer melts and networks
Bo Nystrøm, University of Oslo, Norway	Differentiation of various polymeric structures in dilute and semidilute solution by static and dynamic light scattering
Walther Burchard, University of Freiburg, F.R.G.	Differentiation of various polymeric structures in dilute and semidilute solution by static and dynamic light scattering
Kell Mortensen Risø National Laboratory, Denmark	The Risø Small Angle Neutron Scattering facility
Steen Hansen, Agricultural University, Copenhagen, Denmark	Aspects of analysis of small angle scattering data
Jan Skov Pedersen Risø National Laboratory, Denmark	Analytical treatment of the resolution function in small angle scattering

WORKSHOP ON NEUTRON SCATTERING STUDIES OF NUCLEAR MAGNETISM IN Cu

16 November at Risø

The recent discovery of a new magnetic order in the frustrated fcc antiferromagnet, Cu, was discussed and possible future investigations of magnetism in the ideal nuclear magnetic systems.

Organizing committee:

K.N. Clausen and P.-A. Lindgard, Risø

K.N. Clausen, Risø	Neutron scattering studies of nuclear magnetism in Cu - Introduction
K. Siemensmeyer, Hahn-Meitner Institute, Berlin	Experimental results from the (100) phase in Cu

A. Annila, Helsinki	Experimental results from the (0, 2 3, 2/3) phase and search for new nuclear magnetic peaks along the high symmetry axis
H. Viertio, Helsinki	Monte-Carlo simulation of nuclear magnetic order in Cu
A. Oja, Helsinki	Concluding remarks

The workshop preceeded the following more general topical meeting.

TOPICAL MEETING ON MAGNETISM OF FRUSTRATED SYSTEMS from Nuclear Magnetism to High-T_c Magnetism

17 November 1989 at Risø

The general aspects of magnetic order in frustrated antiferromagnets and in the high T_c superconducting materials were discussed in an international forum with about 50 participants. The meeting was held in the regi of the Danish Physical Society.

Organizer: Per-Anker Lindgård, Risø,
Chairman of the Danish Physical Society, Solid State Section,

The symposium contained the following lectures:

P.-A. Lindgård, Risø	Theory of frustrated antiferromagnet in field
M. Steiner, Mainz	Nuclear antiferromagnetism in fcc Cu, S = 3/2
G. Aeppli, AT&T, USA	Antiferromagnetism in fcc S = ½ and S = 1 systems
J. Reger, Mainz	Simulation results on fcc antiferromagnets
S. Miyashita, Kyoto	Theory of frustrated magnets in d = 2 and d = 3
T. Giamarchi, Paris	Antiferromagnetism and HTC superconductivity in the 2d Hubbard model
M. Nielsen, Risø	Neutron experiments on magnetic dynamics of HTC
P. Hedegård, H.C. Ørsted Inst.	Theory of the dynamics of high-T_c superconductors

H. Viertio, Helsinki

Mean field theory of the magnetic structure in Cu

Poster Session

An abstract booklet is available.

primaries penetrate the deuterium film and reach the underlying substrate. This transition thickness is strongly correlated to the range of hydrogen ions in deuterium. It means that the thin-film enhancement is a result of the interaction between the primary ion and the metallic substrate rather than a beam-independent structural interface effect. The clear increase of the yield for very thick films observed during keV-electron bombardment was not observed.

The results indicate that pellets in fusion plasmas will be sputtered by the fast ions that penetrate the ablation cloud around a solid deuterium pellet. Furthermore, one may expect that this erosion will be more pronounced for particles with a large electronic stopping power, i.e. typically for fast ions generated by the neutron beams.

2.1.4. Energy and mass spectra from particle-irradiated condensed gases

(A. Nordskov, J. Schou, B. Stenum, H. Sørensen and R. Pedrys (Jagellonian University, Cracow, Poland))

The detailed knowledge of the dynamics of the electronic excitations in the condensed gases is usually obtained from either luminescence studies or from investigations of the energy spectra of the ejected particles. In particular, these latter spectra have been important for the identification of the processes that lead to sputtering during particle bombardment[1].

The energy and mass distributions of the ejected particles from the two most important solids used as pellets in plasma experiments - condensed deuterium and neon - have never been measured.

A cryostat has been equipped with a gas-inlet system for producing films of condensed gases at low temperatures. This cryostat has been mounted in the existing setup at the Institute of Physics in Cracow. This is the only existing setup for detection of ejected neutrals in Europe.

The cryostat has been tested for the production of films of frozen deuterium, neon, nitrogen, krypton and xenon. These films have been produced on a substrate suspended below the cryostat. A flexible gas tube kept at about the temperature of liquid nitrogen allows us to produce films of different volatility without changing the thermal couplings. The cryostat has been tested for leaks at liquid helium temperature in the new setup. The measurements will be performed in the spring 1990.

1) Pedrys, R. et al. (1988). Nucl. Instr. Meth B33, 840.

2.1.5. Development of a hydrogen purifier

(A. Nordskov, J. Schou, B. Stenum, H. Sørensen, B. Larsen* and A. Schrøder Pedersen* (*Metallurgic Department, Risø))

The luminescence studies of electron-irradiated solid deuterium have demonstrated that it is difficult to remove small concentrations of impurities from the deuterium. Typically, the stated impurities in deuterium are nitrogen, oxygen and water at a level of 10-30 ppm. In particular, nitrogen in a solid deuterium matrix has turned out to be a strong light emitting source. It is usually desirable to suppress the impurity-induced luminescence bands since they may hide other less intense features.

The purification is performed via formation of magnesium hydride. The hydrogen is stored in magnesium powder as hydride, while the impurities are removed by pumping from the gas container. The hydrogen is liberated from the magnesium hydride at a temperature of about 335°C. This proecdure is expected to deliver extremely pure hydrogen or deuterium. The purifier will be tested for deuterium with known impurites in the near future.

2.1.6. Secondary electron emission from metals

(J. Schou)

The existing theory for secondary electron emission from solids by electron or proton impact[1] has been extended from the standard material aluminium to other nearly-free-electron metals as beryllium and magnesium.

For beryllium the secondary electron yield δ is expressed as

$$\delta = \beta |dE/dx|_e \Lambda ,$$

where β is a dimensionless quantity ($\approx$ 0.5 for primary electrons), $|dE/dx|_e$ the (electronic) stopping power and Λ a material parameter (0.029 nm/eV for Be). This expression that does not contain any adjustable parameters shows an agreement within 20 per cent with existing data for beryllium[2].

1) Schou, J. (1980). Phys. Rev. B22, 2141.

2) Schou, J. (1989). Scan. Micr. 3, 429.

2.1.7. Development of an electrothermal arc module for multiple downstream propellant injection in a high-speed light-gas gun

(S.A. Andersen, L. Bækmark, H. Kossek and J. Thorsen)

From earlier investigations of high-speed pellet acceleration by an arc heated gas gun, it was concluded that an important limitation on the efficiency was set by the excessive convective cooling of the propellant gas in the barrel. This problem is inherent in any conventional gas gun configuration in which high-temperature propellant is supplied at the breech of the barrel, and stays in contact with the barrel over the full acceleration length. This problem is also important for the 2-stage gas gun in which the propellant is heated by adiabatic compression before injection in the breech of the barrel.

In the earlier investigations, where hot propellant gas was produced by electrothermal (arc heated) evaporation of cryo-condensed hydrogen, it was also found difficult to produce a pressure pulse of a sufficiently long duration to match the feeding requirement of the gas gun. However, it was observed that very fast rates of pressure increase could be produced when the arc discharge circuit was adjusted in the "wrong" direction toward shorter time constants. This observation, together with recognition of the propellant/barrel cooling problem, suggests an alternative scheme of propellant supply to a gas gun barrel: multiple downstream injection of hot propellant from fast-acting electrothermal modules in synchronism with the pellet motion along the barrel. With this scheme the energy loss due to propellant/barrel cooling is resolved by requiring the pressure energy of the gas pulse from each injection module to be maintained for only a short barrel length (until the next module takes over). It is then possible to produce a useful average driving force over an extended acceleration path.

Two sets of experiments have been performed to test basic requirements of this scheme. In the first, the requirement of a technique to synchronize a downstream arc module with the passage of a pellet was examined. A simple module consisting of a small arc chamber for electrothermal evaporation of ethanol was connected to a barrel in which a plastic dummy pellet was pre-accelerated by pressurized He-gas. A reliable triggering of the module was obtained by the signal from an upstream pressure probe mounted adjacent to the module. With this simple unit it was possible to increase the velocity of a 38-mg pellet from about 1.3 to 1.7 km/s by discharging 220 J of electrical energy in the arc module loaded with 45 µl of ethanol, corresponding to an efficiency

(pellet energy gain/electrical energy) of about 10%.

In the second set of experiments, the performance of an arc module from which an output of hot hydrogen instead of ethanol could be obtained was optimized with respect to the requirement of a short response time. A module in which hydrogen gas could be cryo-condensed was constructed and tested in a set-up similar to that used for the ethanol module. In this case, the velocity of a 23-mg pellet could be increased from 1.7 to 2.4 km/s by discharging 200 J of electrical energy in the module loaded with about 10 mg of hydrogen. This corresponds to an efficiency of about 17% and was produced with an arc power that reached a maximum of 5 MW within 30 μs. These results indicate that high ultimate pellet velocities may be attained if a number of modules are combined in the proposed multiple downstream injection scheme. It should be noted that the results obtained with only one arc module in this alternative gas gun scheme have already exceeded significantly those found in the earlier work on a conventional arc-heated gas gun.

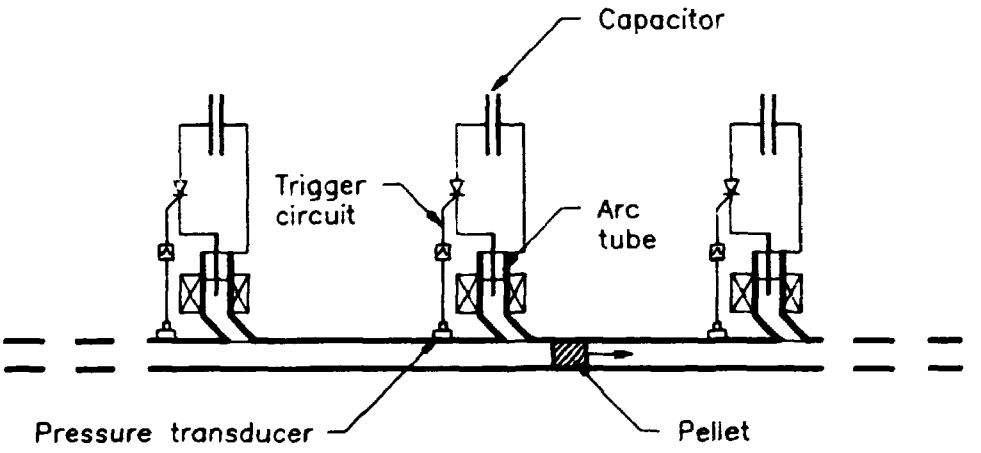

Schematic diagram of multiple downstream propellant injection

2.1.8. The multishot injector test stand

(H. Sørensen, J. E. Hansen, H. Kossek, P. Michelsen, B. Sass, J. Thorsen, K.-V. Weisberg)

In the previous annual report a description was made of a project[1] where a prototype of an 8-shot unit for formation and acceleration of 8 pellets of H_2 and D_2 should be built. This feasibility study should then be followed by construction of multishot pellet injectors for the two Italian experiments FTU in Frascati and RFX in Padova.

In the multishot injector suggested 8 pipe guns are placed around a central liquid helium flow cryostat. The pipe guns are loaded simultaneously through the gun barrels and fired successively with fast valves using H_2 as driver gas. The gun barrels point towards the centre line and are then curved and finally parallel in order that the pellet trajectories become parallel. The 8 pellets can then be transported to the experiment through one guide tube and one diagnostic unit is sufficient for measurement of velocity and mass for all 8 pellets.

The work performed consists of building an 8-shot unit, a diagnostic unit for measurement of velocity and mass, a system for operation and data collection and operation of the 8-shot unit in order to learn its behaviour and limitations and to get results.

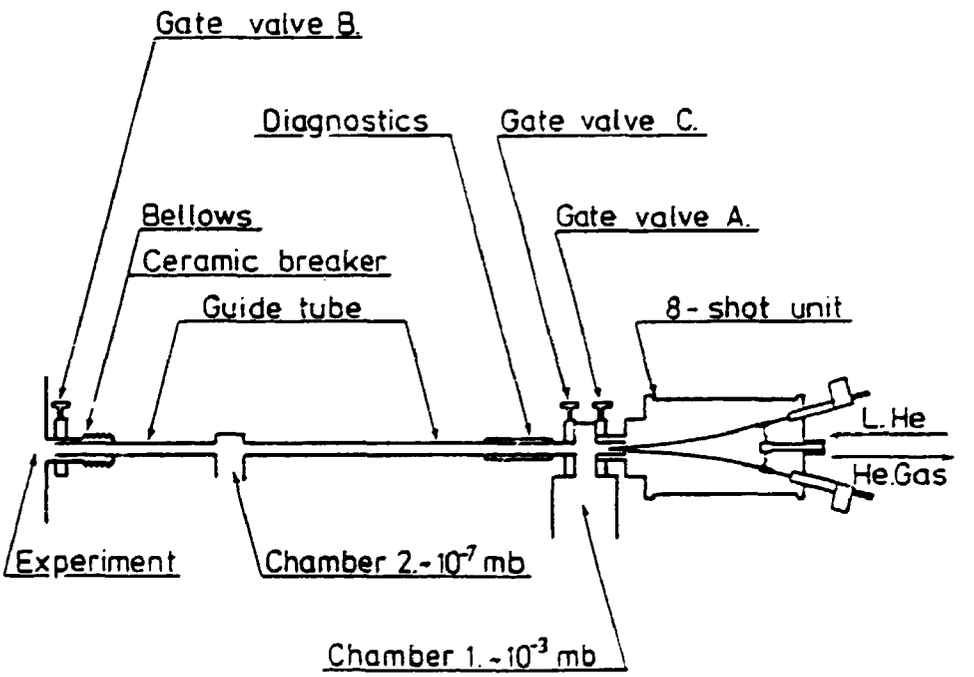

Figure 1. Schematic drawing of an 8-shot pellet injector

The 8-shot unit

A schematic drawing of the 8-shot injector is shown in Fig. 1. A flow cryostat is placed on a support tube on the axis of an assembly flange and the 8 pipe guns are placed symmetrically around it. The barrels are curved in such a manner that the last parts become parallel and close together. The cryostat consists of a stainless steel canister with liquid helium inside. A liquid helium transfer tube enter within the support tube and the helium gas leave through the support tube and is used also to cool the liquid helium transfer line. The liquid helium is forced through the cryostat by pumping. A number of pegs of annealed OFHC copper go through the wall of the canister. The support tube is made from 3 thin walled tubs of stainless steel and two tubes of annealed OFHC copper. Each pipe gun is then cooled by thermal anchoring to the pegs in the canister and to pegs on the two tubes of OFHC copper. The central parts of a pipe gun, i.e. the freezing cell and the outer segments are heated with electrical heaters. The cold parts of the pipe guns are shielded against thermal radiation by means of a radiation shield attached to the outer tube of OFHC copper on the cryostat support.

The 8-shot unit is placed on a bench above a vacuum tank of 400 ℓ volume pumped down to 10^{-3} mbar with a Roots pump in such a manner that the driver gas enters the vacuum tank while the pellets continue along the injector axis.

Three main problems exist in the design

The cryostat shall be designed to give efficient cooling for each pipe gun and the pipe guns should be thermally independent.

The unit actually consists of 8 independent pipe guns. They shall be identical and it shall be possible to load them in such a manner that the pellets become identical in size.

It shall be possible to line the guns up to give parallel pellet trajectories. For this the outer parts of barrel are made parallel by means of three positioning plates

Diagnostics

For diagnostics a microwave cavity was designed and built in collaboration with Elektronikcentralen. It was built together with two optical detectors for time of flight measurements to form an integrated unit[2,3]. The pellet trajectories are close together and one diagnostic unit is sufficient for all pellet trajectories.

Operation and data collection

For operation of a pipe gun a number of electromagnetical valves and electrical heaters should be activated successively in periods of preset length. The operation of an 8-shot unit follows the same scheme, but in some cases 8 heaters or valves are operated and in some cases

common valve. The 8-shot unit can then be operated by means of a PLC in the same manner as a single pipe gun.

Following this scheme a set up with PLC, power supplies for heaters and valves, etc. was built. A number of actions outside the 8-shot unit are also controlled by the PLC.

The data collected during a run may be divided in two groups, fast data from the diagnostic unit and slow data from temperature measurements for parts of the pipe gun. The outputs from the diagnostic unit are read and stored successively shot by shot by a transient recorder. The transient recorders used do, however, not allow intervals between shots below 40 ms.

The data from a shot are recorded by an Olivetti M380-XP1 personal computer supplied with a Keithley 570 data acquisition workstation and a GPIB-interface (General Purpose Instrumentation Bus)

The software for handling data consists of a LabTech "Notebook programme" for collection of and presentation of the temperatures during a shot. The data collection from the transient recorders is handled by a special developed programme written in Turbo Pascal, that also performs the calculation of pellet masses and velocities. Plotting of production data and analog signals from

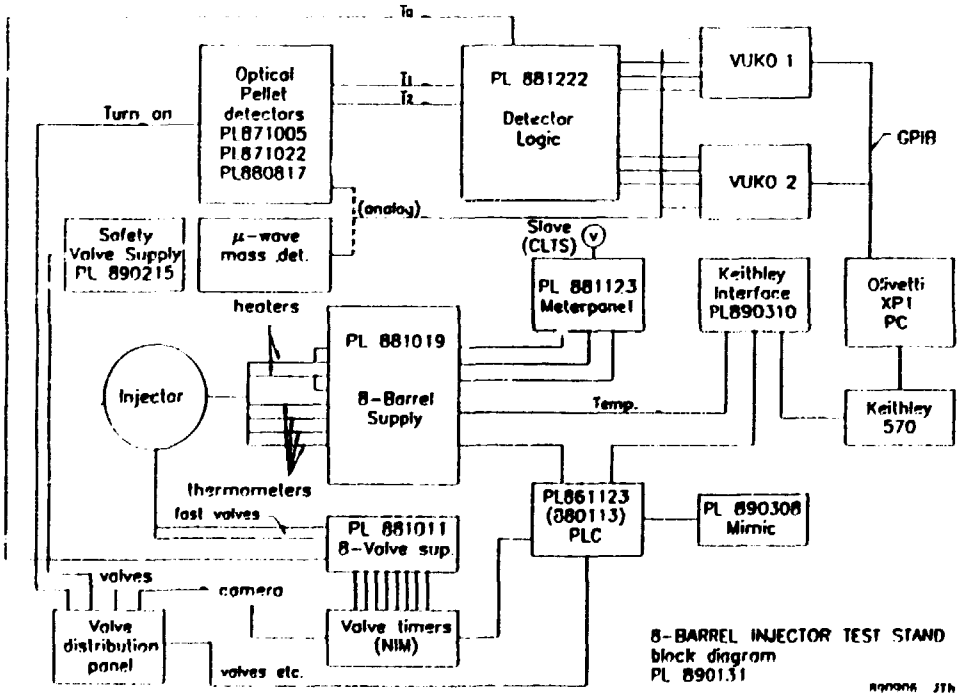

Figure 2. Block diagram for operation of an 8-shot injector in the laboratory

the pellet detectors is done by another Pascal programme.

The set up for data collecting and handling is shown in Fig. 2.

Before starting a shot it is possible to change parameters and the new parameters should be entered manually by the operator.

Results

Two 8-shot units were built, the first with 8 barrels of 2.05 mm inner diameter and the second one with 4 barrels of 1.4 mm inner diameter and 4 barrels of 2.05 mm inner diameter. For the last unit the cryostat was improved and a cryopump was attached to the cryostat.

The first problem solved in the first 8-shot unit was to make the thermal couplings so that sufficient cooling was obtained. Based on these results the cryostat for the second 8-shot unit was modified.

For the first unit there were a slight reduction in velocity for the last two pellets with time intervals of 100 ms between shots. For the second unit it was possible to fire with time intervals of 1000 ms between shots without affecting the velocities of the last pellets. A cryopump with active carbon was further attached to the cryostat. It appeared to be very effective and able to replace a turbopump.

The suggested method for operation of the 8-shot unit worked very well. The set up for data collection also worked without problems.

An 8-shot unit is actually 8 independent pipe guns and these pipe guns should be made so that they make up 1 or 2 identical groups and should be operated so that they give 1 or 2 sets of identical results. With the first 8-shot unit we got some experience in operating a unit and with the second unit we have made some actual measurements on stability and behaviour.

To show the behaviour we give result for acceleration of H_2 pellet in unit 2 with 50 ms between shots in Table 1. 21 series of shots were fired and average velocities in km/s and masses in 10^{20} atoms/pellet were for the 8 barrels:

Table 1

Barrel	1	2	3	4	5	6	7	8	
Average Size	1.78	1.77	1.72	1.57	4.52	3.82	4.59	4.49	10^{20} at/pel.
Std.dev.	4	6	6	19	8	12	3	4	per cent
Velocity	1.35	1.40	1.35	1.54	1.54	1.53	1.41	1.33	km/s
Std.dev.	1.5	2.4	2.4	3.1	2.4	5.8	1.5	2.2	per cent

We see the quality of pellets varies somewhat from one barrel to another. Barrels 4, 5 and 6 are apparently not quite satisfactory.

This showed up more clearly when lower driver gas pressures were used. Here pellets often stuck in the barrels at pressures below 20 bar.

Most of the work was made with H_2 pellets. Some work was made with D_2 pellets. They were slower because of the higher mass, they were longer than H_2 pellets made under same conditions because of a different vapour pressure curve and they were more tricky to handle.

A method for fixing the outer parts of the barrel so they were parallel was developed and with this method it was possible to fire 8 pellets through a hole of less than 20 mm diameter 4 m in front of the barrels. It actually corresponded to a precision in direction for each barrel of better than ± 0.025 degree. With this accuracy of firing it was possible to calibrate the microwave cavity as described[2,3].

During these measurements Allen Bradley carbon resistors have been used for low temperature thermometry, first resistors bougth more than 20 years ago and next resistors bougth very recently. It appeared that the newest thermometers are no longer reliable. The change in resistance when cooled to low temperature is not as large as for old resistors, the resistors may be divided into two groups with respect to the change and we have in one case seen a resistor go from one group to another after some use. The work has to some extent been hampered by this.

1) Sørensen, H., Hansen, J.E., Nordskov, A., Sass, B., Weisberg, K-V. (1989), Development of a multishot pellet injector, Risø-R-566, 79-81.
2) Sørensen, H., Hansen, J.E., Michelsen, P., Sass, B., Weisberg, K-V. Knudsen, O. and Michelsen, E. Submitted to Rev. Sci. Instr. for publication.
3) A microwave cavity for pellet mass measurement. (see 2.1.10)

2.1.9. Design of multishot injectors for FTU, Frascati and RFX, Padova

(H. Sørensen, J.E. Hansen, B. Sass and K.-V. Weisberg, J. Bundgaard* and J. Sejr Olsen* (*Electronics Department, Risø), B. Bukholt**, P. Hersom Jensen** and P. Sanderhof** (**Construction Department, Risø))

A number of meetings were held with colleagues from RFX in Padova and FTU in Frascati. During these meetings a construction for the injectors for RFX and FTU were suggested and discussed and tenders for delivery of turnkey injectors by Risø National Laboratory were given in September. These tenders are now being discussed.

2.1.10. A microwave cavity for pellet mass measurement

(H. Sørensen, J. E. Hansen, P. Michelsen, B. Sass, K.-V. Weisberg, O. Knudsen* and E. Michelsen* (*Elektronik-centralen, Copenhagen, Denmark))

A microwave cavity for nondestructive measurement of the mass of high-speed pellets of solid hydrogens has been made. The cavity is for use at the multishot pellet injector, where 8 pellets are fired successively with trajectories being parallel and symmetrical around the injector axis.

The cavity is cylindrical with the axis coinciding with the injector axis. When a pellet passes through the cavity through holes of 15-16 mm diameter the change in resonant frequency is proportional to the pellet mass. Due to symmetry the sensitivity will be the same for all pellets. The frequency shift is measured directly and is converted to a voltage proportional to the size of the pellet.

The cavity was calibrated with pellets of H_2 and D_2 containing around 6×10^{20} atoms and with velocities between 1200 and 1500 m/s. The sensitivity was was found to be 60 ± 3 mV/10^{20} atoms in both cases. This is in fair agreement with estimates made from the dielectric constant of solid H_2 and D_2.

The cavity is built together with two optical detectors for time of flight measurements to form an integrated diagnostic unit.

2.1.11. Singular behaviour of a reacting ablated flow of a spherical hydrogen pellet under the impact of plasma electrons

(C. T. Chang)

When dissociation and ionization effect are presented in the ablated cloud of a spherical hydrogen pellet, the governing equations become singular whenever the flow velocity of the ablatant reaches the local equilibrium sound speed, a_e, or equivalently, the local equilibrium Mach number, M_e, tends to unity. Due to the presence of the dissociation and ionization effect, M_e is not a monotonic increasing functon of the cloud radius, r; multiple singularities are possible. At the first singular radius, r_* (denoted by x in the figure), breakdown of the solutions of the governing equations is prevented through the balance between the expansion and heating of the ablated cloud and the local energy flux of the plasma electrons. For some combinations of the local pellet radius and the state of the plasma electrons, breakdown of the solution of the system of governing equations can occur when this delicate balance is absent (see the point marked by o in the figure).

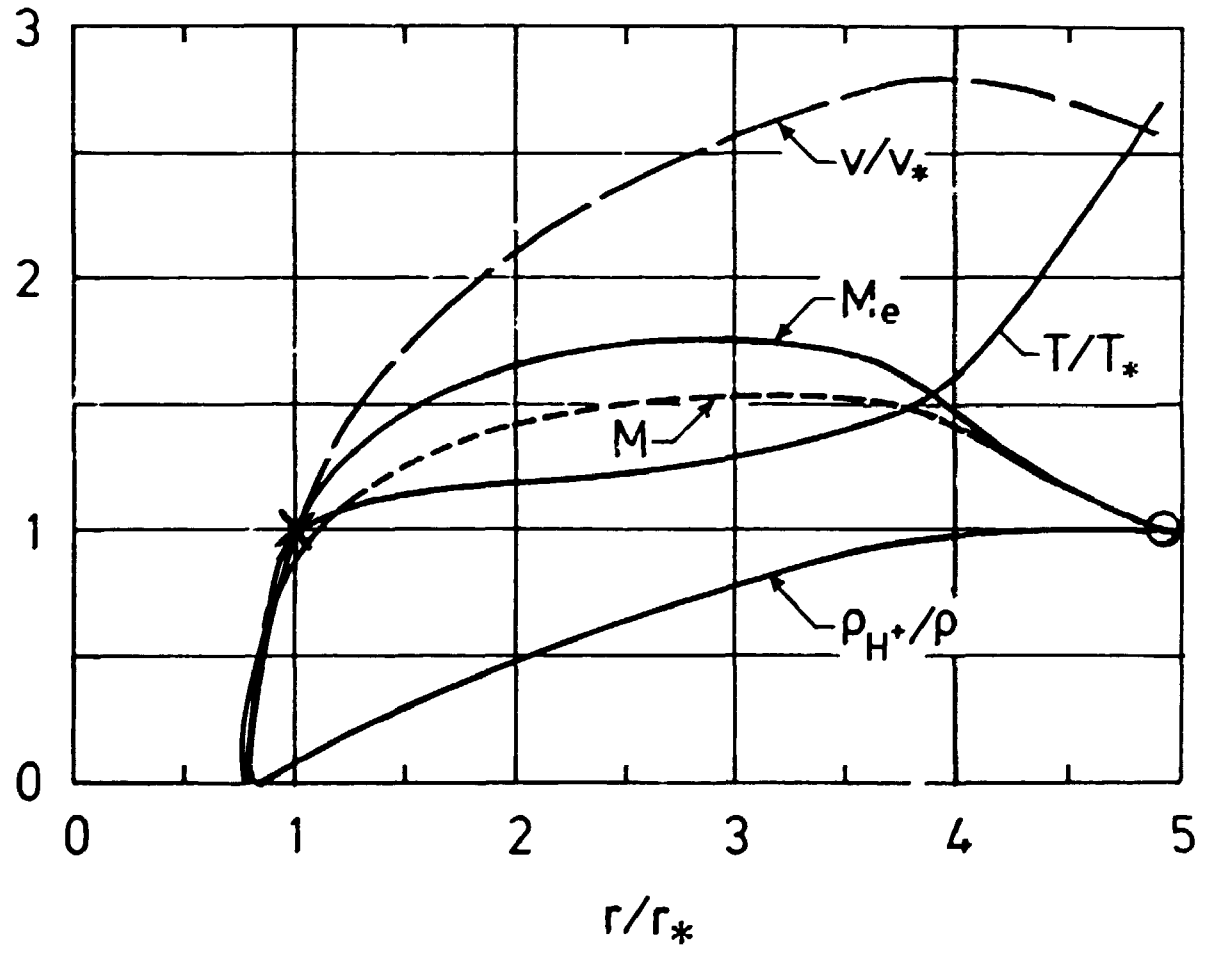

2.1.12. The ionization radius of a spherical hydrogen pellet during its passage in a tokamak

(C.T. Chang)

Assuming the ablatant is a 4-species mixture, H_2, H, H^+ and e, and their relative concentraton is determined by the condition of local thermodynamic equilibrium, the ionization radius, r_i, of a spherical hydrogen pellet of radius r_p during its passage in a tokamak is studied. Using the dimensional reasoning, it is shown that the ratio, r_i/r_p, is a function of the parameter, $p_e/K_i(T_e)$, where p_e and $K_i(T_e)$ are the local pressure and ionization equilibrium constant of the plasma electrons. When $p_e/K_i(T_e) > 2\times10^{-12}$ r_i/r_p approaches a constant ($\approx$ 11), as shown in the figure.

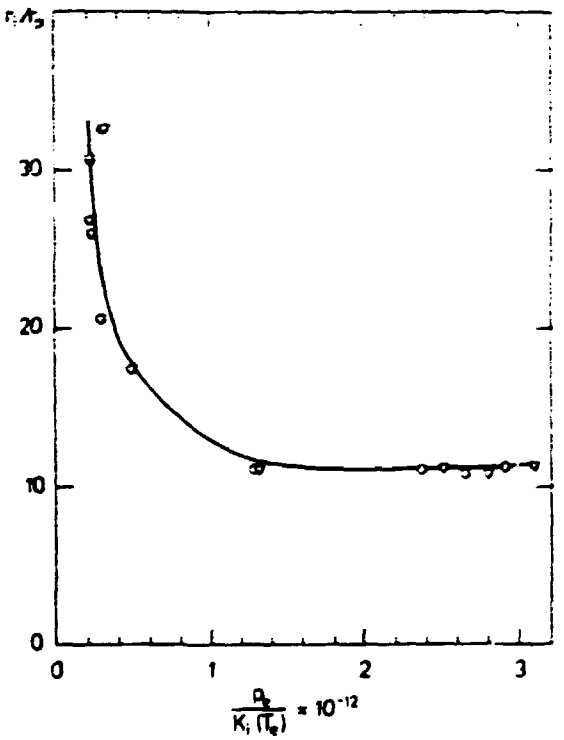

The points shown by triangles (▽) are calculated using the full model while the points shown by circles (o) are obtained using the approximation $K_i(T_e) \simeq 4.826\cdot10^9\,T^{2.5}$ dyn/cm^2.

2.1.13. Steady plane ablated flow of a solid hydrogen slab under the impact of an electron beam

(F. L. Tang (Institute of Mechanics, Academia Sinica, Beijing, China) and C. T. Chang)

To study the effect of the expansion geometry of the ablated flow and the stopping of energetic electrons in a medium of variable density, an ablation model of a plane slab of solid hydrogen under the impact of an electron beam is constructed. Due to the lack of area change during the expansion process, the flow is subsonic everywhere. As a result, the ablation rate of the slab is very sensitive to the temperature, T_v and the velocity, u_v of the ablatant leaving the slab surface. At a given T_v (e.g. $T_v \geq T_s$, the surface temperature of the slab), two limiting cases of u_v are of special interest: $u_v \approx 0$ and $u_v \approx u_s$, the sonic speed. The first case corresponds to the existence of an effective energy absorbing region (the ablation mode). The second case corresponds to the existence of the rocket effect, thus offers a feasibility study of the acceleration of a pellet to high speed by an

electron beam. Computational result showed that to reach a pellet velocity of 10 km/sec., at a current I = 30 kA, a beam energy around 0.35 MW is required.

2.1.14. The ablation of a spherical hydrogen pellet under the impact of an ion beam

(F.L. Tang (Institute of Mechanics, Academica Sinica, Beijing, China) and C.T. Chang)

To study the possible contribution of hot ions on the ablation of a hydrogen pellet, we have modified the neutral shielding model of electron impact[1] by taking the appropriate loss function, L(E)[2,3], and the total elastic scattering cross section, σ(E)[3,4] for the slowing down of hydrogen ions in a molecular hydrogen gas into consideration. Compared with the ablation rate of the pellet due to plasma electrons in the central region of existing large tokamaks, the results of the analyses showed that at the level of the power and energy of the neutral beam used, the contribution of ions to the ablation of the pellet cannot be neglected.

1) Parks, P.B. and Turnbull, R.J. (1978). Phys. Fluids 21, 1735.
2) Schou, J. (1989). In: "Structure-Property Relationships in Surface-Modified Ceramics", edited by J. McHargue et al., 61-102.
3) Lindhard, J., Nielsen, V. and Scharff, M. (1968). Mat. Fys. Medd. Dan. Vid. Selsk. 33, No. 10.
4) Sigmund, P. (1971). Penetration of charged particles, lecture notes at H.C. Ørsted Institute, University of Copenhagen.

2.1.15. Studies of wavepropagation in JET-plasma

(H. Bindslev)

JET Contract No. JE8/9008 was completed. Under this contract the effects of density turbulence on the performance of the JET diagnostic, KG4, was studied.KG4 is intended to measure velocity distributions of alpha particles and other fast ions by collective Thomson scattering af 2 mm waves. Initial work on this contract was reported last year[1].

An existing ray tracing code[2] was modified to model the propagation of Gaussian beams in a Tokamak plasma[3]. In addition a set of codes were developed to analyze the intersection of two beams giving, among other parameters, the volume-integrated product of beam intensities. With the aid of these codes the dependence on plasma conditions and turbulence level of a range of geometrical parameters, of significance to the performance of KG4, were investigated. The work has been reported and will appear as a JET report soon. Also the codes have been documented.

After completion of the contract, work has continued on KG4 but on an entirely different front. It is attempted to develop a fully relativistic theory for the Thomson scattering of EM-waves in the case where vacuo propagation cannot be assumed. In particular it is expected that such a theory will resolve the singularity in the scattering cross section for X-mode waves near the R-cutoff and upper hybrid resonance found with the cold plasma model.

1) Bindslev, H., Hansen, F.R., Lynov, J.P. and Pécseli, H.L. (1989), Risø-R-566, p. 84.
2) Hansen, F.R., Lynov, J.P. and Michelsen, P.M. (1985). Plasma Phys. Contr. Fusion 27, 1077.
3) Hansen, F.R., Lynov, J.P., Michelsen, P.M. and Pécseli, H.L. (1988). Nucl. Fusion 28, 769.

2.1.16. Correlation reflectometry

(P. Michelsen, H.L. Pécseli and J.P. Lynov)

Experiments on JET on correlation reflectometry has initiated a theoretical/numerical study with the purpose to improve the interpretation of the experimental results. Correlation reflectometry is a rather new technique based on microwave reflectometry for diagnosing density microturbulence. Two independent reflectometers operating with microwave frequencies close to each other probe the plasma along the same light of sight. They are reflected at two positions close to each other. Fluctuations in the plasma will have two principal effects on the phase: they will cause a variation in the local value of the refractive index, and in the position of the reflecting layer. In order to calculate the phase change of the reflected signal for a given plasma profile, it is necessary to solve the Maxwell equations together with the equation of electron motion as a two-point boundary value problem. A numerical code for this kind of problems was developed in the group earlier and with some modifications it should be well suited also for this problem.

2.1.17. Autonomous models for two-dimensional turbulence

(J.P. Lynov, A.H. Nielsen, H.L. Pécseli and J. Juul Rasmussen)

We have continued our numerical studies of autonomous models for two-dimensional turbulence[1]. This model is initiated with a linear superposition of a large number of structures with Gaussian shape

$$\phi_j(\mathbf{r}-\mathbf{r}_j) = a_j \exp(-(\mathbf{r}-\mathbf{r}_j)^2/\delta_j) \qquad (1)$$

where the initial positions $\mathbf{r}_j$, with $j = 1...N$, are chosen by a random number generator. Interpreting ϕ as a stream function we define an interaction between individual structures as a simple convection, i.e.

$$\frac{d\mathbf{r}_j}{dt} = \sum_{\ell \neq j} \nabla\phi_\ell(\mathbf{r}_j-\mathbf{r}_\ell) \times z$$

where $\hat{z}$ is a unit vector perpendicular to the configuration plane. We have extended the previous investigations by allowing the interacting structures to have different sizes defined through the parameters a_j and δ_j. Compared with the simple system with only identical structures, this system cannot properly be put in a Hamiltonian form. Negative temperature states, described by Onsager[2] are not simply defined for this system. Although a condensation of the system have not been observed in the

computer simulation, it might be possible that the system contained a kind of negative temperature states.

The analysis of Wandel and Kofoed Hansen[3] as applied by Pécseli and Mikkelsen[4] accounts also very well for both Eulerian and Lagrangian correlation functions of this system, and we have not observed any major difference in the results as compared to the result for the simple system.

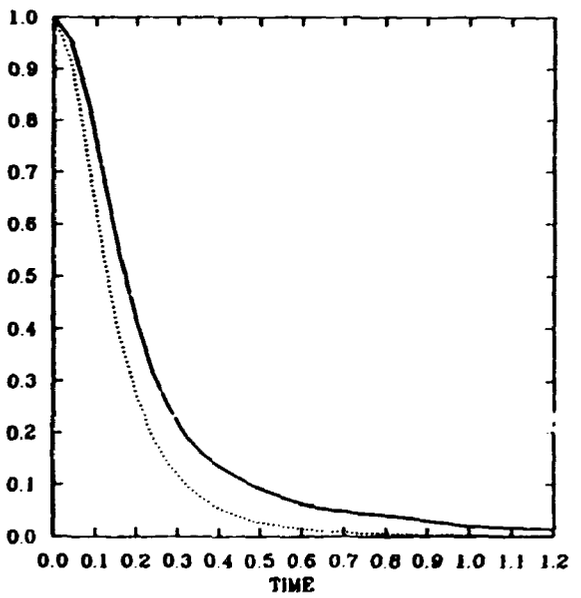

As an example of this the figure shows the Lagrangian correlation function for two kind of structures, where one is three times larger than the other. The solid line show the numerical result, and the dotted line the theoretical.

1) Physics Department, Annual Progress Report 1988, Risø-R-566, p. 87.

2) Onsager, L. (1949). Nuovo Cimento, Suppl. 6, 279.

3) Kofoed-Hansen, O. and Wandel, C.F. (1967). On the relation between Eulerian and Lagrangian averages in the statistical theory of turbulence. Risø, Report, Risø-R-50.

4) Pécseli, H.L. and Mikkelsen, T. (1985). J. Plasma Physics 34, 77.

2.1.18. Spectral solution of the two-dimensional Hasegawa-Mima equation

(J.P. Lynov, A.H. Nielsen, J. Nycander (Uppsala University, Sweden))

The Hasegawa-Mima equation is a nonlinear equation describing quasi two-dimensional fluctuations caused by electrostatic low frequency drift waves in strongly magnetized plasma. These waves are believed to be important for the explanation of anomalous transport in magnetically confined plasmas. Similar equations has long been known to describe large-scale motion of the atmosphere, and in particular nonlinear Rossby-waves. In the short wavelength limit the Hasegawa-Mima equations reduce to the Euler-equations and in the long wavelength limit one obtains the modified Hasegawa-Mima equation having the form

$$\frac{\partial \phi}{\partial t} + V \cdot \nabla \nabla^2 \phi = 0 \qquad (1)$$

where ϕ is the electrostatic potential and V is the E×B drift velocity. The modified Hasegawa-Mima equation is solved numerically in a two-dimensional domain with periodic boundary conditions. We have employed a spectral collocation method with a fully dealiasing scheme, to obtain high accuracy in the numerical solution.

In particular we have investigated the time evolution of the spectrum in order to examine a possible blow-up of the spectrum. This effect is a known feature for e.g. the nonlinear Schrödinger type equations[1]. Here the power-spectrum has the form: $k^{-\alpha(t)}e^{-\delta(t)k}$, $\alpha,\delta > 0$ and at the time when $\delta(t') = 0$ a singularity develops in configuration-space. In the figure we show the time evolution of the power-spectrum for equation (1). As an initial condition all modes in the interval $2 < |k|^2 < 16$ has been activated, and the figure displays the first 1000 time-steps. The result is that this spectrum has the form $k^{-\alpha(t)}$, and we find empirically that $\alpha(t) \propto \log t/\tau$ where τ is a characteristic time. This indicates that a singularity may develop for $t \to \tau$. An analytical explanation for this is yet unknown.

1) Sulem, C., Sulem, P.L., Frisch, H. (1983). J. Computational Physics **50**, 138-161.

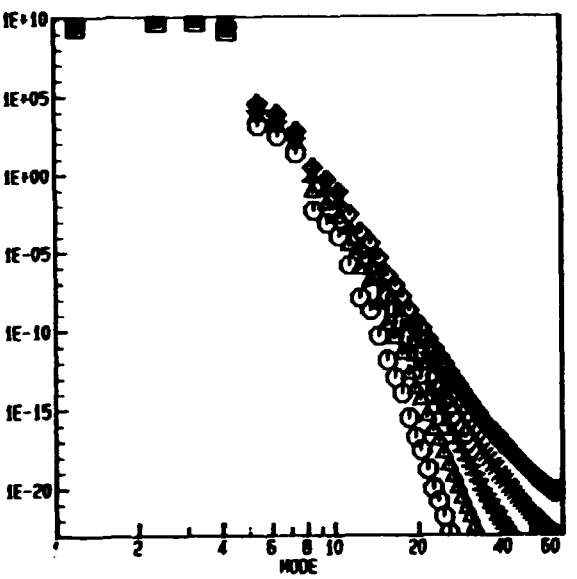

2.1.19. Numerical studies of the transition to turbulence in the edge region of a cylindical confined plasma

(E. A. Coutsias, T. Huld and J.P. Lynov)

The dynamical evolution of low frequency, electrostatic perturbations of a plasma in a plane perpendicular to a strong magnetic field can be modelled by the two-dimensional Euler equations. These equations are equivalent to the dynamical equations for incompressible, inviscid fluid flow in two dimensions. The Euler equations are used in numerical studies of the transition to turbulence in the edge region of a cylindrical confined plasma. These investigations are relevant to the understanding of anomalous transport in magnetic fusion experiments. For the numerical studies, an efficient and accurate spectral scheme developed at Risø was employed.

In the numerical experiments, a strong radial shear is slightly modulated in order to trigger the Kelvin-Helmholtz instability, which breaks up the flow into a number of large scale coherent structures. The rotational symmetry of the flow is weakly perturbed initially, and the subsequent non-linear interactions between the coherent structures are analysed. As an example of the numerical results, the figure shows the evolution of the electric charge density from a state with mode number 7 to a state with a predominant mode number equal to 2, indicating a strong inverse cascade process.

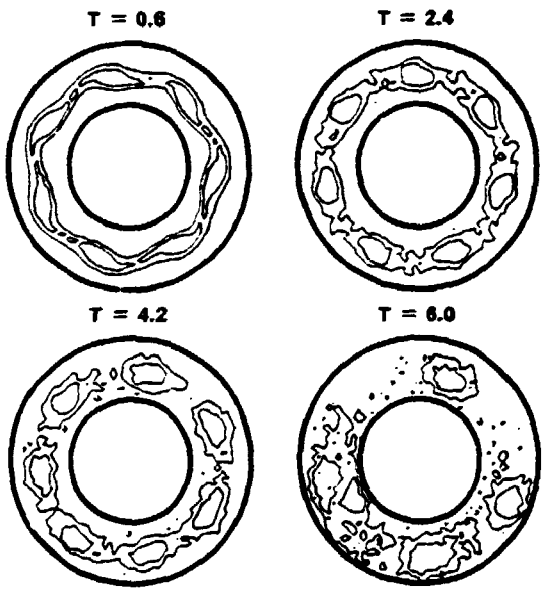

2.1.20. Spectral solution of the Navier-Stokes equations in two dimensional bounded geometries

(E. A. Coutsias and J.P. Lynov)

In numerical simulations of two dimensional turbulence in inviscid fluids, the generation of increasingly shorter wavelength structures such as filaments can cause serious degradation of the accuracy of the numerical solution. This behaviour has been observed under various conditions in numerical solutions of the Euler equations. Employing the Navier-Stokes equations, which include viscosity effects, as model equations, allows the short wavelength stuctures to be dissipated in a controlled way.

Usually, the Navier-Stokes equations are solved in the velocity-pressure formulation and an elaborate fractional time stepping scheme is used to advance the solution in time. An alternative scheme based on the vorticity-stream function formulation simplifies the calculations in two dimensions since only one component of the vorticity field is required to advance in time as oppossed to two for the velocity, and the pressure calculation is replaced by the conceptually simpler calculation of the stream function via solution of Poisson's equation. Also incompressibility is automatically satisfied, while in the velocity-pressure formulation it must be enforced seperately. However, the no-slip boundary condition is given on the velocity and its inclusion in the vorticity-stream function formulation has been a source of difficulties. We have developed an accurate spectral scheme for efficient solution of this problem in an annulus or a slab in 2D, where the no-slip condition is expressed by integral constraints on the spectral expansion coeffients of the vorticity. These constraints are included as so-called "tau conditions" in the implicit time integration of the viscous term. The algorithm is used to study the Kelvin-Helmholtz instability in linear and circular shear flows in a guiding center plasma. The figure shows an example of the evolution of the electric charge density in slab geometry. The generation of wall turbulence is clearly seen.

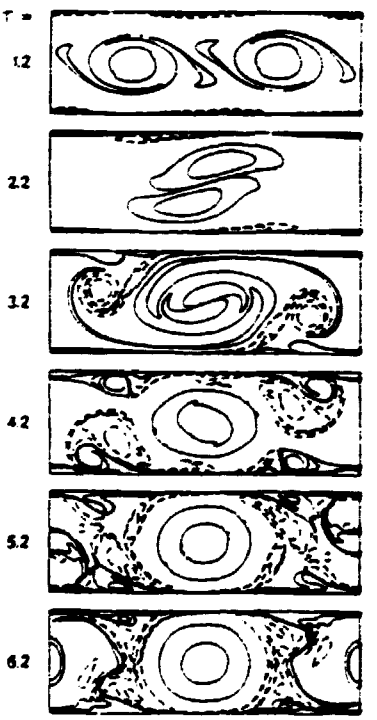

2.1.21. Localized solutions of the Euler equations

(E.A. Coutsias, J. Nycander (Uppsala University, Uppsala, Sweden) and J. Juul Rasmussen)

We have considered the possible localized stationary solutions of the Euler equations governing the evolution of two-dimensional, inviscid, incompressible flows:

$$\omega_t + J(\omega,\psi) = 0$$

Here J is the Jacobian of the vorticity, ω, and the stream function, ψ ($J(\omega,\psi) = \omega_x\psi_y - \omega_y\psi_x$). ω and ψ are related by $\omega = -\nabla^2\psi$. The condition for stationary solutions is $J(\omega,\psi) = 0$ which implies that ω is functionally dependent on ψ : $\omega = f(\psi)$, and the level lines of ω and ψ coincides everywhere. We define localized solutions as solutions having a closed stream line separating space into an inner and an outer region and specialize to cases where ω is constant in the outer region. The aim is to construct the stationary solutions that exist in a general (imposed) outer field. The investigation is motivated by the observations of long-lived coherent vortical structures in experiments and numerical simulations of two-dimensional turbulence. The outer field is then produced by the other structures and our investigation may be considered as a precursor for the development of an interaction theory for vortical structures.

Our results obtained sofar include:

i) The general vortex solutions when the bounding stream line is a circle and the function f is linear in the interior.

ii) The general perturbative solutions when the bounding stream line is nearly circular and f is a weakly nonlinear function in the interior. The perturbation parameter is measuring the departure from circular shaped vortices.

We have also investigated the stability of the structures. Preliminary results show that the lowest order vortex solutions (monopoles and dipoles) are stable for a restricted class of perturbations. This appears to agree with experimental and numerical evidence of long-lived vortex structures.

2.1.22. Coherent structures in flute type electrostatic turbulence

(T. Huld, A.H. Nielsen, H.L. Pécseli and J. Juul Rasmussen)

We have investigated the appearance of relatively long lived vortex-like structures in a background of wide-band turbulent fluctuations. The fluctuations are generated by a sheared azimuthal plasma flow in the residual plasma surrounding the main plasma column of the Q-machine[1]. We have employed a conditional statistical analysis[2] of the turbulence to reveal possible large potential structures and determine their average properties. For this purpose we considered the azimuthal component, E, of the fluctuating electric field, as a reference signal. This is measured as the potential difference between two closely spaced probes. For the low frequency fluctuations in question the radial component of the velocity fluctuations, v, is directly determined as the $E \times B_0$ velocity; $v = E/B_0$.

The electrostatic potential measured by a movable Langmuir probe is subsequently analyzed subject to certain conditions on the reference signal. In the simplest type of conditional analysis we used sets of time series containing simultaneous records of signals from the reference and the movable probe. The records were obtained with a sampling rate of 50 kHz with 8 bit resolution and a duration of 500 ms. Choosing a certain prescribed value, E_1, the digitized time series was searched for times where the reference signal takes a value within a narrow interval around E_1 with a positive time derivative of the signal. Each time this condition is satisfied a subseries over a time invertal $\{t'-\tau, t'+\tau\}$ is selected from the potential record from the movable probe. The time τ is taken to be the correlation time associated with the turbulent fluctuations. The conditionally chosen time series are then considered as independent realizations for the ensuing statistical analysis. The procedure is repeated for probe positions in a grid of 8×13 positions with 3 mm resolutions in the plane perpendicular to the magnetic field. The same analysis is carried out with the fluctuations in plasma density being monitored by recording the fluctuating ion current to the movable probe. In the figure we show contours of the conditionally averaged potential variations for various times with reference to the actual time where the condition on the reference signal is fulfilled. Negative contours are given by dashed lines. The position and size of the reference probes measuring E are marked by • (Note that with full time records available it is possible to investigate the average time evolution before as well as after the reference time). The formation, propagation and decay of conditional vortices, or eddies, having the form of a double vortex is

clearly observed. The life time of the vortices of around 100 μs corresponds to a displacement of a particle convected by the vortex of around 5 mm - 10 mm. Thus, they may significantly influence the transport of particles by the turbulence.

1) Huld, T., Iizuka, S., Pécseli, H.L. and Juul Rasmussen, J. (1988), Plasma Phys. Contr. Fusion **30**, 1297.

2) Pécseli, H.L. and Trulsen, J., in Turbulence and Anomalous Transport in Magnetized Plasmas, ed. D. Gresillon and M.A. Dubois, Edition Physique, Orsay, France (1987), p. 319. Johnsen, H., Pécseli, H.L. and Trulsen, J. (1987), Phys. Fluids **30**, 2239.

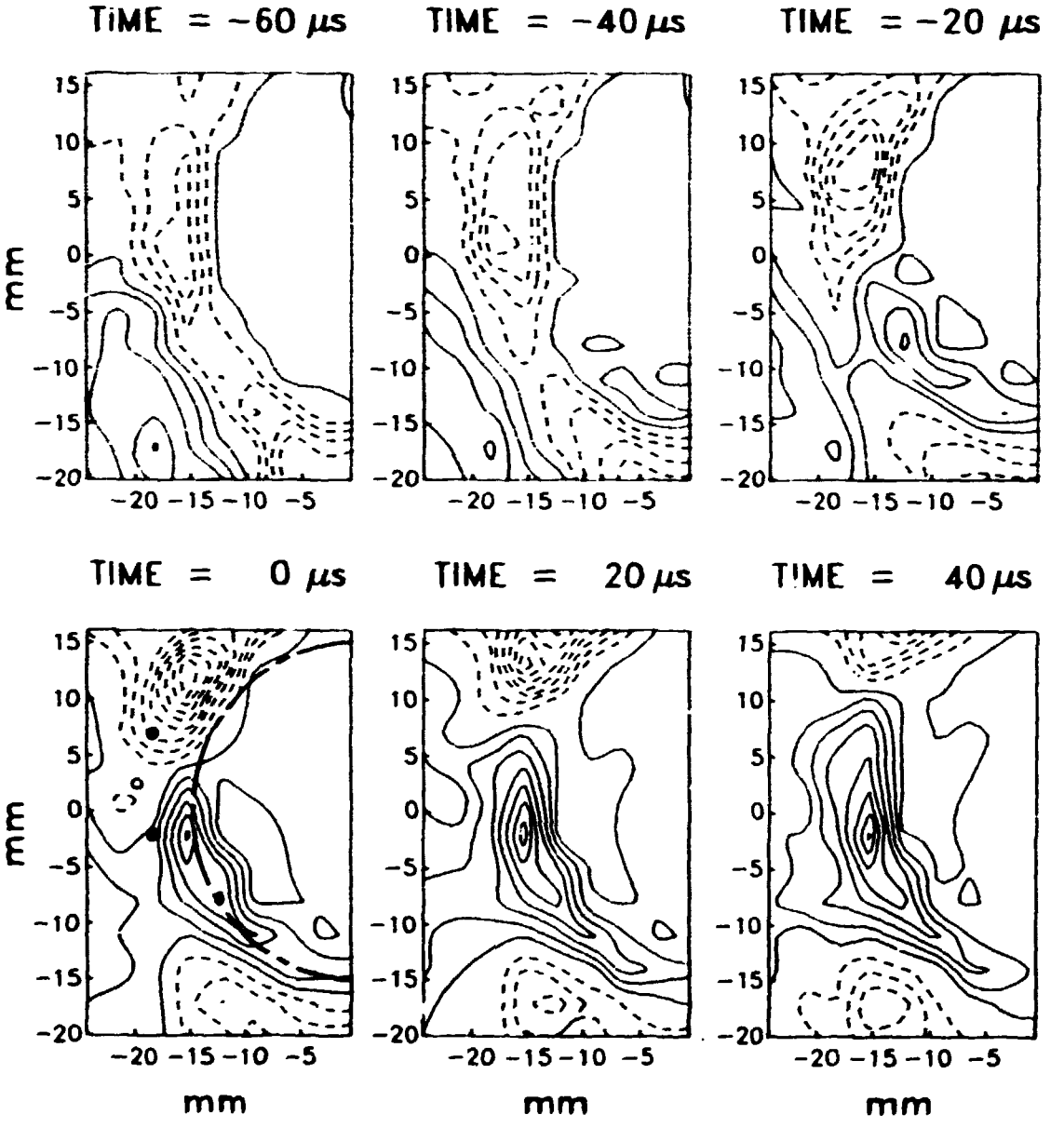

2.1.23. Cross-field plasma transport caused by vortices in flute type turbulence

(T. Huld, A.H. Nielsen, H.L. Pécseli and J. Juul Rasmussen)

The anomalous plasma transport across the magnetic field lines associated with low frequency flute type turbulence is investigated in the Q-machine plasma by measuring and analyzing the radial plasma flux[1] $\Gamma = nv$. Here n is the density fluctuation and v is the radial component of the velocity fluctuations determined from the radial component of the $E \times B_0$ - velocity (see 2.1.22). In particular, we have investigated the importance of large scale coherent structures, which were found to be present in the turbulence (2.1.22), for the anomalous plasma transport. To do that we analyzed the (simultaneously obtained) individual electric field and density fluctuation records which constitute the flux signal at the reference position. The conditionally averaged flux $<\Gamma(t)|E \geq \xi\sigma>$ is obtained subject to the imposed condition that E (the azimuthal component of the fluctuating electric field) is larger than a certain value $\xi\sigma$ measured in units of the rms-value σ for the fluctuating azimuthal electric field component and simultaneously $\partial_t E \geq 0$. The temporal variation of this averaged flux is shown in Fig. 1 for $\xi = 1.5$. The time integral of curves like the one in Fig. 1 will thus

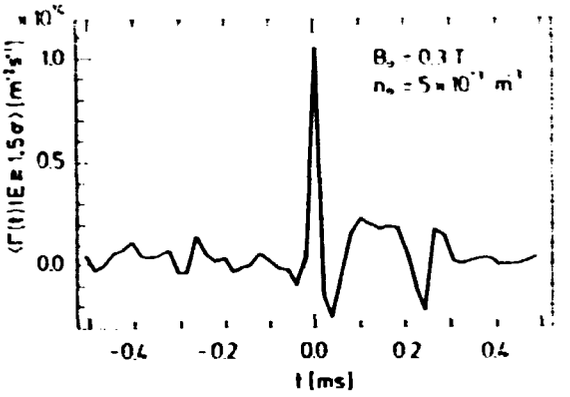

Figure 1

give

$$\Lambda(\xi) = \frac{1}{2t}\int_{-t}^{t} <\Gamma(R\,t,\eta_0)|\,E \geq \xi\sigma > dt\ ,$$

at the reference position (R, η_0), i.e. the net plasma flux associated with structures having a peak value above $\xi\sigma$. Performing this integration for various values of ξ we obtain the results shown in Fig. 2. Because of the cylindrical

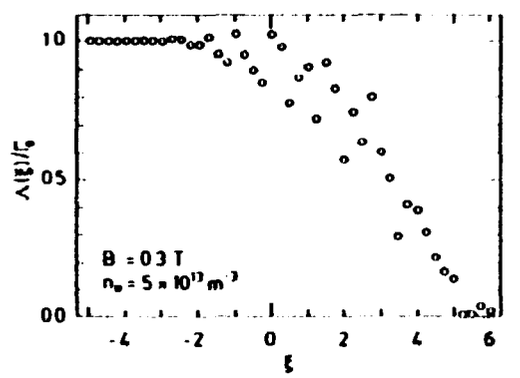

Figure 2

symmetry of the problem, all azimuthal positions, η_0, are statistically equivalent for a given R. Evidently, all structures contribute to the plasma transport indicating that the presence of large

coherent vortices will not necessarily imply a dramatic degradation of plasma confinement. Although our results are obtained in a specific plasma device it should be noted that the basic characteristics of the turbulence described in Ref. 1 are very similar to the results from e.g. the ISX-B Tokamak[2], indicating that we are dealing with universal phenomena.

1) Huld, T., Iizuka, S., Pécseli, H.L. and Juul Rasmussen, J. (1988), Plasma Phys. Contr. Fusion **30**, 1297.

2) Hallock, G.A., Wootton, A.J. and Hickok, R.L. (1987), Phys. Rev. Lett. **59**, 1301.

2.1.24. Phase-space diffusion in turbulent plasmas

(H.L. Pécseli and J. Trulsen (University of Tromsø, Norway))

The analysis of phase-space diffusion of charged particles in turbulent plasmas is reformulated in terms of conditionally averaged potential variations. Considering only electrostatic turbulence an equation is derived for the ensemble averaged Green function for a charged particle released in the turbulent plasma. The analysis requires as input the probability density $P(\phi)$ for the fluctuating potential and correlation functions of the form $R_n(x,t) = <\phi^n(\xi,t)\phi(x+\xi, t+t)>$ for $n = 0,1,2...N$, where N is a free parameter. The quantities $P(\phi)$ and $R_n(x,t)$ are readily measurable quantities.

2.1.25. Experiments on the two-stream instability in an unmagnetized plasma

(T. Huld, M. Nielsen, H.L. Pécseli, B. Reher and J. Juul Rasmussen)

Initial investigations have been performed on the two-stream instability in a plasma with an ion beam of finite diameter. The experiments were carried out in the Risø Double-Plasma device where a collimated beam of low-energy (< 20 eV) ions can be injected into an unmagnetized plasma. Sufficiently dense ion beams will excite the two-stream or beam instability in the plasma. The instability generates a broad band noise spectrum as the unstable modes saturate. Examples of these are shown in the figure. In a) is shown the noise spectrum in the centre of the beam at various distances z from the injection point. It is clearly seen that the instability grows within the first few cm. Unlike earlier investigations[1] with beams filling the entire experiment, which showed a single hump in the spectrum, this experiment reveals a double-humped form. This is thought to be due to radial modes propagating inside the beam region at oblique angles. These are partially reflected at the beam

edge due to the change in refractive index.

In Figs. b) and c) are shown spectra obtained at various radial distances from the beam centre at two different values of z. It is seen here that the spectrum changes considerably with radial distance. This too is thought to be due to partial reflection of oblique modes. It is also seen that part of the noise generated inside the beam region propagates outside the beam.

The measurements were obtained with a standard spectrum analyzer. In the near future more detailed investigations of the beam-generated turbulence will be initiated. These will use a high-frequency digital oscilloscope to map coherent structures in the turbulence.

1) Johnsen, H. (1986). Phys. Scripta 33, 84.

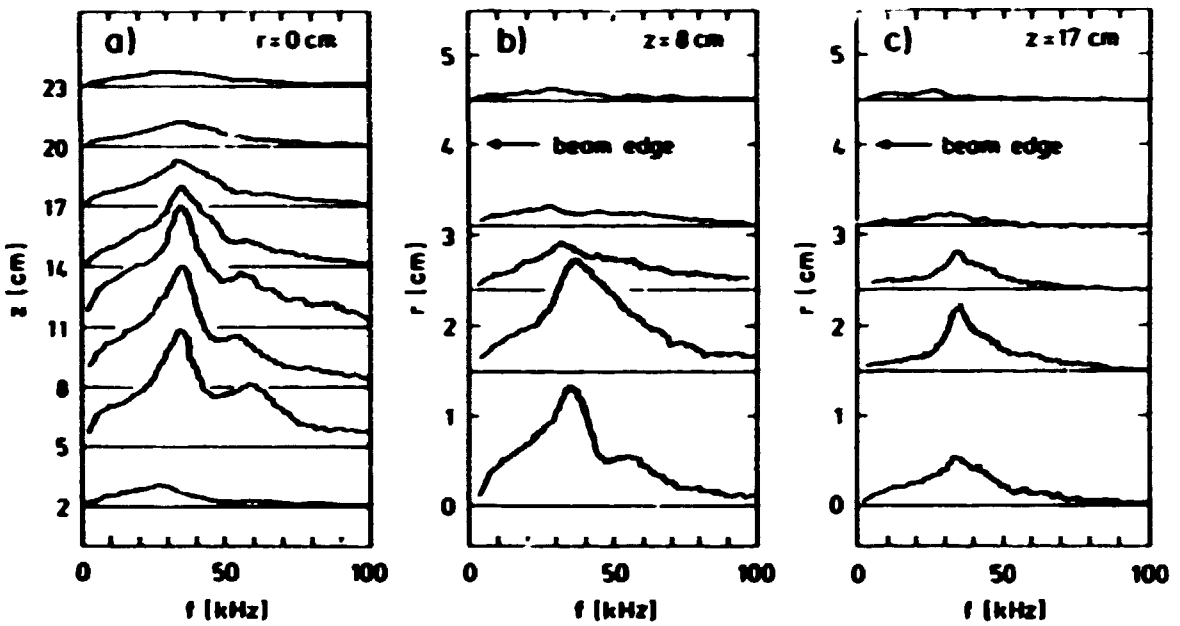

2.1.26. Wavenumber-in-cell simulation of Langmuir turbulence

(H.L. Pécseli and J. Trulsen (University of Tromsø, Norway))

A simple model for describing Langmuir turbulence was proposed by Vedenov et al.[1] on semi-intuitive grounds. In normalized form their equations are

$$\partial_t F(x,\kappa,t) + \kappa \partial_x F(x,\kappa,t) - \frac{1}{2}\partial_x n(x,t)\partial_\kappa F(x,\kappa,t) = 0 \qquad (1)$$

$$\partial_t^2 n(x,t) - \partial_x^2 n(x,t) = \partial_x^2 \int F(x,\kappa,t)\,d\kappa \qquad (2)$$

Physically $\int F\,d\kappa$ can be interpreted as a wave action density, while n denotes the bulk plasma density. In this physical model F(x,κ,t) denotes the density of wavepackets at a position x at time t with a central wavenumber κ. These wavepackets (or quasi-particles) are in the WKB limit propagating in a plasma with varying index of refraction caused by the varying density n(x,t), and their orbits are consequently perturbed. Gradients in density give rise to an effective "force" $-\frac{1}{2}\partial_x n(x,t)$ acting on the wavepackets, see Eq. (1). The spatially modulated wave field will in turn perturb the plasma if the wave intensity is sufficiently large. A gradient in wave intensity will thus act on the light component of the plasma, i.e. the electrons, by ponderomotive forces. The resulting electron displacement gives rise to an ambipolar electric field, which subsequently sets also the ions in motion, and a perturbation of the bulk plasma density results. This process is in the quasi neutral limit accounted for by the term on the right hand side Eq. (2).

The set of equations (1)-(2) were solved numerically by a procedure similar to the one used in collisonless plasma simulations. Thus a "wavenumber-in-cell" simulation was developed for the self-consistent movement of quasi-particles as described by their position x and respective wavenumber κ, according to the characteristics (1). The integral in (2) is obtained in each spatial grid point, and the equation solved by fast Fourier transform in the spatial variable using periodic boundary conditions.

With the code we verified theoretical results[1] for damping and growth of ion sound waves caused by resonant interaction of quasi-particles, a process very similar to Landau damping and growth. An equilibrium solution to (1)-(2) is $n = 0$ and $F = F_0(\kappa)$. Solutions of the dispersion relation

$$u^2 - 1 = \frac{1}{2}\fint_{-\infty}^{\infty} \frac{F_0'(k)}{\kappa - u}\,d\kappa, \qquad (3)$$

with $u \equiv \Omega/K$, were compared with results from the simulations for the case where $F_0(\kappa) = A(2\pi\Delta)^{-\frac{1}{2}}\exp(-\frac{1}{2}(\kappa-\kappa_0)^2/\Delta)$. The symbol $\fint$ denotes the usual Landau contour of integration, while $F_0'(\kappa) \equiv dF_0(\kappa)/d\kappa$. Only those solutions

close to the sound wave branches $u^2 = 1$ were considered. Typical results are shown in Fig. 1.

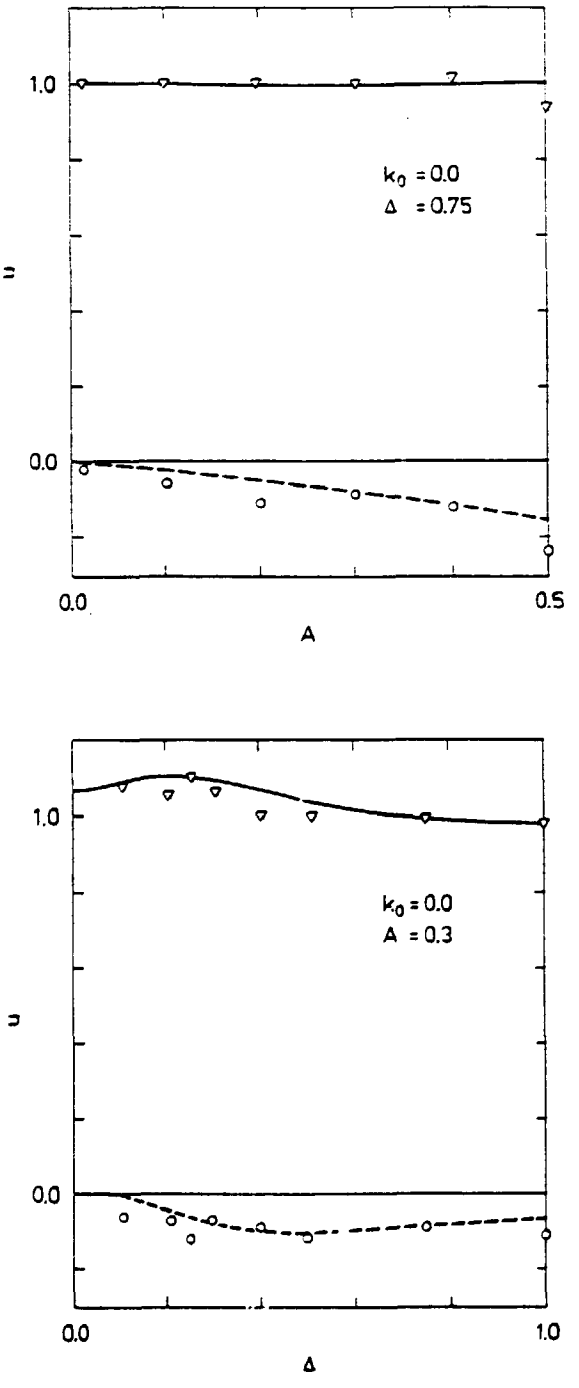

Figure 1

The code was applied also for a study of large amplitude phenomena. Fig. 2 shows the evolution of density n and the corresponding variation of $\rho \equiv \int F dk$ as functions of x for different times.

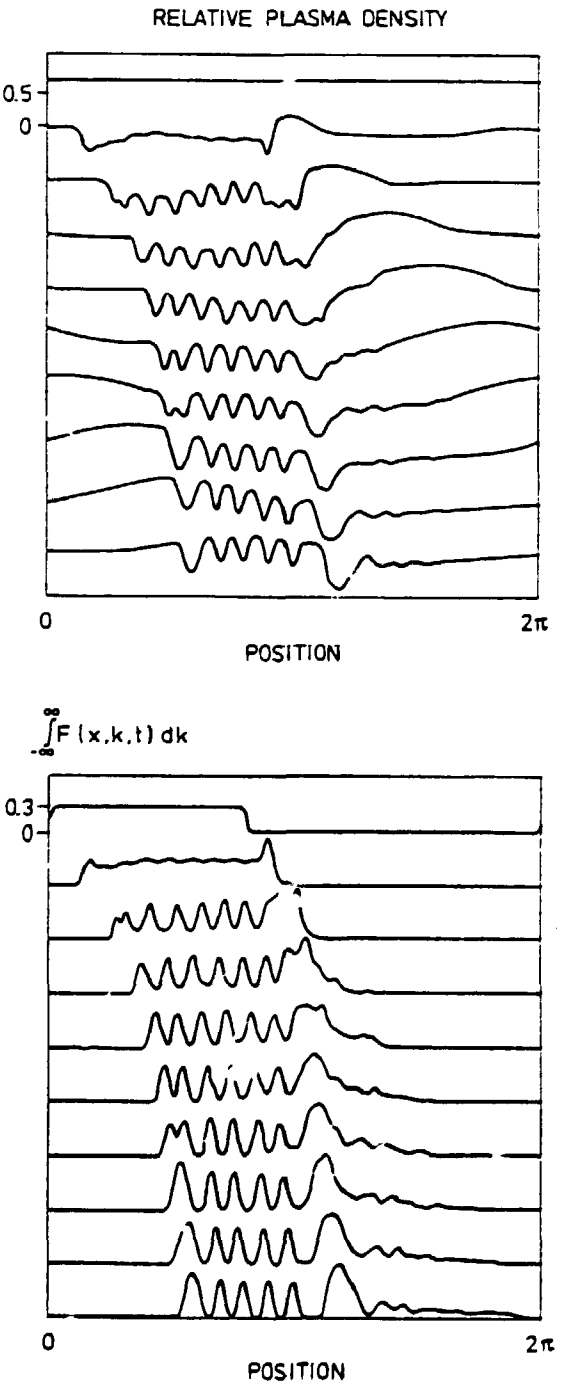

Figure 2a,b

Initial conditions were n(t = 0) = 0 and ρ = 0.1 in an interval [0;0.4L] where L is the length of the system. Initially F is chosen to be a Gaussian with standard deviation 0.075 around κ = 0.75 i.e. a characteristic group velocity below C_S. The figures contain several of the important features of general results. The intense wave-burst is digging a cavity which traps parts of the wave-field, while the rest is slowly dispersing. The plasma removed from the cavity escapes in the form of free sound pulses. Inside the cavity a modulational instability develops. The instability saturates in an array of density cavities (Fig. 2a), filled with a "hot" plasmon gas (Fig. 2c) which maintains an equilibrium very much similar to Bernstein - Grene - Kruskal phase space equilibria. The figures show clearly a coalescence of some of these cavities, which is a process well known for phase space vortices. Figures like Fig. 2c show that the interaction which leads to coalescence between cavities is mediated by an exchange of quasi-particles.

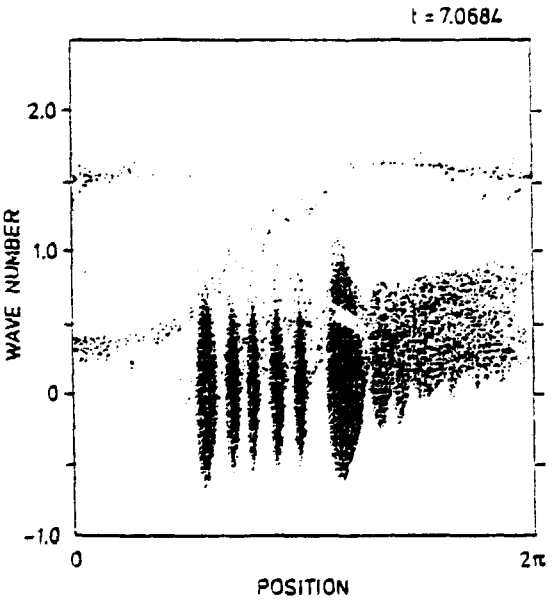

Figure 2c

1) Vedenov, A.A., Gordeev, A.V. and Rudakov, L.I. (1967), Plasma Phys. 9, 719.

2.1.27. Nonlinear stage of the modulational instability of whistler waves

(F.R. Hansen, T. Huld, V.I. Karpman (IZMIRAN, Moscow, U.S.S.R.), J.P. Lynov, H.L. Pécseli and J. Juul Rasmussen)

Numerical investigations have shown that the two-dimensional modulational instability of whistler waves evolves in a quasi-recurrent manner. The main part of the energy is residing in the fundamental mode of the initial modulation, and the energy is spreading slowly to higher mode numbers. The detailed evolution depends on the initial conditions and the spreading of the energy to higher mode numbers proceeds faster for higher amplitudes and/or when the direct harmonics of the

initial modulation are unstable. In the figure we show an example of the evolution of the amplitude spectra of $|\psi|^2(\mathbf{K})$ (a) and $\nu(\mathbf{K})$ (b) for a high amplitude case. ψ is the complex amplitude of the modulation of the whistler wave and ν is the slowly varying density. The fundamental mode excited initially is $(K_{xo}, K_{zo}) = (0.19, 0.019)$ and 32×32 Fourier-modes were employed in the numerical solutions. After one period of almost perfect recurrence, where the main part of the energy resides in the fundamental mode, the higher modes start getting excited. This development accelerates for $T \geq 6000$ because some of the (nonlinearly excited) higher modes happen to be linearly unstable. From the observed development we conjecture that the energy will ultimately cascade to arbitrary high wave numbers giving rise to an apparently chaotic or random wave field. We note that recurrent behavior is generally expected for bounded systems having a finite number of "effective" degrees of freedom. For the present system we have not been able to find an upper limit to the number of "effective" degrees of freedom, which supports the conjecture above.

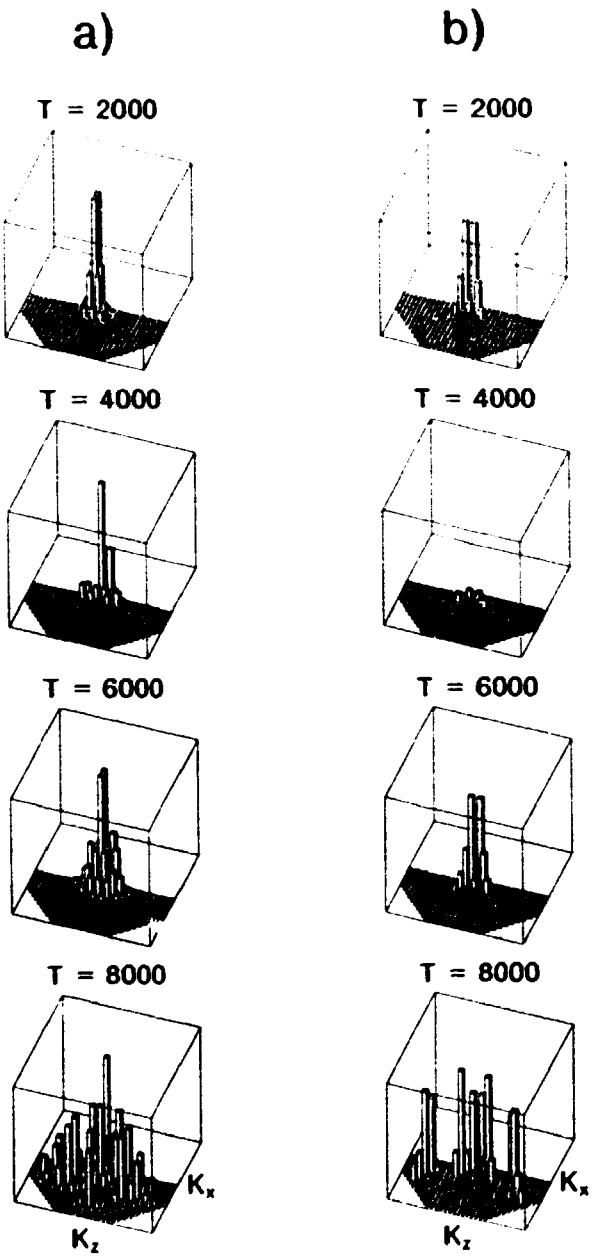

2.2. PARTICIPANTS IN THE WORK IN PLASMA PHYSICS

Scientific Staff

Andersen, Stig Albjerg
Chang, Che Tyan
Ellegård, Ole (part time (25%))
Hansen, Flemming Ramskov (until January 31)
Jensen, Vagn O.
Kofoed Hansen, Otto
Lynov, Jens-Peter
Michelsen, Poul
Pécseli, Hans L.
Rasmussen, Jens Juul
Schou, Jørgen
Sørensen, Hans
Weisberg, Knud V.

Ph.D. Students

Andersen, Annette* (from December 1)
Bindslev, Henrik* (from May 1)
Huld, Thomas
Stenum, Bjarne
Nielsen, Anders Henry

Technical Staff

Bækmark, Lars
Hansen, John
Kossek, Henryk
Nielsen, Mogens O.
Nordskov, Arne
Reher, Børge
Sass, Bjarne
Thorsen, Jess

Secretaries

Astradsson, Lone
Frederiksen, Lajla
Kjøller, Kæth
Kloster, Margit (from February 1)

---

* At present working at JET, U.K.

Guest Scientists

Coutsias, E V.	University of New Mexico, U.S.A.
Tang, F.L.	Chinese Academy of Science, Beijing, China

Short time visitors (more than one week)

Jovanoviç, D.	Institute of Physics, Beograd, Yugoslavia
Knorr, G.	University of Iowa, U.S.A.
Nycander, J.	University of Uppsala , Sweden
Ohe, K	Nagoya Institute of Technology, Japan
Pedrys, R.	Jagellonian University, Cracow, Poland
Rothard, H.	University of Johan Wolfgang, Frankfurt am Main, F.R.G.
Schrittwieser R.	University of Innsbruck , Austria
ter Haar, D.	Oxford University, U.K.
Taniuti,T.	The Japanese Society for Plasma Physics and Thermonuclear Research, Japan

Awards and degrees

Pécseli, H.L.	Appointed external professor at the University of Tromsø, Norway in plasma physics (November).
	Received the annual physics prize of the Danish Physical Society for 1989 together with O. Kofoed-Hansen, for works on plasma turbulence.
Kofoed-Hansen, O.	Received the annual physics prize of the Danish Physical Society for 1989 together with H. Pécseli, for works on plasma turbulence.

Students working for the master degree

Andersen, Annette
Bindslev, Henrik

IAESTE-student

Haid, G.	**Canada**

2.3. PUBLICATIONS AND EDUCATIONAL ACTIVITIES IN PLASMA PHYSICS

2.3.1. Publications

ALS-NIELSEN, J., ANDERSEN, N.H., CLAUSEN, K.N., MICHELSEN, P. and POULSEN, F.W. (1989). Experiments on palladium- and titanium-deuterium systems with reference to studies on "Cold Fusion". Risø-M-2806, 12 pp.

BUNDGAARD, J., HANSEN, K.B. and WEISBERG, K.-V. (1989). Electronics for microchannel photomultipliers in the LIDAR Thomson scattering diagnostic on JET. Rev. Sci. Instrum. **60** (10), 3265-3269.

CHANG, C.T. (1989). General remarks concerning the ablation of a fuelling pellet. In: Pellet Injection and Toroidal Confinement. (IAEA, Vienna, 1989), IAEA-TECDOC-534, 205-215.

COUTSIAS, E.A., HANSEN, F.R., HULD, T., KNORR, G. and LYNOV, J.P. (1989). Spectral methods in numerical plasma simulation. Phys. Scripta **40**, 270-279.

COUTSIAS, E.A., HANSEN, F.R., HULD, T. and LYNOV, J.P. (1989). An efficient spectral algorithm for guiding center simulations in cylindrical coordinates. In: Proceedings of the 13th Conference on the Numerical Simulation of Plasmas, Santa Fe, USA 17-20 September (American Physical Society Division of Plasma Physics, Santa Fe), PT8 (4p).

Fusionsforskning på Risø. En beskrivelse af Plasmafysiksektionen i Fysikafdelingen på Forskningscenter Risø. (Fusion research at Risø, Risø National Laboratory, Roskilde, Denmark 1989) 22 pp.

HANSEN, F.R., KNORR, G., LYNOV, J.P., PÉCSELI, H.L. and RASMUSSEN, J. JUUL (1989). A numerical plasma simulation including finite Larmor radius effects to arbitrary order. Plasma Phys. Contr. Fusion **31**, 173-183.

HULD, T., IIZUKA, S., PÉCSELI, H.L. and RASMUSSEN, J. JUUL (1989). Investigations of flute-type electrostatic turbulence. In: "The Physics of Ionized Gases", invited contributions from the SPIG-88 Symposium, Sarajevo, Yugoslavia, 15-19 August 1988, (edited by L. Tanoviç, N. Konjeviç and N. Tanoviç) (Nova Science Publishers, New York) 611-625.

HULD, T., IIZUKA, S., PÉCSELI, H.L. and RASMUSSEN, J. JUUL (1989). Experimental investigations of flute type electrostatic turbulence. In: "Nonlinear Phenomena of Vlasov Plasmas" (edited by F. Doveil), Editions de Physique, Orsay, France, 1989, 323-326.

HULD, T., IIZUKA, S., PÉCSELI, H.L. and RASMUSSEN, J. JUUL (1989). Experimental investigations of flute type electrostatic turbulence. In: Proceedings of the 16th European Conference on Controlled Fusion and Plasma Physics, Venice, Italy, March 13-17 (edited by S. Segre, H. Knoepfel, E. Sindoni), Vol. **13B**, part IV, 1579-1582.

HULD, T., NIELSEN, A.H., PÉCSELI, H.L. and RASMUSSEN, J. JUUL (1989). Coherent structures in cross-field plasma turbulence. In: Proceedings of the 1989 International Conference on Plasma Physics, New Delhi, India, 22-28 Nov. (edited by A. Sen and P.K. Kaw) Vol. III, 889-892.

IIZUKA, S., HULD, T., PÉCSELI, H.L. and RASMUSSEN, J. JUUL (1989). Forced organization of flute-type fluctuations by convective cell injection. Plasma Phys. Contr. Fusion 31, 855-871.

JENSEN, V.O. (1988). Fusionsforskning og det fælleseuropæiske fusionsforskningseksperiment JET (Fusion research and the joint European Fusion Research Experiment JET). Fysisk Tidsskrift 80 nr. 4, 145-168.

JENSEN, V.O. and ULRIKSEN, J.M. (1989). Sønderø - en anløbsplads fra yngre jernalder og vikingetid (Sønderø, a place of call from the late iron age and the viking age). ROMU, Årsskrift for Roskilde Museum 1988, 5-14.

JOVANOVIÇ, D., PÉCSELI, H.L. and RASMUSSEN, J. JUUL (1989). Interaction of plasma vortices with resonant particles. In: Proceedings of the 16th European Conference on Controlled Fusion and Plasma Physics, Venice, Italy, March 13-17 (edited by S. Segre, H. Knoepfel, E. Sindoni), Vol. 13B, part IV, 1341-1344.

JOVANOVIÇ, D., PÉCSELI, H.L. and RASMUSSEN, J. JUUL (1989). Kinetic theory of plasma vortices - application to reduced MHD. In: Proceedings of the XIX International Conference on Phenomena in Ionized Gases, Belgrade, Yugoslavia, July 10-14 (edited by J.M. Labat), Vol. 1, 26-27.

KARPMAN, V.I., RASMUSSEN, J. JUUL and TURITSYN, S.K. (1989). Hamiltonian structure of the reduced equations for the ponderomotive interaction between a whistler and fast magnetic sound waves. Phys. Lett. 139A, 423-425.

KARPMAN, V.I., HANSEN, F.R., HULD, T., LYNOV, J.P., PÉCSELI, H.L. and RASMUSSEN, J. JUUL (1989). Nonlinear evolution of the modulational instability of whistler waves. In: "Nonlinear World". Proc. IV International Workshop on Nonlinear and Turbulent Processes in Physics, Kiev, U.S.S.R., October 9-22 (edited by A.G. Sitenko, V.E. Zakharov, V.M. Chernousenko) (Naukova Dumka, Kiev), Vol. 1, 333-336.

KNORR, G. and PÉCSELI, H.L. (1989). Asymptotic state of the finite Larmor-radius guiding-centre plasma. J. Plasma Phys. 41, 157-170.

KOFOED-HANSEN, O., PÉCSELI, H.L. and TRULSEN, J. (1989). A statistical analysis of ion-beam generated plasma turbulence. In: "The Physics of Ionized Gases", invited contributions from the SPIG-88 Symposium, Sarajevo, Yugoslavia, 15-19 August, 1988, (edited by L. Tanoviç, N. Konjeviç and N. Tanoviç), (Nova Science Publishers, New York), 595-609.

KOFOED-HANSEN, O., PÉCSELI, H.L. and TRULSEN, J. (1989). Coherent structures in numerically simulated plasma turbulence. In: Selected papers with Otto-Kofoed-Hansen as coauthor and résumé of talks presented at the celebration on 28 April 1989 at Risø (edited by H.L. Pécseli) (Risø National Laboratory, Roskilde) 79-86.

KOFOED-HANSEN, O., PÉCSELI, H.L. and TRULSEN, J. (1989). Coherent structures in numerically simulated ion-acoustic turbulence. Europhys. Lett. 9, 681-687.

KOFOED-HANSEN, O., PÉCSELI, H.L. and TRULSEN, J. (1989). Coherent structures in numerically simulated plasma turbulence. Physica Scripta 40, 280-294.

LOMAS, P.J., THOMSEN, K. the JET team. (1989). An overview of JET results. Plasma Phys. Contr. Fusion 31, 1481-1496.

LYNOV, J.P. and MICHELSEN, P. (1989). Tokamakken - En rapport om fusionsforskning til brug i fysikundervisningen i gymnasiet og HF. (The Tokamak - A report on fusion research for use in the physics education at high school level). Risø-M-2830, 21 pp.

MICHELSEN, P. (1989). Fusionsenergi ved stuetemperatur? (Fusion energy at room temperature?). Dansk Energi Tidsskrift, Vol. 7, May, 10-11.

MICHELSEN, P., ANDERSEN, P., ANDERSEN, S.A., BÆKMARK, L., HANSEN, B.H., JENSEN, V.O., KOSSEK, H. and WEISBERG, K.-V. (1989). Experimental results on acceleration of D_2-pellets by an arc-heated gas gun. In: Proceedings of the 15th Symposium on Fusion Technology, Utrecht, The Netherlands, September 1988, (edited by A.M. van Ingen, A. Nijsen-Vis, H.T. Kippel) (North-Holland, Amsterdam), Vol. 1, 700-703.

MIKKELSEN, T., KRISTENSEN, L., THYKIER-NIELSEN, S. and PÉCSELI, H.L. (1989). Validation experiments for near-site region atmospheric dispersion models. in: Radiation Protection Programme. Progress Report 1988. (Commission of the European Communities, Brussels) (EUR-12064), 1703-1707.

PÉCSELI, H.L. (1989). Plasmafysik (Plasma physics). Naturens Verden, 78-88.

PÉCSELI, H.L. (1989) (ed.). Selected Papers with Otto Kofoed-Hansen as coauthor and résumé of talks presented at the celebration April 28, 1989 at Risø (Risø National Laboratory, Roskilde, Denmark), 155 pp.

PÉCSELI, H.L. (1989). Turbulence in fluids and plasmas. In: SelectedPapers with Otto Kofoed-Hansen as coauthor and résumé of talks presented at the Celebration April 28, 1989 at Risø (edited by H.L. Pécseli), (Risø National Laboratory, Roskilde, Denmark), 35-39.

PÉCSELI, H.L., RASMUSSEN, J. JUUL and SCHRITTWIESER, R. (1989). An experimental investigation on the influence of neutral collisions on the current-driven electrostatic ion-cyclotron instability. Physica Scripta 39, 480-484.

PÉCSELI, H.L., PRIMDAHL, F. and BAHNSEN, A. (1989). Low-frequency electrostatic turbulence in the polar cap E-region. J. Geophys. Res. 94, 5337-5349.

PÉCSELI, H.L. and TRULSEN, J. (1989). A statistical analysis of numerically simulated plasma turbulence. Phys. Fluids, B1, 1616-1636.

PÉCSELI, H.L. and MIKKELSEN, T. (1989). Diffusion in weakly turbulent shear flows. In: "Proceedings of the 5th EPS Liquid State Conference, Moscow, U.S.S.R., October 16-21 (edited by K. Bethge and G. Thomas) (Europhysics conference abstracts) 191-194.

PEDRYS, R., OOSTRA, D.J., HARING, A., de VRIES, A.E. and SCHOU, J. (1989). Energy distributions from electron-sputtered solid nitrogen. Rad. Eff. Def. Solids 109, 239-244.

RASMUSSEN, J. JUUL and RYPDAL, K. (1989). Blow-up in nonlinear Schrödinger equations. In: "Structure, Coherence and Chaos in Dynamical Systems" (edited by P.L. Christiansen and R.D. Parmentier), (Manchester University Press, Manchester), 541-545.

RYPDAL, K. and RASMUSSEN, J. JUUL (1989). Stability of solitary structures in the nonlinear Schrödinger equation. Phys. Scr. 40, 192-201.

SALZMANN, H., BUNDGAARD, J., GADD, A., GOWERS, C., GUSEV, V., HANSEN, K.B., HIRSCH, K., NIELSEN, P., REED, K., SCHRÖDTER, C. and WEISBERG, K.V. (1989). The LIDAR Thomson scattering diagnostic on JET. JET-R(89)07, 23 pp.

SCHOU, J. (1989). Ion energy dissipation and sputtering during bombardment of multicomponent materials. In: Structure-Property Relationships in Surface-Modified Ceramics, NATO ASI series E, (edited by C.J. McHargue, R. Kossowsky and W.O. Hofer) (Kluwer Academic, Dordrecht, The Netherlands), 61-102.

SCHOU, J., STENUM, B., SØRENSEN, H. and GÜRTLER, P. (1989). Observation of fluorescence from heavy rare-gas hydrides and deuterides in electron-irradiated matrices of solid hydrogen and deuterium. Phys. Rev. Lett. **63**, 969-971.

SCHOU, J. (1989). Secondary electron emission: Progress and prospects. Scan. Micr. **3**, 429-433.

STENUM, B., SCHOU, J., SØRENSEN, H. and GÜRTLER, P. (1989). Erosion and luminescence from pure and impure solid deuterium. Rad. Eff. Def. Solids **109**, 235-238.

SØRENSEN, H. (1989). A multishot pellet injector design. In: Pellet Injection and Toroidal Confinement. (IAEA, Vienna 1989) IAEA-TECDOC-534, 255-260.

SØRENSEN, H., ENGBÆK, P., NORDSKOV, A., SASS, B., VILLORESI, P. and WEISBERG, K.-V. (1989). A multishot pellet injected design. In: "Fusion Technology" Proceedings of the 15th Symposium on Fusion Technology, Utrecht, The Netherlands, 19-23 September 1988, (edited by A.M. van Ingen, A. Nijsen-Vis, H.T. Kippel) (North-Holland, Amsterdam 1989), 704-708.

TANG, F.L. and CHANG, C.T. (1989). On the plane steady flow of an ablating pellet under the impact of plasma electrons. Risø-M-2775, 23 p.

TANG, F.L. and CHANG, C.T. (1989). Ablation of a solid hydrogen disc under the impact of plasma electrons in a uniform magnetic field. In: Proceedings of the 16th European Conference on Controlled Fusion and Plasma Physics, Venice, Italy, March 13-17, (edited by S. Segre, H. Knoepfel, E. Sindoni), Vol. 13B, Part IV, 1397-1400.

TRULSEN, J., and PÉCSELI, H.L. (1989). A wavenumber-in-cell simulation of Langmuir turbulence. In: Proceeding of the 13th Conference on the Numerical Simulation of Plasmas, Santa Fe, U.S.A. 17-20 September 1989. (American Physical Society Division of Plasma Physics, Santa Fe, U.S.A.), Paper IM7 (4 p).

TURITSYN, S.K., RASMUSSEN, J. JUUL and RAADU, M.A. (1989). Stability of shocklike solutions in weakly dispersive media. In: "Nonlinear World" Proc. IV International Workshop on Nonlinear and Turbulent Processes in Physics, Kiev, U.S.S.R. 9-22 October (edited by A.G. Sitenko, V. E. Zakharov, V.M. Chernousenko) (Naukova Dumka, Kiev), Vol. 1, 187-190.

VALKEALAHTI, S., SCHOU, J. and NIEMINEN, R.M. (1989). Energy deposition of keV electrons in light elements. J. Appl. Phys. **65**, 2258-2266.

VILLORESI, P. and CHANG, C.T. (1989). Ablation of a cylindrical hydrogen pellet in a magnetized plasma. In: Proceedings of the 16th European Conference on Controlled Fusion and Plasma Physics, Venice, Italy, March 13-17 (edited by S. Segre, H. Koepfel, E. Sindoni), Vol. 13B, Part IV, 1401-1404.

WEISBERG, K.-V. (1989). Timing and control problems in pellet injection. In: Proceedings of the 15th Symposium on Fusion Technology, Utrecht, The Netherlands, 19-23 September 1988, (edited by A.M. van Ingen, A. Nijsen-Vis, H.T. Kippel) (North-Holland, Amsterdam 1989), 1697-1701.

2.3.2. Conference contributions

CHANG, C.T., The ionization radius of the ablated cloud during the passage of a hydrogen pellet in a tokamak. 31st Annual Meeting, Division of Plasma Physics, American Physical Society, Anaheim, U.S.A. (November).

CHANG, C.T., Singular behavior of an ablated flow with a nonlinear heat source. 42nd Annual Meeting, Division of Fluid Dynamics of the American Physical Society, Palo Alto, U.S.A. (November).

COUTSIAS, E.A. and RASMUSSEN, J. JUUL, Localized solutions of the Euler equations. The 3rd European Fusion Theory Conference, Trinity College, Oxford, England (September).

COUTSIAS, E.A., HANSEN, F.R., HULD, T. and LYNOV, J.P., An efficient spectral algorithm for guiding center simulations in cylindrical coordinates. 13th Conference on the Numerical Simulation of Plasmas, Santa Fe, U.S.A. (September).

COUTSIAS, E.A. and LYNOV, J.P., A spectral algorithm for the Navier-Stokes equation in 2d bounded geometries in the vorticity-stream function formulation. Meeting on Theory and Numerical Methods for Initial-Boundary Value Problems, Oberwolfach, F.R.G. (December).

HULD, T., IIZUKA, S., PÉCSELI, H.L. and RASMUSSEN, J. JUUL, Forced organization of flute-type turbulence by convective cell injection. The 24th Nordic Plasma and Gas Discharge Symposium, Gausdal, Norway (February).

HULD, T., IIZUKA, S., PÉCSELI, H.L. and RASMUSSEN, J. JUUL, Experimental investigation of flute type electrostatic turbulence.16th European Conference on Controlled Fusion and Plasma Physics, Venice, Italy (March).

HULD, T., NIELSEN, A.H., PÉCSELI, H.L. and RASMUSSEN, J. JUUL, Coherent structures in cross-field plasma turbulence. 1989 International Conference on Plasma Physics, New Delhi, India (November).

HULD, T., NIELSEN, A.H., PÉCSELI, H.L. and RASMUSSEN, J. JUUL, Investigations of edge turbulence and the associated anomalous transport. The 8th European Tokamak Workshop, Gut Ising, F.R.G. (December).

JOVANOVIÇ, D., PÉCSELI, H.L. and RASMUSSEN, J. JUUL, Interaction of plasma vortices with resonant particles. 16th European Conference on Controlled Fusion and Plasma Physics, Venice, Italy (March).

JOVANOVIÇ, D., PÉCSELI, H.L. and RASMUSSEN, J. JUUL, Kinetic theory of plasma vortices - application to reduced MHD. XIX International Conference on Phenomena in Ionized Gases, ICPIG XIX, Belgrade, Yugoslavia (July).

KARPMAN, V.I., HANSEN, F.R., HULD, T., LYNOV, J.P., PÉCSELI, H.L. and RASMUSSEN, J. JUUL, Nonlinear evolution of the modulational instability of whistler waves. IV International Workshop on Nonlinear and Turbulent Processes in Physics, Kiev, U.S.S.R. (October).

KOFOED-HANSEN, O., Investigations of turbulence in fluids and plasma. The Annual Meeting of the Danish Physical Society, Risø, Denmark (November).

LOMAS, P.J., THOMSEN, K., the JET team, An overview of the JET results. 16th European Conference on Controlled Fusion and Plasma Physics. Venice, Italy (March).

LYNOV, J.P., NIELSEN, A.H., PÉCSELI and RASMUSSEN, J. JUUL, Autonomous models for two-dimensional turbulence. The 24 Nordic Plasma and Gas Discharge Symposium, Gausdal, Norway (February).

LYNOV, J.P., NIELSEN, A.H., PÉCSELI, H.L. and RASMUSSEN, J. JUUL, Autonomous models for two-dimensional turbulence. The 26th Culham Plasma Physics Summer School, Culham, U.K. (July).

MICHELSEN, P., Non-emission of neutrons from a titanium-deuterium system. The Second Meeting on "Cold Fusion in the European Community", Harwell, U.K. (May).

PÉCSELI, H.L., Turbulent diffusion in plasmas. IAEA, United Nations Educational, Scientific and Cultural Organization, International Centre for Theoretical Physics, Trieste, Italy (May).

PÉCSELI, H.L., Coherent structures in turbulence. Interdisciplinary Workshop on Complexity and Chaos. One-day open meeting, Risø National Laboratory, Roskilde, Denmark (June).

PÉCSELI, H.L., Cross-field plasma diffusion in weakly turbulent shear flows. The 3rd European Fusion Theory Conference, Trinity College, Oxford, England (September).

PÉCSELI, H.L., Identification of coherent structures in plasma turbulence (invited paper). CRPE - Workshop on Plasma Turbulence, Issy-Les-Moulineaux, France (October).

PÉCSELI, H.L. and MIKKELSEN, T., Diffusion in weakly turbulent shear flows. 5-th EPS Liquid State Conference on Turbulence, Moscow, U.S.S.R. (October).

PÉCSELI, H.L., Cross-field plasma diffusion in turbulent shear flows (invited paper). 1989 International Conference on Plasma Physics, New Delhi, India (November).

PÉCSELI, H.L., A review of plasma turbulence. The Annual Meeting of the Danish Physical Society, Risø, Denmark (November).

SCHOU, J., STENUM, B., SØRENSEN, H. and GÜRTLER, P., Luminescence of rare gas hydrides and deuterides in doped solid hydrogen and deuterium. Meeting on Desorption from van der Waals Solids and Related Phenomena, DESY, Hamburg, F.R.G. (April).

SCHOU, J., Secondary electron emission from solids by electron and proton bombardment. IAEA Advisory Group Meeting on Particle-Surface Interaction Data for Fusion, Wienna, Austria (April).

SCHOU, J., Electronic sputtering from insulators. IAEA Advisory Meeting on Particle-Surface Interaction Data for Fusion, Wienna, Austria (April).

SCHOU, J., ELLEGAARD, O., STENUM, B., SØRENSEN, H., PEDRYS, R., OOSTRA, D.J., HARING, A. and de VRIES, A.E., Electronic sputtering of solid nitrogen and oxygen by light ions. 13th International Conference on Atomic Collisions in Solids, Århus, Denmark (August).

STENUM, B., SCHOU, J., SØRENSEN, H. and GÜRTLER, P., Sputtering and luminescence from solid H_2 and D_2. Meeting on Desorption from van der Waals Solids and Related Phenomena, DESY, Hamburg, F.R.G. (April).

STENUM, B., SCHOU, J., SØRENSEN, H. and GÜRTLER, P., Sputtering and luminescence from electron-bombarded solid hydrogens. The 26th Culham Plasma Physics Summer School, Culham, U.K. (July).

STENUM, B., ELLEGAARD, O., SCHOU, J. and SØRENSEN, H., Sputtering of solid deuterium by light keV ions. 13th International Conference on Atomic Collisions in Solids, Århus, Denmark (August).

TANG, F.L. and CHANG, C.T., On the feasibility of high speed pellet injection by a steady electron beam. 31st Annual Meeting, Division of Plasma Physics, American Physical Society, Anaheim, U.S.A. (November).

TANG, F.L. and CHANG, C.T., Ablation of a solid hydrogen disc under the impact of plasma electrons in a uniform magnetic field. 16th European Conference on Controlled Fusion and Plasma Physics, Venice, Italy (March).

TRULSEN, J. and PÉCSELI, H.L., A wavenumber-in-cell simulation of Langmuir turbulence. 13th Conference on the Numerical Simulation of Plasmas, Santa Fe, New Mexico, U.S.A. (September).

TURITSYN, S.K., RASMUSSEN, J. JUUL and RAADU, M.A., Stability of shocklike solutions in weakly dispersive media. IV International Workshop on Nonlinear and Turbulent Processes in Physics, Kiev, U.S.S.R. (October).

VILLORESI, P. and CHANG, C.T., Ablation of a cylindrical hydrogen pellet in a magnetized Plasma. 16th European Conference on Controlled Fusion and Plasma Physics, Venice, Italy (March).

2.3.3. Lectures

JENSEN, V.O., 56 lectures during two courses on fusion plasma physics. The Technical University of Denmark, Lyngby, Denmark.

JENSEN, V.O., Fusionsenergi, fremtidens energikilde (Fusion energy, the energy source of the future).

1) Roskilde University Centre, Denmark (February)
2) University Extension, Roskilde, Denmark (April)
3) Post-Graduate Training College of Denmark (May)
4) Roskilde University Centre, Denmark (October).

JENSEN, V.O., Discussion on cold fusion, Danish radio, MONDORAMA (April).

MICHELSEN, P., Fusionsforskning (Fusion research). Risø, Denmark (May).

PÉCSELI, H.L., Low frequency turbulence in the ionospheric E-region over Greenland. University of Tromsø (April).

PÉCSELI, H.L., Statistical analysis of ionospheric turbulence. University of Oslo, Norway (April).

PÉCSELI, H.L., Coherent structures in plasma turbulence. Université Libre de Bruxelles, Belgium (November).

RASMUSSEN, J. JUUL, Turbulence, turbulent diffusion and related problems. University of Innsbruck, Austria (June).

RASMUSSEN, J. JUUL, Problems in two-dimensional turbulence. Institute for Automation and Electrometry, Novosibirsk, U.S.S.R. (October).

SCHOU, J., Theory of secondary electron emission from solids. J.W. Goethe-University of Frankfurt, F.R.G. (January).

SCHOU, J., Sputtering and luminescence from electron-bombarded solid deuterium and neon. Sandia National Laboratory, Livermore, U.S.A. (May).

SCHOU, J., Fusionsenergi (Fusion energy). University Extension, Roskilde, Denmark (October).

2.3.4. Conferences and schools

A one day symposium was organised at Risø, April 28 in honour of the first head of the physics department Professor O. Kofoed-Hansen. Six lectures were presented giving a review of his research. A summary of the lectures were printed together with selected papers with O. Kofoed-Hansen as author or co-author.

3. PARTICIPATION IN THE UA_2 COLLABORATION AT CERN

(O. Kofoed-Hansen)

The UA_2 experiment at CERN has continued with data analysis and writing of papers, UA_2 has now been upgraded and is again taking data. Work is in progress on understanding the details of the experiment in its present form. Real results will not be available until the spring at the earlies.

Participants

Bern[1], CERN[2], Copenhagen (NBI)[3], Heidelberg[4], Orsay (LAL)[5], Pavia[6], Perugia[7], Pisa[8], Saclay (CEN)[9], Parkville, Australia[10], collaboration.
R. Ansari[5], P. Bagnaia[2], M. Banner[9], R. Battiston[7], K. Bernlöhr[4], C.N. Booth[2], K. Borer[1], M. Borghini[2], G. Carboni[8], V. Cavasinni[8], P. Cenci[2],a, J.-C. Chollet[5], A.G. Clark[2], C. Conta[6], C. Corona[8], F. Costantini[8], P. Darriulat[2], B. De Lotto[5], T. Del Prete[8], L. Di Lella[2], J. Dines-Hansen[3], K. Einsweiler[2], L. Fayard[5], R. Ferrari[6], M. Fraternali[6], D. Froidevaux[5], J.-M. Gaillard[5], O. Gildemeister[2], V.G. Goggi[6], C. Gössling[2], B. Hahn[1], H. Hänni[2,a], J.R. Hansen[2], P. Hansen[3], K. Hara[1], N. Harnew[2], E. Hugentobler[1], E. Iacopini[8,b], L. Iconomidou-Fayard[5], K. Jakobs[4], P. Jenni[2], E.E. Kluge[4], O. Kofoed-Hansen[3], S. Lami[8], E. Lançon[9], P. Lariccia[8], M. Livan[6], S. Loucatos[9], B. Madsen[3], B. Mansoulié[9], G.C. Mantovani[7], L. Mapelli[2,c], K. Meier[2], B. Merkel[5], R. Møllerud[3], M. Moniez[5], R. Moning[1], M. Morganti[8], C. Onions[2], T. Pal[2], M.A. Parker[2], G. Parrour[5], F. Pastore[6], M. Pepe[7], C. Petridou[2], H. Plothow-Besch[4], M. Polverel[9], L. Rasmussen[2], J.-P. Repellin[5], A. Roussarie[9], V. Ruhlmann[9], G. Sauvage[5], J. Schacher[1], S. Stapnes[2], F. Stocker[1,d], M. Swartz[2], J. Teiger[9], S.N. Tovey[10], W.Y. Tsang[e], M. Valdata-Nappi[8], V. Vercesi[6], A.R. Weidberg[2], M. Wunsch[4] and H. Zaccone[9].

3.1. Publications in the work with UA_2

UA_2 collaboration. (1988). Measurement of the strong coupling constant α_s from a study of W bosons produced in association with Jets. Phys. Lett. B215, 175-185.

UA_2 collaboration. (1988). Direct photon production in pp collisions at $\sqrt{s} = 630$ GeV. Z. Phys. C41, 395-404.

Risø National Laboratory **Risø–R–574**

Title and author(s)

PHYSICS DEPARTMENT ANNUAL PROGRESS REPORT

1 JANUARY - 31 DECEMBER 1989

edited by J. Als-Nielsen , J. Skov Pedersen, J. Juul Rasmussen and B. Lebech

ISBN	ISSN 0106-2840
87–550–1618-9	ISSN 0107-8348

Department or group	Date
Physics Department	February 1990

Pages	Tables	Illustrations	References
124	4	66	71

Abstract (Max. 2000 char.)

Abstract

Research in the Physics Department covers two main fields: condensed matter physics and plasma physics. The principal activities in these fields are presented in this Progress Report covering the period from 1 January to 31 December 1989.

The condensed matter physics research is predominantly experimental utilising diffraction of neutrons and x-rays. The research topics range from studies of two- and three-dimensional structures, magnetic ordering, heavy fermions, phase transitions in model systems to studies of texture and recrystallization kinetics with a more applied nature. The discovery of the high T_c superconductors in 1986 has opened an important new research area, where neutron and x-ray diffraction are used to elucidate the basic mechanism responsible for the superconductivity and in the analysis of the solid state syntheses used in producing the materials.

The plasma physics research is partly experimental and partly theoretical. The plasma physics programme is also of a wide scope ranging from fundamental studies of wave propagation, instabilities, solitons and turbulence in plasmas to refuelling a fusion reactor by deuterium-tritium pellets.

Descriptors INIS/EDB

MAGNETISM; PLASMA; PROGRESS REPORT; RISOE NATIONAL LABORATORY; SOLID STATE PHYSICS; SUPERCONDUCTIVITY; THERMONUCLEAR REACTIONS

Available on request from Risø Library,
Risø National Laboratory (Risø Bibliotek, Forskningscenter Risø)
P.O. Box 49, DK–4000 Roskilde, Denmark
Phone + 45 42 37 12 12, ext. 2268/2269. Telex 43 116. Telefax + 45 46 75 56 27

Sales distributors:
G.E.C. Gad Strøget
Vimmelskaftet 32
DK-1161 Copenhagen K, Denmark

Available on exchange from:
Risø Library,
Risø National Laboratory,
P.O. Box 49, DK-4000 Roskilde, Denmark
Phone +45 42 37 12 12 ext. 2268/2269
Telex 43 116, Telefax +45 46 75 56 27

ISBN 87-550-1618-9
ISSN 0106-2840
ISSN 0107-8348